Maximum Likelihood Time-Domain Beamforming Using Simulated Annealing

by

Kevin Xu

Submitted in partial fulfillment of the
requirements for the degree of

Master of Science in Oceanographic Engineering

at the

MASSACHUSETTS INSTITUTE OF TECHNOLOGY

and the

WOODS HOLE OCEANOGRAPHIC INSTITUTION

September 1999

Author ..... K. Xu .....
Department of Ocean Engineering, MIT
and the MIT-WHOI Joint Program in Oceanographic Engineering
August 22, 1999

Certified by ....
Nicholas C. Makris
Assistant Professor, Massachusetts Institute of Technology
Thesis Supervisor

Accepted by ....
Michael S. Triantafyllou
Chairman, Joint Committee for Oceanographic Engineering, Massachusetts Institute of Technology and Woods Hole Oceanographic Institution

Maximum Likelihood Time-Domain Beamforming Using Simulated Annealing

by

Kevin Xu

Submitted to the Department of Ocean Engineering on August 22, 1999, in partial fulfillment of the requirements for the degree of Master of Science in Oceanographic Engineering

Abstract

An algorithm is developed for underwater acoustic signal processing with an array of hydrophones. With various acoustic signals coming from different directions, the maximum likelihood approach is used to estimate the source bearings and time series. Simulated annealing is used to implement the resulting time-domain beamformer. Broadband signals in spatially correlated noise are treated. Previous time-domain beamformers did not consider the correlation between random noise, and they did not use the concept of maximum likelihood, which is asymptotically optimal. We show that improved resolution can be achieved using this new method.

Thesis Supervisor: Nicholas C. Makris
Title: Assistant Professor, MIT

Acknowledgements

It is with deep appreciation that I express my thanks to my academic and research advisor, Dr. Nicholas C. Makris, who with his clear guidance provided me this excellent opportunity and led me to the completion of the thesis. I also appreciate his support and mentorship during the past two years, and his encouragement and patience when I struggled and made mistakes. The time, effort and care which he has taken to shape my research career will be appreciated forever.

I am especially grateful to Mr. Wen Xu for all kinds of help, from courses to research, from FrameMaker to Matlab.

My thanks also go to the Ocean Acoustics Group graduate students at MIT Room 5-435 and other friends. They are Yi-San Lai, Vicent Lupien, Peter Daly, Chin-Swee Chia, Brian Sperry, Kyle Becker , Yanwu Zhang, Yuriy Dudko, Pierre Elisseeff, Dianne Egnor, and Irena Veljkovic.

I would like to thank Ms. Jean Sucharewicz at MIT Ocean Engineering Administration Office, who assisted me in many ways during this work.

Contents

List of Figures

Chapter 1

Introduction

1.1 Beamforming

The problem solved in this thesis will be the determination of the bearing and time series of a broadband acoustic source in additive white noise. Assume that a plane-wave signal is propagating in a medium. An array of sensors is present in the medium. Each sensor is assumed to record the acoustic signal at its spatial position with perfect fidelity. The waveform measured at each sensor is the sum of the signal with a time delay and noise. The noise is due to disturbances propagating in the medium or to noise generated internally in the sensor or in the associated electronics. The outputs of the sensors are summed with weights and time delays to form a beam. This process is beamforming.

The idea of beamforming is to get a precise adjustment of the propagation delays of a signal presumed to be propagating in a direction so as to reinforce it. Signals from other directions and the noise are not reinforced. The energy in the beam is computed for many directions-of-look by manipulating the time delays. Maxima of this energy as a function of the directions-of-look are assumed to correspond to acoustic sources, and the source bearings correspond to the locations of these maxima.[1]

1.2 Time-domain beamforming

The standard time-domain approach is delay-and-sum beamforming. It has some limitations in practice.

William A. Kuperman, Michael D. Collins, etc., solved this problem using a time-domain approach. [2][3] In their approach, Least Squares cost function is used as the energy. Good estimation of the source bearings and time series are obtained by optimizing the energy (corresponding to the peak in the ambiguity function). The results are better

than using conventional beamforming techniques, such as the delay-and-sum beamformer. The parameter search space is large and the computational load is heavy. However, it is not "optimal beamformer" as it is called in papers [2] and [3] unless the noise is Gaussian distributed, uncorrelated, and the signals are deterministic.

1.3 Maximum likelihood and least squares estimation

To make the time-domain beamforming truly optimal, maximum likelihood approach instead of least squares is used in our research. Both maximum likelihood and least squares are very popular in parameter estimation. However, maximum likelihood is asymptotically optimal because it is asymptotically unbiased and it asymptotically reaches the Cramer Rao Lower Bound for large data samples.[4][5][6]

1.4 Simulated Annealing

The maximum likelihood beamforming is implemented numerically on a digital computer. Simulated annealing refers to a class of numerical algorithms that imitate the slow cooling (annealing) of a substance to obtain a crystalline or glass-like state.[7] In numerical analysis, simulated annealing has been successfully applied to in various optimization problems.

1.5 Thesis overview

In our research, maximum likelihood cost function is used to optimize the energy instead of the least squares cost function. The random noise is considered to be spatially correlated. The random noise could also be correlated in time, but because it is very time consuming to compute the time covariance matrix and its inverse, usually, in practice, prewhitening method is applied to decorrelate temporal correlation. The ocean noise is usually wind generated noise, mammalian noise and distant ship noise. Due to the multi-path, when the noise arrives at the array sensors (hydrophones), there is correlation between the

noise on each hydrophone. The surface noise generated by wind is almost always there, so it's more important than other types of noise.

In chapter 2, problem and data models are given. In section 2.1, the problem of time-domain beamforming is described. In section 2.2, data model and signal models are given in detail.

In chapter 3, maximum likelihood estimation algorithm is described in detail. Section 3.1 describes the ocean ambient noise. Section 3.2 describes maximum likelihood parameter estimation in general. Section 3.3 describes the specific maximum likelihood time-domain beamforming algorithm, and its difference with least squares estimation.

In chapter 4, simulated annealing algorithms are applied to implement the maximum likelihood time-domain beamformer. Section 4.1 describes the simulated annealing algorithms in general, section 4.2 describes a fast simulated annealing algorithm.

Simulation results are given in chapter 5. Several cases are given. Arrays consisted of different number of hydrophones are used to find different signals from various directions. The signal are detected from different random noise environments. The estimated bearings and time series using both maximum likelihood beamforming and least squares beamforming are compared. The results show that using maximum likelihood beamforming, higher resolution could be achieved than least squares beamforming when the array is present in correlated noise.

Chapter 6 is conclusions and discussions.

Chapter 2

Problem and Data Model

2.1 Problem definition

The problem is an array signal processing problem. Some plane-wave signals with different waveforms and in different directions are propagating in the medium. A single array of sensors is present in the medium. Each sensor measures the acoustic pressure of the signals. Then the sensor data are used as the inputs to a beamformer. The output of the beamformer -- the bearings and time series of the signals, are of interest to us.

Suppose the source is located in the far field. Spatially, the signal is regarded as a plane wave relative to the receiving array so that the wavefronts are parallel. Temporally, the spectrum of the signal of interest consists of a broadband or narrowband waveform, or a discrete set of frequency lines. [8] Here we are primarily interested in broadband signals, since efficient narrowband methods already exist.

A single array is present in the medium and is used to measure the acoustic field. The array could be horizontal and vertical, it could be linear and non-linear.

A common form of array is the towed array, in which a set of sensors is deployed in a linear configuration some distance behind a moving ship. Modern towed arrays often consist of a set of subarrays, each designed for a specific frequency range. A high-frequency subarray can be obtained by using the more closely spaced set of sensors. A low-frequency subarray, on the other hand, can be realized by using the more separated set of sensors. The longer the array, the lower is the frequency range for which acceptable performance can be achieved.

However, towed arrays also have some disadvantages. For example, a source can be located only relative to a conic angle, which means that it is impossible to separate this

conic angle into azimuth and elevation components without additional information, particularly, we can not determine on which side of the array the source is located without additional information. Another shortcoming arises from the fact that the array is never perfectly horizontal nor vertical straight. This results to uncertainties in sensor positions and thus degrade the beamforming calculation without perfect correction.

A second class of array is the hull-mounted array of sensors. Such arrays are often two-dimensional, which allows the determination of the arimuth and elevation of the source. Because of the restrictions on array size, these arrays in general do not have good low-frequency response. Also, because the sensors are mounted on the hull, they are exposed to a higher noise environment (both from the noise due to the medium and from noise transmitted through the hull) than the sensors in the towed array.

Assume the acoustic pressure of each signal is represented by the symbol $p_m(t)$, where m represents the m th source. The signals could have different source time series, with arbitary center frequency and bandwidth, and could come from different directions.

An array of N equally spaced sensors is deployed to estimate bearings and time series of the sources. A typical configuration of the array is illustrated in figure 2.1.

In this problem, the bearings and the time series of the M signals are all unknowns, because we have no a priori information. The knowns are the acoustic pressure we measured on the array sensors. Our task is to estimate the time series and their bearings correctly based on these sensor data. The algorithm of the beamformer must have the ability to suppress the noise.

2.2 Data model and signal model

Suppose θ_m is the bearing of the m th signal with respect to the array. When the m th signal arrives at the array, it has a time delay τ_m between two adjacent sensors. The

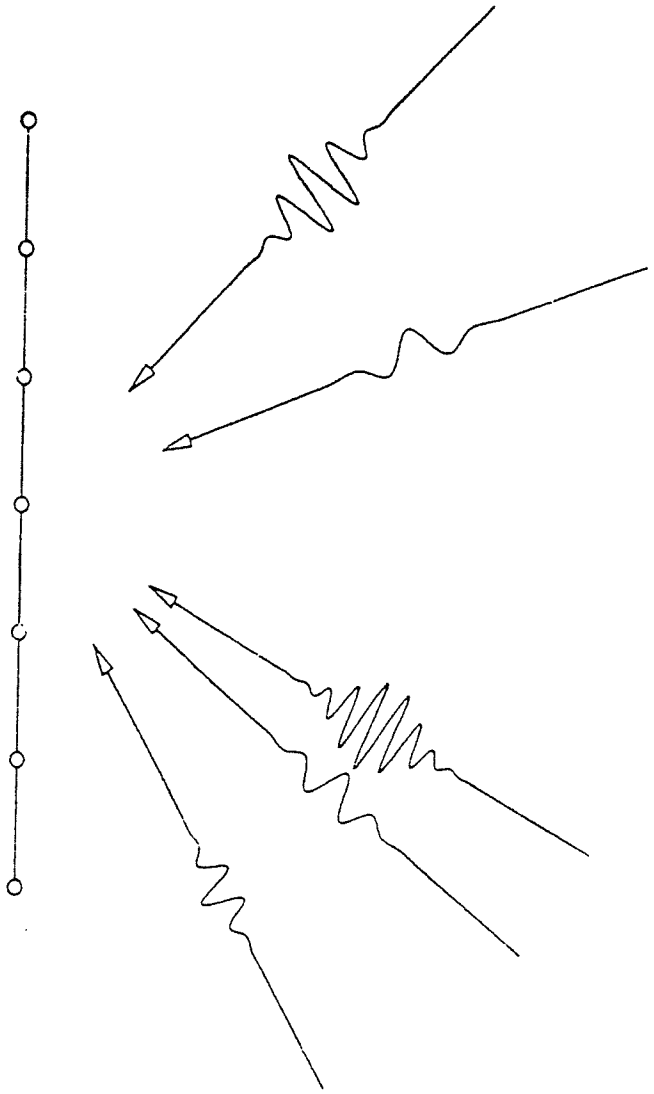

Figure 2.1: Configuration of the array and sources

relationship between the bearing and the time delay is

$$\tau_m = \frac{h \sin \theta_m}{c} \tag{2.1}$$

where c is the sound velocity in the medium, and h is the hydrophone spacing. Here we assume the ocean is a homogeneous media in our problem, and the sound velocity c

remains the same value through the water depth range.

The acoustic pressure measured at the n th sensor is:

$$P_n(t) = \sum_{m=1}^{M} p_m(t - n\tau_m) + \Psi_n(t) \tag{2.2}$$

This is the data model. It is the sum of all the acoustic signals arriving at the sensors with corresponding time delays. In this equation, $p_m(t)$ is the time series of the m th plane wave source, it could be either deterministic signal or random signal, or both. In our problem, we assume that all the signals are deterministic, they can be broadband signals or narrow band signals. The time delay corresponding to the bearing θ_m of the m th source is τ_m. $\Psi_n(t)$ is the noise series, they are random, broadband. At each sensor, the noise has spatial and temporal correlation because of multipath or other reasons. Usually, the ocean ambient noise consists of sea surface generated noise, mammalian vocalization noise and distant shipping noise.

The replica pressure at the n th sensor is defined as the sum of the test time series with corresponding test delays. It is given by the following equation

$$Q_n(t) = \sum_{m=1}^{M} q_m(t - n\sigma_m) \tag{2.3}$$

This is the signal model. In this equation, $q_m(t)$ is the test time series corresponding to the m th plane wave source, the test time delay corresponding to the m th plane wave source is σ_m.

The task is to match $P_n(t)$ using $Q_n(t)$, match $p_m(t)$ using $q_m(t)$, and match τ_m using σ_m. We will solve this problem in time domain, and estimate the true values of the time series and time delays based on the raw sensor data.

Kuperman's time domain beamforming[2][3] is a good solution for this problem when the random noise at each sensor is uncorrelated. In that case, the Least Squares cost function is used. Although Kuperman calls it "optimal time domain beamforming", in fact, it is not optimal. Also, the noise model in Kuperman's paper is uniform distributed random noise, which is not always true in practice. In general, the noise at each sensor is spatially correlated to each other, so we use Maximum Likelihood cost function instead of Least Squares cost function. Maximum Likelihood estimation is asymptotically unbiased, asymptotically reaching Cramer Rao Bound, so it is asymptotically optimal. This is described in detail in the next chapter.

Chapter 3

Maximum Likelihood Estimation

3.1 Ocean ambient noise

The ocean acoustic signals are almost always accompanied by ocean ambient noise. When we estimate or detect the signals, to remove the noise is a major problem. Therefore, before discussing the Maximum Likelihood Estimation, we must discuss the mechanisms of the ocean ambient noise.

Generally, to sonar systems or other underwater acoustic devices, noise is composed of ocean ambient noise, self-noise, and radiated noise.

Self-noise is the noise generated by the vessels (ships, submarines, and torpedoes) on which the hydrophones are located. Radiated noise is generated by the vessels and transmits through the sea and appears as underwater sound at a distant hydrophone. There are three major classes of self-noise and radiated noise - machinery noise, propeller noise, and hydrostatic noise. Of the three classes of noise, machinery noise and propeller noise dominate the spectra of self-noise and radiated noise under most conditions. The relative importance of the two depend upon frequency, speed, and depth. At very low speeds, the hydrophone "sees" the ambient noise of the sea itself. With increasing speed, machinery noise tends to dominate the low-frequency end of the spectrum, and a combination of propeller and hydrodynamic noise becomes important at high frequencies.[9]

In our problem, we suppose the array of hydrophones is still in the ocean, so the ambient noise is the dominating noise to the hydrophones. We only consider the ambient noise, and ignore the self-noise and radiated noise which are not important to this problem.

Ocean ambient noise is defined as the noise of the sea itself. It is that part of the total noise background observed with a nondirectional hydrophone which is not due the hydro-

phone and its manner of mounting called "self noise", or to some identifiable localized source of noise. [9] Ambient noise surrounds the hydrophone on all sides, though unequally and in a nonisotropic manner. In deep water, the ambient noise of the sea has a directionality of its own.

Ocean ambient noise can be generated by the ocean itself and other objects in the ocean. Usually it is generated by ocean surface agitation, mammalian vovalization, and distant shipping. The noise could be affected by sound propagation properties of the ocean when it travels from its source to the array.

Ocean ambient noise is sound in the ocean, but it is not of our interest. Because it interferes the signals and the sonar systems and other underwater sound devices, it is unwanted. The ambient noise can not be reduced by system operators except using receiving arrays or frequency filters. When the noise and the signals are in the same frequency band, the noise can not be totally removed. In our problem, both the noise and the signals are broadband. So how to effectively suppress the noise is what we are interested in.

The noise sources in deep water and in shallow water are not the same.

In deep water, ambient noise sources include tides and hydrostatic effects of waves, seismic disturbances, oceanic turbulence, ship traffic, surface waves and thermal noise, etc.

The tides may generate noise with very low frequency, in the pressure spectrum of frequencies corresponding to 1 or 2 cycles/day. Such pressure changes are far below the frequencies of interest in underwater sound and are restricted to narrow regions of the spectrum. [9]

Surface waves are also a source of hydrostatic pressure changes at a depth in the sea. However, the pressure amplitude falls off rapidly with increasing depth and with decreasing wavelength of the surface waves. The attenuation is extremely rapid with increasing

depth. In shallow water, however, the depth may not be great enough to completely eliminate the pressure effects of waves passing over a bottomed hydrophone; in such instances, the rough surface can become the dominant source of the low-frequency background of a pressure-sensitive hydrophone.

Seismic disturbance is likely an important cause of low-frequency noise in the sea. Microseismis has a nearly regular periodicity of about 1/7 Hz and a vertical amplitude on land of the order of 10^{-4} cm. It is roughly of the same level as that measured as the ambient noise pressures at frequencies below 1 Hz. In addition, intermittent seismic sources such as individual earthquakes and distant volcanic eruptions are undoubtedly transient contributions to the low-frequency background of the deep sea.

Oceanic turbulence, in the form of irregular random water currents of large or small scale, is also a probably cause of low-frequency noise.

Distant ship traffic is generated by the traveling ships, it is a dominant source of noise at frequencies around 100 Hz, in the decade of 50Hz to 500 Hz.

Ocean ambient noise is governed by the roughness of the sea surface at higher frequencies. The noise level is correlated with the local wind speed over the measurement hydrophone. In the frequency range from 500 Hz to 25 kHz, the sea surface generates the major portion of the ambient noise through some processes such as breaking white caps, flow noise, cavitation, wave-generating action of the wind on the surface of the sea, and, second-order effect of sea-surface wave motion.

Thermal noise of the molecules of the sea places a limit on hydrophone sensitivity at high frequencies.

In shallow waters, such as in coastal water and in bays and harbors, the noise sources are highly variable, both from time to time and from space to space. However, at a given frequency in shallow water the noise background is the mixture of three different types of

noise: (1) shipping and industrial noise, (2) wind noise, and (3) biological noise. At a particular time and space, the "mix" of these sources will determine the noise level, and because the mix is variable with time, the existing noise levels will exhibit considerable variability from time to time and from space to space. At bays and harbors, the man-made noises of industrial activity and the noises produced by marine life and by the turbulence of tidal currents all conspire to create a noisy ambient environment.

In coastal waters, such as the continental shelves, wind speed appears to determine the noise level over a wide frequency range. The various processes by which the wind conceivably generates noise - hydrostatic effects of wind-generated waves, whitecaps, and direct sound radiation from the rough sea surface - all play a part in determining the level of the noise in seashore locations.

When shipping and biological noise sources are absent, and when wind noise is sole contributor to the background, the shallow-water noise levels depend only on wind speed, and are independent of hydrophone depth, water depth, and other site characteristics. On the other hand, when shipping or other man-made noises exist, or when biological organisms contribute to the noise background, shallow water is a noisy and exceedingly variable environment for most sonar operations.

In a dynamic, active area where shipping creates an important and changeable form of environmental noise pollution, the standard deviation of a series of noise levels as measured over a period of time is relatively large. On the other hand, at higher frequencies and in the absence of biological noises, the variability of the wind speed during the observation period is an important factor.

Intermittent sources of ambient noise include biological sounds, twenty-cycle pulses, rain and explosions. For other sonar applications, the noise of fish and other forms of life in the sea is an annoying, though readily identified, hindrance to sonar operations and

forms an erratic and, in large part, unpredictable part of the ambient background in which the sonars must operate.

Falling rain may be expected to increase ambient noise levels to an extent depending on the rate of rainball and perhaps on the area over which the rain is falling. The spectrum of the noise of heavy rain is nearly white between 1 and 10kHz.

The simplest possible noise model of the ocean is an infiinte layer of uniform water with a plane surface along which the sources of noise are uniformly distributed. With this elemental model, one could predict the ambient-noise level to be independent of depth, except for frequencies above about 10 kHz, where absorption would cause the level to decrease with increasing depth.

Ambient noise has a complex Gaussian field distribution at moderate depths. This is consistent with the view that the noise originates through a great many sources of random amplitude and phase. Although ambient noise is Gaussian over short time periods, it is clearly non-stationary over long time periods because of the variability of the sources of noise.[9]

3.2 Maximum likelihood parameter estimation

Problems of statistical estimation deal with deriving parameters of quantities that can be observed. These problems may deal with finding the parameters for the model of a signal from direct measurements of that signal or for estimating one signal from another (say a clean transmitted signal from a received noisy and distorted one).

Maximum likelihood parameter estimation is a very important method in this area. The problem of parameter estimation can be thought of having observations of a random variable described by a probability density function of some known form, but with a parameter whose value is unknown. The density function is thus denoted by $f_{x;\theta}(x;\theta)$.

For a given fixed set of observations, say $x = x_0$, the maximum likelihood estimate of the parameter is the value θ that maximizes $f_{x;\theta}(x_0;\theta)$. This value or estimate of θ will be denoted by $\hat{\theta}_{ml}$, where $\hat{\theta}_{ml}$ is a function of the data x_0.

When $f_{x;\theta}(x;\theta)$ is viewed as a function of θ, it is known as the likelihood function. The maximum likelihood estimate of a parameter maximizes the likelihood function. If the likelihood function is continuous, and the maximum does not occur at boundary, then the maximum likelihood estimate for a real scalar parameter θ can be found through either the necessary conditions

$$\frac{\partial}{\partial\theta} f_{x;\theta}(x;\theta)\Big|_{\theta = \hat{\theta}_{ml}} = 0 \tag{3.1}$$

or

$$\frac{\partial}{\partial\theta} \ln f_{x;\theta}(x;\theta)\Big|_{\theta = \hat{\theta}_{ml}} = 0 \tag{3.2}$$

These equations are sometimes referred to as the likelihood equation and the log likelihood equation, respectively. The log likelihood equation follows from the likelihood equation because the logarithm is a strictly monotonic increasing function. This form is convenient in many problems where the likelihood function involves an exponential, such as Gaussian distribution. For vector parameters $\underline{\theta}$ the corresponding likelihood and log likelihood equations involve setting the gradient or vector of derivatives with respect to all components of the parameter vector to zero.

The maximum likelihood estimate for a parameter θ can be written as

$$\hat{\theta}_{ml}(x) = \arg max f_{x;\theta}(x;\theta) \tag{3.3}$$

It is clear that the estimate is a function of the observations. Moreover, since the observations are a random vector, the estimate itself is a random variable and has a mean, cova-

riance, density function, and so on. Not all estimates are maximum likelihood estimates. The estimate for the mean of a Gaussian random signal

$$\hat{m}_x = \frac{1}{N} \sum_{n=0}^{N} x[n] \tag{3.4}$$

is a maximum likelihood estimate.

An estimate $\hat{\theta}_N$ is unbiased if

$$E\{\hat{\theta}_N\} = \theta \tag{3.5}$$

Otherwise the estimate is biased with bias $b(\theta) = E\{\hat{\theta}_N\} - \theta$. An estimate is asymptotically unbiased if

$$\lim_{N \to \infty} E\{\hat{\theta}_N\} = \theta \tag{3.6}$$

Maximum likelihood estimation is asymptotically unbiased.[10]

An estimate $\hat{\theta}_N$ is consistent if

$$\lim_{N \to \infty} Pr[\left|\hat{\theta}_N - \theta\right| < \varepsilon] = 1 \tag{3.7}$$

for any arbitrarily small number ε. The sequence of estimates $\{\hat{\theta}_N\}$ is said to converge in probability to the parameter θ.

An estimate $\hat{\theta}_N$ is said to be efficient with respect to another estimate $\hat{\theta}'$ if the difference of their covariance matrices $\underline{C}_{\hat{\theta}'} - \underline{C}_{\hat{\theta}}$ is positive definite ($\underline{C}_{\hat{\theta}'} - \underline{C}_{\hat{\theta}} > 0$). This implies that the variance of every component of $\hat{\theta}$ must be smaller than the variance of the corresponding component of $\hat{\theta}'$. If $\hat{\theta}_N$ is unbiased and efficient with respect to $\hat{\theta}_{N-1}$ for all N, then Θ_N is a consistent estimate.

The Chebychev inequality states that

$$Pr[\left|\hat{\theta}_N - \theta\right| \geq \varepsilon] \leq \frac{Var(\hat{\theta}_N)}{\varepsilon^2} \tag{3.8}$$

Thus, if the variance of $\hat{\theta}_N$ decreases with N, the probability is that $\left|\hat{\theta}_N - \theta\right| \geq \varepsilon$ approaches zero as $N \rightarrow \infty$. In other words, the probability is that $\left|\hat{\theta}_N - \theta\right| < \varepsilon$ approaches one.

The variance of any unbiased estimate can be bounded by the Cramer Rao Bound, which is in the right-hand side of the following inequality:

$$Var[\hat{\theta}] \geq \frac{1}{E\left\{\left(\frac{\partial}{\partial\theta}\ln f_{x;\theta}(x;\theta)\right)^2\right\}} = \frac{1}{-E\left\{\frac{\partial^2}{\partial\theta^2}\ln f_{x;\theta}(x;\theta)\right\}} \tag{3.9}$$

and $E\left\{\left(\frac{\partial}{\partial\theta}\ln f_{x;\theta}(x;\theta)\right)^2\right\}$ is called the Fisher information. The Cramer Rao Bound gives the absolute lower bound for the variance of any unbiased estimator satisfying regularity conditions.[11]

The two alternate expressions on the right-hand side are valid as long as the partial derivatives exist and are absolutely integrable. Maximum likelihood estimation can reach the Cramer Rao Bound asymptotically. Estimators that achieve the Cramer Rao Bound are said to be efficient. For large data size, the ML estimates are asymptotically efficient or consistent.

An estimate satisfying the bound with equality is known as a minimum-variance estimate. It can be shown that if an unbiased minimum variance exists and the maximum likelihood estimate does not occur at a boundary, then the maximum likelihood estimate is that minimum-variance estimate.

3.3 Maximum Likelihood time-domain beamforming

As we just discussed in the previous section, maximum likelihood estimation is an asymptotically optimal method in parameter estimation problems, because it is asymptotically unbiased, and asymptotically reaches the Cramer Rao Bound.

Suppose the noise has a Gaussian distribution with zero mean, $\Psi_n(t) \sim N(0, \sigma^2)$.

Let $\underline{P}(t)$ and $\underline{\underline{Q}}(t)$ are column vectors of the data and replica pressure

$$\underline{P}(t) = \begin{bmatrix} P_1(t) \\ P_2(t) \\ \cdots \\ P_N(t) \end{bmatrix}, \underline{\underline{Q}}(t) = \begin{bmatrix} Q_1(t) \\ Q_2(t) \\ \cdots \\ Q_N(t) \end{bmatrix} \tag{3.10}$$

The probability density function is given by

$$p(\underline{P}(t);\underline{\underline{Q}}(t)) = \frac{1}{(2\pi)^{\frac{N}{2}}|\underline{\underline{C}}|^{\frac{1}{2}}} \exp\left(-\frac{1}{2}[\underline{P}(t) - \underline{\underline{Q}}(t)]^{\dagger} \underline{\underline{C}}^{-1} [\underline{P}(t) - \underline{\underline{Q}}(t)]\right) \tag{3.11}$$

where $\underline{\underline{C}}$ is the covariance matrix, it is defined as

$$\underline{\underline{C}} = \begin{bmatrix} c(\underline{r_1}, \underline{r_1}) & c(\underline{r_1}, \underline{r_2}) & \cdots & c(\underline{r_1}, \underline{r_N}) \\ c(\underline{r_2}, \underline{r_1}) & c(\underline{r_2}, \underline{r_2}) & \cdots & c(\underline{r_2}, \underline{r_N}) \\ \cdots & \cdots & \cdots & \cdots \\ c(\underline{r_N}, \underline{r_1}) & c(\underline{r_N}, \underline{r_2}) & \cdots & c(\underline{r_N}, \underline{r_N}) \end{bmatrix} \tag{3.12}$$

where

$$c(\underline{r_i}, \underline{r_j}) = E[(P_i(t) - Q_i(t))(P_j(t) - Q_j(t))^{\dagger}] \tag{3.13}$$

and the symbol † stands for the conjugate transpose for a complex value.

We want to find those values that maximize the probability density function to get the optimal estimation. Because the probability density function is in exponential form, it is monotonically increasing, we can take natural logarithm and the result is the same.

$$\ln(p(\underline{P}(t);\underline{Q}(t))) = \ln\left\{\frac{1}{(2\pi)^{\frac{N}{2}}|\underline{C}|^{\frac{1}{2}}}\right\} - \frac{1}{2}[\underline{P}(t)-\underline{Q}(t)]^{\dagger}\underline{C}^{-1}[\underline{P}(t)-\underline{Q}(t)] \quad (3.14)$$

Because the first term in the right-hand side is a constant, so the problem of maximizing the logarithm term in the left-hand side becomes to minimize this term

$$[\underline{P}(t)-\underline{Q}(t)]^{\dagger}\underline{C}^{-1}[\underline{P}(t)-\underline{Q}(t)] \quad (3.15)$$

We use this term to define our cost function.

We define energy as

$$E = \int_{-t_J}^{t_J}[\underline{P}(t)-\underline{Q}(t)]^{\dagger}\underline{C}^{-1}[\underline{P}(t)-\underline{Q}(t)]dt \quad (3.16)$$

and

$$E_0 = \sum_{n=1}^{N}\int_{-t_J}^{t_J}\Psi_n^{\,2}(t)dt \quad (3.17)$$

where $-t_J$ and t_J are the observation starting and ending time index. In the computation, it turns out to be

$$E = \sum_{j=1}^{N}\left(\sum_{i=1}^{N}A_{ij}(P_i(t)-Q_i^{*}(t))(P_j(t)-Q_j(t))\right) \quad (3.18)$$

where A_{ij} is the element on the ith row and the jth column of the inverse of the covariance matrix $\underline{C}$.

In temporally uncorrelated noise, minimizing E leads to the maximum likelihood time-domain beamformer. The physical significance of this method is that we are, in effect, choosing the value of the parameter of interest which most likely caused the given observed signals to occur.

E_0 is the value of E for $q_m(t) = p_m(t)$ and $\sigma_m = \tau_m$. If noise is present, E_0 is not necessarily the minimum of E because the optimal time-domain beamformer is degraded as the test time series attempt to cancel both the signal and the noise.

For independent identically distributed random noise, the covariance matrix is diagonal, i.e., $\underline{C} = \sigma^2 \underline{I}$, the correlation matrix is the identity matrix, then

$$E = \sigma^2 \sum_{n=1}^{N} \int_{t_J} [P_n(t) - Q_n(t)]^2 dt \tag{3.19}$$

This is Least Squares Estimation. Since σ^2 is a constant, we can define E as

$$E = \sum_{n=1}^{N} \int_{t_J} [P_n(t) - Q_n(t)]^2 dt \tag{3.20}$$

It is a special case of Maximum Likelihood Estimation, when noise data are completely uncorrelated. In this case, the maximum likelihood estimation and the least squares estimation get the same result.

Chapter 4

Fast Simulated Annealing Algorithm

4.1 Simulated annealing algorithms

Simulated annealing refers to a class of numerical algorithms. It imitates the slow cooling (annealing) process of a substance to obtain a crystalline or glass-like state. The cooling process of an annealing procedure is usually done very slowly so that the number of defects in the crystal structure is reduced, and the potential energy stored in the molecular structure is minimized.[7] Simulated annealing was originally suggested by Metropolis in 1953. But it was in 1980s, simulated annealing algorithms were developed successfully in many diverse applications in numerical optimization such as, optimizing VLSI layout and routing problems arising in the design of computer systems, travelling salesman problem, image restoration of noisy blurred images, and communications code design.

In numerical analysis, simulated annealing has been employed successfully in various optimization algorithms. Generally, an optimization problem is to maximize (or minimize) an objective cost function of many variables. These variables can be analogies to the molecules of a dynamical system, and the objective cost function maybe identified with the potential energy of the system. Simulated annealing seeks to maximize (or minimize) this potential energy by defining an appropriate temperature for the system. This temperature is slowly reduced over time, and the function variables will tend to settle in a low energy configuration.

Simulated annealing has also been applied to optimization problems arising in estimation theory and signal processing. An annealing algorithm for finding the maximum likelihood estimates for a set of model parameters from noisy data measurements is described

in this thesis. This fundamental problem arises in many areas including spectral analysis, signal detection, image processing, and sensor array processing, which is the application considered in this thesis.

Now we are going to describe a fairly general simulated annealing algorithm that could be applied to a variety of unconstrained optimization problems.

Simulated annealing is a form of stochastic optimization that is based on the Boltzman statistical properties of large numbers of molecules (variables) in thermal equilibrium. One of its most important features is that it can escape from local stationary points in the cost function. This allows the algorithm to proceed to find a globally optimal solution.

Let $f(\underline{\theta})$ be a cost function that is to be maximized, where $\underline{\theta}$ is a column vector of parameters to be found. The problem is to find a set of optimal parameters $\underline{\theta}_{opt}$ that yields a global maximum of the cost function, or one of the maxima if the objective function has several identically valued global maxima.

We define the energy E to be the objective cost function,

$$E = f(\underline{\theta}) \tag{4.1}$$

The algorithm involves an artificial quantity called the system temperature, denoted by T_k.

The algorithm is started with an initial guess at the optimal parameters $\underline{\theta}_0$. Let $\{\underline{\theta}_k, k = 0, 1, 2, \ldots\}$ be a sequence of estimates of the function parameters produced by the simulated annealing procedure, and let E_k be the corresponding energies due to these parameters, i.e.,

$$E_k = f(\underline{\theta}_k) \tag{4.2}$$

At the kth iteration, a random change to the parameters, $\Delta\underline{\theta}_k$, is proposed, and the energy E_k' associated with these new parameters is computed. This random change to the

current parameters is chosen according to a certain generating probability density function, which will normally be dependent on the system temperature. The change, ΔE_k, in the energy arising from these new parameters is also evaluated,

$$\Delta E_k = E_k' - E_k \tag{4.3}$$

This energy change may be negative, indicating that the new parameters lead to a reduction to the cost function. If the energy change is positive, the new parameters are always accepted, and the algorithm continues to choose another set of parameters. If on the other hand the change is negative, and the cost has reduced, then the new parameters are accepted stochastically, with a certain probability called the acceptance probability. The acceptance probability distribution is a function of both the magnitude of the energy change and the system temperature.

The procedure of choosing new parameters and stochastic acceptance is continued for several iterations, and then the system temperature is reduced according to the annealing schedule. By making the acceptance probability a monotonic decreasing function of temperature, then, as the temperature is reduced, the probability of accepting downward changes in the cost function is also reduced, and if the generating and accepting probabilities are chosen correctly, the algorithm will tend to settle in maximum energy states. Note that the algorithm can accept both increases and decreases in the cost function and it is this feature that allows escape from local stationary points.

Geman and Geman have discussed convergence properties of the simulated annealing algorithm when a Boltzman acceptance probability function is used.[12] The probability of accepting lower cost is,

$$Pr = \exp\left(-\frac{\Delta E_k}{T_k}\right) \tag{4.4}$$

It was also shown that in this case, that if the annealing schedule has the inverse logarithmic form,

$$T_k = \frac{T_0}{\log(1+k)}. \tag{4.5}$$

where T_0 is an appropriate initial temperature, convergence will occur in infinite time, but no guarantee are made for finite time.

Simulated annealing is a Monte Carlo optimization technique in which the temperature (an artificial control parameter) is gradually lowered until a nearly perfect crystal (the global minimum of the ambiguity function) is obtained. The cooling process consists of a Markov process in which each step involves randomly perturbing the parameters, evaluating an energy (ambiguity) function, and testing if the energy is lowered. When we use equation (3.16) or (3.20) as the energy function, if the energy is lowered, the perturbation is accepted; if the energy is raised, the perturbation is accepted according to a Boltzman probability distribution to allow escape from local minima.

The analogy between the thermodynamics of annealing and large combinatorial optimization problems is useful for developing and understanding simulated annealing algorithms. For example, the concept of critical temperature is central to simulated annealing. The most general simulated annealing algorithm converges asymptotically to an optimal solution if the initial temperature is sufficiently high and the temperature decreases inverse logarithmically with the number of iterations.

Simulated annealing has been applied to narrow-band beamforming in the presence of noise and to various other problems. Since the advantages of simulated annealing are the greatest for the problems involving a large number of parameters, the method should be most useful for time-domain problems in which source bearings and time series are unknowns.

4.2 Fast simulated annealing algorithm

A fast simulated annealing algorithm that could converge with an inverse linear cooling schedule by occasionally allowing relatively large perturbations was developed in [13]. It leads to significantly improved convergence rates compared with classical annealing algorithms such as in the inverse logarithmic form. The fast simulated annealing algorithm employs a Cauchy generating density and a Boltzman acceptance probability. Under these conditions the annealing schedule follows an inverse law instead of an inverse logarithmic law, i.e.,

$$T_k = \frac{T_0}{1+k} \tag{4.6}$$

However, convergence is not guaranteed even in infinite time. The fast simulate annealing schedule uses a Cauchy density for the generation of new candidate parameter estimates. The density has the following functional form,

$$d_{\underline{\theta}}(\underline{\Theta}) = \frac{\alpha T}{(|\underline{\Theta}|^2 + \alpha T^2)^{(N+1)/2}} \tag{4.7}$$

where α is a scalar parameter that controls the width of the density, and N is the number of the parameters to be found. The generating probability is a function of temperature, at high temperatures the density has a wide spread and new parameters are essentially chosen at random, while at lower temperatures a more local sampling takes place.

The probability of accepting the lower cost is given by the Boltzman distribution,

$$Pr = \frac{1}{1+\exp\left(-\frac{\Delta E_k}{T_k}\right)} \tag{4.8}$$

The acceptance probability tends to zero as the temperature tends towards zero. Thus, at low temperatures the algorithm only accepts increases in the cost function. At higher tem-

peratures both increases and decreases can be accepted, which allows the algorithm to escape from local maxima.

In this thesis, a time-domain signal processing method for bearing and time series estimation is applied in simulations. The method is based on a fast simulated annealing algorithm that is analogous to the cooling of a mixture of liquids. The unknown bearings have a higher freezing temperature than the unknown time series, and standard simulated annealing algorithms (which are analogous to the cooling of a pure substance) are not effective because the bearings freeze out of the mixture as separate (imperfect) crystals.

Simulated annealing algorithms consist of a sequence of iterations involving random perturbations of the unknown parameters. The perturbations are influenced by an artificial control parameter, the temperature T, which decreases slightly after each iteration. All perturbations that produce decreases in E are accepted (i.e., the test parameters are modified) at all values of T. Perturbations that produces increases in E are accepted with a probability that decreases with T (a random number generator is used to determine whether or not to accept the perturbations). Since E must be computed many times, it is important to have a means for computing E efficiently.

We use equation (3.16) and (3.20) as our energy functions. We work with dimensionless variables, where the sound speed is unity. Hydrophone data is assumed to be available at $t = t_j = j\Delta t$ for $-J \le j \le J$ and E is evaluated numerically over $(-t_J, t_J)$. The test time series values $q_{m,j} = q_m(t_j)$ are initialized with zeros, and the test delays are also initialized with zeros. The control parameter T is initially assigned the value T_0, and $T = \frac{T_0}{i}$ at the ith iteration, which involves randomly perturbing the test parameters in two steps.

For the first step, only the values of the time series are perturbed. The perturbed value for the jth value of the mth time series is

$$q_{m,\,j} = \begin{cases} q_{m,\,j} - \Delta q & if \quad \chi_q(m,\,j) \le \frac{1}{2} \\ q_{m,\,j} + \Delta q & if \quad \chi_q(m,\,j) > \frac{1}{2} \end{cases} \tag{4.9}$$

where the random numbers $\chi_q(m,\,j)$ are selected uniformly from (0,1) at each iteration. The grid size Δq for the time series discretization is small relative to the maximum of $|P_n(t)|$ over n and t. Thus only small perturbations are allowed for the time series. The energy change due to this perturbation is

$$\Delta E = E(q'_{m,\,j}) - E(q_{m,\,j}) \tag{4.10}$$

If $\exp\left(-\frac{\Delta E}{T}\right) > \varphi_q(m,\,j)$, the perturbation is accepted and $q_{m,\,j}$ is replaced by $q'_{m,\,j}$, where the random numbers $\varphi_q(m,\,j)$ are selected uniformly from the interval (0,1) at each iteration. In particular, the perturbation is accepted if $\Delta E < 0$ (i.e., lower energy states are always accepted).

In this step, because the n th hydrophone acoustic pressure $P_n(t)$ is a linear function of the source pressures $p_m(t)$,

$$P_n(t) = \sum_{m\,=\,1}^{M} p_m(t - \tau_m) + \Psi_n(t) \tag{4.11}$$

when we take partial derivative with respect to $p_m(t)$ and set it to zero to get the minimum values, we can see that there's only one global minimum in the energy function, the perturbation is accepted only when energy is lowered. There's no problem of ecsaping the local minima.

$$\frac{\partial}{\partial p_m} P_n(t) = 0 \tag{4.12}$$

One the other hand, because $P_n(t)$ is a non-linear function of the time delays τ_m, when we take derivative with respect to τ_m and set it to zero to get the minima, there might exist more than one minima,

$$\frac{\partial}{\partial \tau_m} P_n(t) = 0 \tag{4.13}$$

Thus, the algorithm must have the ability to escape from the local minima and converge to the global minima.

One of the keys to the usefulness of a simulated annealing algorithm is to be able to compute ΔE efficiently. Since the time series perturbations result in local perturbations of the Q_n, most of the terms in the sums representing in integrals in $E(q'_{m,j})$ are identical to terms in the sums representing the integrals in $E(q_{m,j})$. Thus it is possible to compute ΔE efficiently by summing a relatively small number of terms.

For the second step, the time delays are perturbed for one source at a time. The perturbed value of the m th time delay is

$$\sigma_m' = min(h, max(-(h, \sigma_m + h\chi_\sigma^3(m)))) \tag{4.14}$$

where the random numbers $\chi_\sigma(m)$ are chosen uniformly from the interval (-1,1) at each iteration and h is the hydrophone spacing. Thus large perturbations in the time delays are possible, but small perturbations are more likely to occur. The energy change due to this perturbation is

$$\Delta E = E(\sigma_m') - E(\sigma_m) \tag{4.15}$$

If $\exp\left(-\frac{\Delta E}{T}\right) > \varphi_\sigma(m)$, the perturbation is accepted and σ_m is replaced by σ_m', where the numbers $\varphi_\sigma(m)$ are selected uniformly from the interval (0,1) at each itera-

tion. This process is repeated at each iteration for $m = 1, 2, \ldots, M$. It is not possible to compute ΔE as a perturbation for this step. However, this does not seriously degrade efficiency because it is necessary to compute ΔE only M times for this step (as opposed to $2 \times J \times M$ times for the first step).

Like the original fast simulated annealing algorithm, this algorithm performs well with a linear cooling schedule because large perturbations are occasionally allowed for the time delays. Thus the time delays appear to be more important than the values of time series in some sense. The importance of the delays is apparently analogous to the fact that compounds with different freezing temperatures crystallize separately from a mixture.

Chapter 5

Simulation Results

In this chapter, some simulation results in different cases are given.

In section 5.1, the noise is spatially correlated Gaussian noise. In subsection 5.1.1, the diagonal elements of the covariance matrix are inhomogeneous. A single source is propagating in the medium, it could be an impulse, short pulse, long pulse, sinusoidal signal with different frequencies, and a general broadband signal - a sinusoidal signal with exponential attenuation. An array of 3 hydrophones is employed for this case. In subsection 5.1.2, the diagonal elements of the covariance matrix are homogeneous. In this case, both single source and multi-source are used. The single source takes the form of a broadband signal and a multi-impulse. An array of 3 hydrophones is used. For the multi-source case, 3 broadband signals are estimated by an array of 5 hydrophones and an array of 25 hydrophones, respectively.

In section 5.2, the noise is surface generated noise in a ocean waveguide. The waveguide is bounded above by a pressure release surface and below by a pressure release bottom.

In section 5.1 and 5.2, both maximum likelihood estimation and least squares estimation are employed to estimate the time series and the bearings. The results show that the maximum likelihood estimation gets better results than the least squares estimation in all cases.

In section 5.3, the noise is spatially uncorrelated noise. This is a special case. For this case, because the covariance matrix is reduced to a diagonal matrix, the maximum likelihood estimation and the least squares estimation get the same result.

In all of these cases, the noise is uncorrelated in time.

We use the standard deviation of the difference between the resulting estimated test time series and the real signal to analysis the performance of the quality of the beamforming.

For example, when only one signal is present, the acoustic pressure measured at the n th sensor is:

$$P_n(t) = p(t - n\tau) + \Psi_n(t) \tag{5.1}$$

The replica pressure at the n th sensor is

$$Q_n(t) = q(t - n\sigma) \tag{5.2}$$

where $Q_n(t)$ are the estimations of $P_n(t)$. The variance between them is

$$var(P_n(t) - Q_n(t)) = \frac{1}{N}\sigma^2 \tag{5.3}$$

and the standard deviation is

$$std(P_n(t) - Q_n(t)) = \frac{1}{\sqrt{N}}\sigma \tag{5.4}$$

Thus the smaller the standard deviation, the better the performance of the estimator.

5.1 In spatially correlated Gaussian noise

In this section, we work with dimensionless variables. Suppose the sound velocity $c = 1$ and the hydrophone spacing $h = 20$. In subsections 5.1.1.1, 5.1.1.2, 5.1.1.4 (5.1.1.4.1, 5.1.1.4.2, 5.1.1.4.3), 5.1.2.1, 5.1.2.2, and 5.1.2.3 (5.1.2.3.1, 5.1.2.3.2), the source signals are broadband. In subsection 5.1.1.3, the source signal is narrow band.

5.1.1 The diagonal elements of the covariance matrix are inhomogeneous

The noise is a correlated Gaussian random process in space, but uncorrelated in time.

The noise is generated by the following process. Suppose $x_1(t)$, $x_2(t)$ and $x_3(t)$ are random processes with Gaussian distribution, and they are independent. Let

$$\underline{X(t)} = \begin{Bmatrix} x_1(t) \\ x_2(t) \\ x_3(t) \end{Bmatrix} \tag{5.5}$$

and

$$\underline{Y(t)} = \begin{Bmatrix} y_1(t) \\ y_2(t) \\ y_3(t) \end{Bmatrix} \tag{5.6}$$

$\underline{Y(t)}$ is a linear combination of $\underline{X(t)}$, and is given by

$$\underline{Y(t)} = \underline{A}\,\underline{X(t)} \tag{5.7}$$

where

$$\underline{A} = \begin{bmatrix} a & b & d \\ b & a & b \\ d & b & a \end{bmatrix} \tag{5.8}$$

In this case, $x_1(t)$, $x_2(t)$ and $x_3(t)$ have Gaussian distribution: $x_1(t) \sim N(0, 1)$, $x_2(t) \sim N(0, 1)$, $x_3(t) \sim N(0, 10000)$. The diagonal elements of the covariance matrix are inhomogeneous.

$$y_1(t) = ax_1(t) + bx_2(t) + dx_3(t) \tag{5.9}$$

$$y_2(t) = bx_1(t) + ax_2(t) + bx_3(t) \tag{5.10}$$

$$y_3(t) = dx_1(t) + bx_2(t) + ax_3(t) \tag{5.11}$$

where $y_1(t)$, $y_2(t)$ and $y_3(t)$ are linear combinations of $x_1(t)$, $x_2(t)$ and $x_3(t)$, therefore, they also have Gaussian distributions. Because $x_1(t)$, $x_2(t)$ and $x_3(t)$ are independent random processes, we have the mean values

$$\mu_{y_1} = a\mu_{x_1} + b\mu_{x_2} + d\mu_{x_3} = 0 \tag{5.12}$$

$$\mu_{y_2} = b\mu_{x_1} + a\mu_{x_2} + b\mu_{x_3} = 0 \tag{5.13}$$

$$\mu_{y_3} = d\mu_{x_1} + b\mu_{x_2} + a\mu_{x_3} = 0 \tag{5.14}$$

and the variance

$$\sigma^2_{y_1} = a^2\sigma^2_{x_1} + b^2\sigma^2_{x_2} + d^2\sigma^2_{x_3} = a^2 + b^2 + 10000d^2 \tag{5.15}$$

$$\sigma^2_{y_2} = b^2\sigma^2_{x_1} + a^2\sigma^2_{x_2} + b^2\sigma^2_{x_3} = b^2 + a^2 + 10000b^2 \tag{5.16}$$

$$\sigma^2_{y_3} = d^2\sigma^2_{x_1} + b^2\sigma^2_{x_2} + a^2\sigma^2_{x_3} = d^2 + b^2 + 10000a^2 \tag{5.17}$$

and the covariance

$$\sigma^2_{y_1y_2} = E\{(y_1 - \mu_{y_1})(y_2 - \mu_{y_2})\} = E\{y_1y_2\} - \mu_{y_1}\mu_{y_2} = E\{y_1y_2\} \tag{5.18}$$

$$\sigma^2_{y_1y_2} = E\{(ax_1 + bx_2 + dx_3)(bx_1 + ax_2 + bx_3)\} \tag{5.19}$$

$$\sigma^2_{y_1y_2} = abE\left\{x_1^2\right\} + abE\left\{x_2^2\right\} + bdE\left\{x_3^2\right\} \tag{5.20}$$

$$\sigma^2_{y_1y_2} = ab\sigma^2_{x_1} + ab\sigma^2_{x_2} + bd\sigma^2_{x_3} \tag{5.21}$$

For the same reason,

$$\sigma^2_{y_2y_3} = bd\sigma^2_{x_1} + ab\sigma^2_{x_2} + ab\sigma^2_{x_3} \tag{5.22}$$

$$\sigma^2_{y_1y_3} = ad\sigma^2_{x_1} + b^2\sigma^2_{x_2} + ad\sigma^2_{x_3} \tag{5.23}$$

Also, we have

$$\sigma^2_{y_2y_1} = \sigma^2_{y_1y_2} \tag{5.24}$$

$$\sigma^2_{y_3y_2} = \sigma^2_{y_2y_3} \tag{5.25}$$

$$\sigma^2_{y_3y_1} = \sigma^2_{y_1y_3} \tag{5.26}$$

Take $a = 1$, $b = 0.5$ and $d = 0.01$, we have

$$\underline{C} = \begin{bmatrix} 2.25 & 51.0 & 100.26 \\ 51.0 & 2501.25 & 5000.505 \\ 100.26 & 5000.505 & 10000.2501 \end{bmatrix} \tag{5.27}$$

This is the theoretical value. The inverse covariance matrix is

$$\underline{C}^{-1} = \begin{bmatrix} 3.1677 & -3.3979 & 1.6673 \\ -3.3979 & 4.8832 & -2.4077 \\ 1.6673 & -2.4077 & 1.1873 \end{bmatrix} \tag{5.28}$$

The generated noise is shown in figure 5.1.

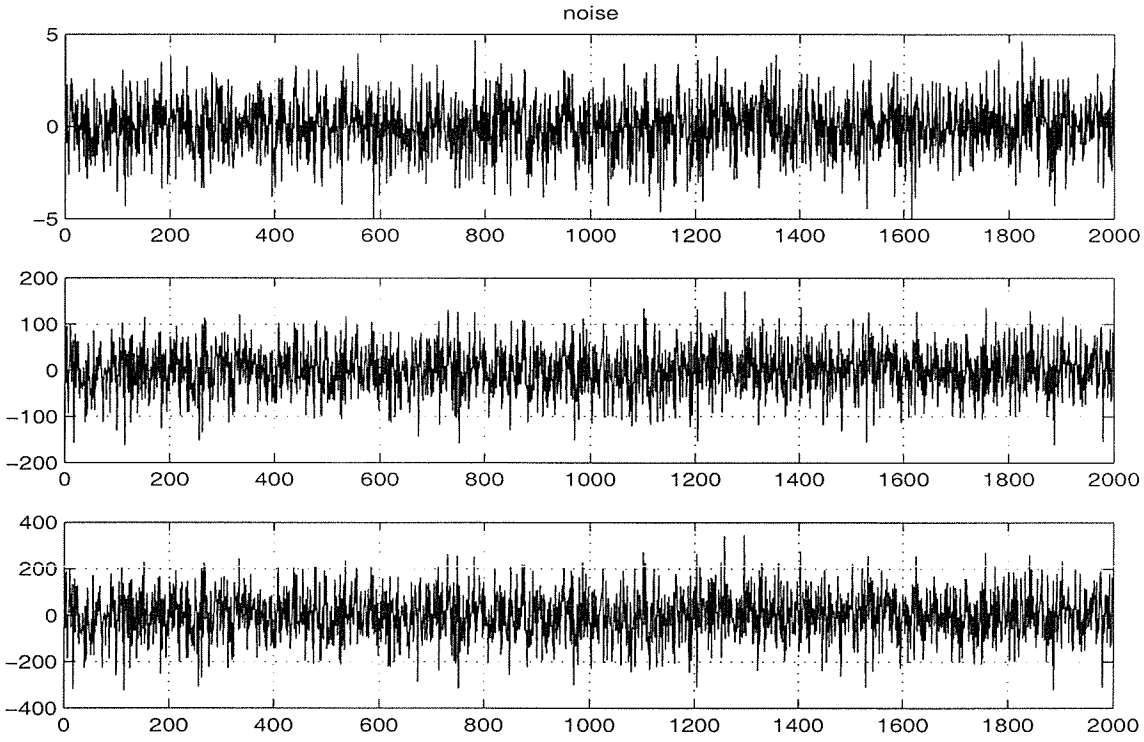

Figure 5.1: The spatially correlated Gaussian noise with different variance

5.1.1.1 Source signal is an impulse

The plane wave source signal is an impulse, shown in figure 5.2.

$$p(t) = A\delta(t) \tag{5.29}$$

The Fourier transform for $p(t)$ is

$$S(\omega) = \frac{1}{2\pi}\int_{-\infty}^{\infty} p(t)e^{-j\omega t}dt \tag{5.30}$$

For this signal, $S(\omega) = \frac{A}{2\pi}$ is a constant for all ω. Thus its bandwidth is $B = \infty$. We have $\frac{c}{2B} \ll L$, which is the length of the array. Therefore the signal is a broadband signal. The amplitude of the signal is $A = 350$, its bearing is $\theta = 20°$.

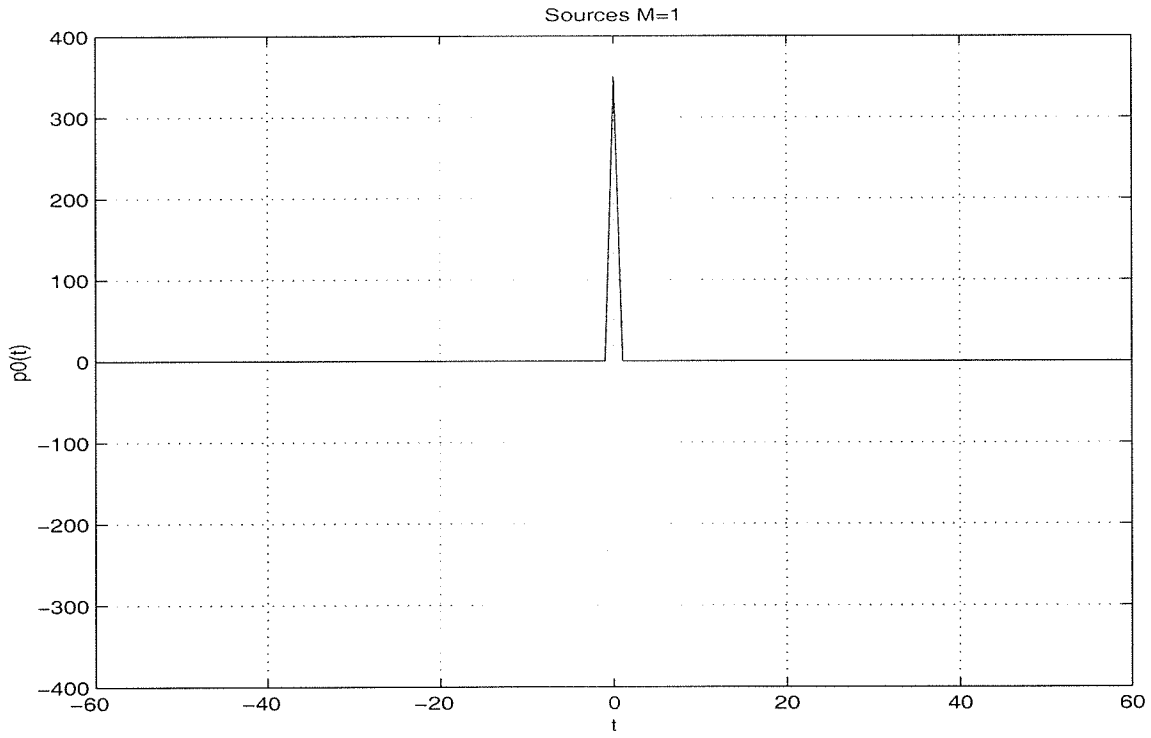

Figure 5.2: Plane wave source signal - an impulse

We use an array of three hydrophones to solve this problem. The length of the array is $L = 40$. The hydrophone data is consisted of signal and noise. The hydrophone data is shown in figure 5.3.

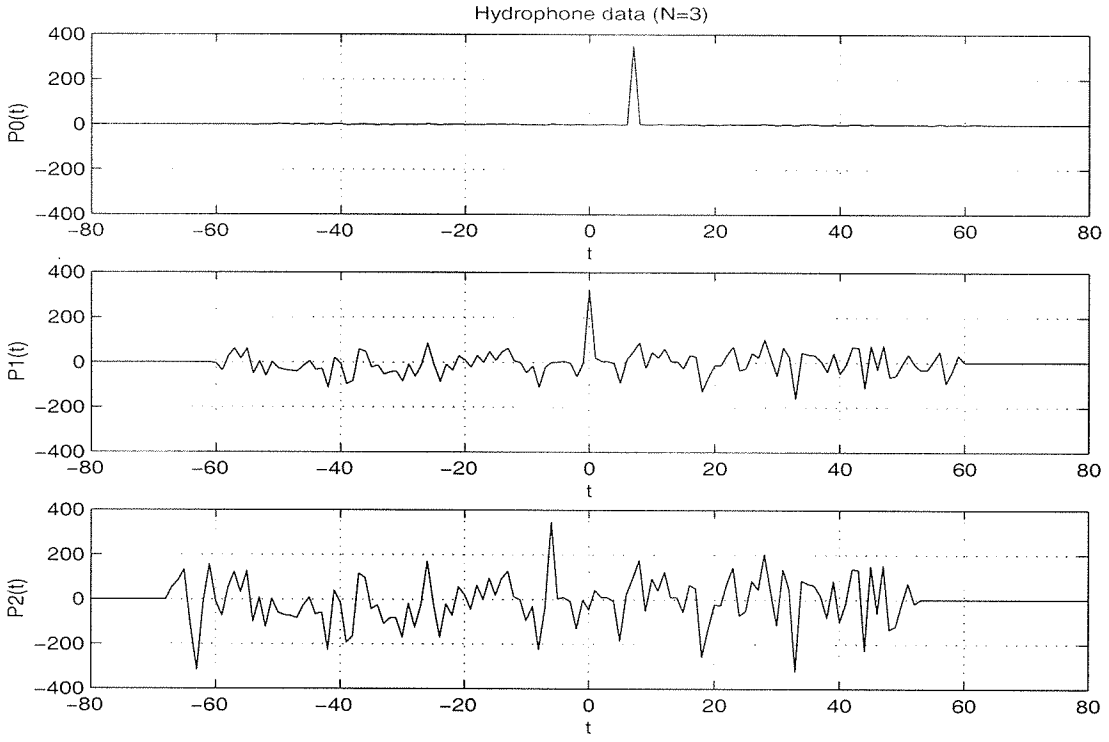

Figure 5.3: Hydrophone data with an impulse signal

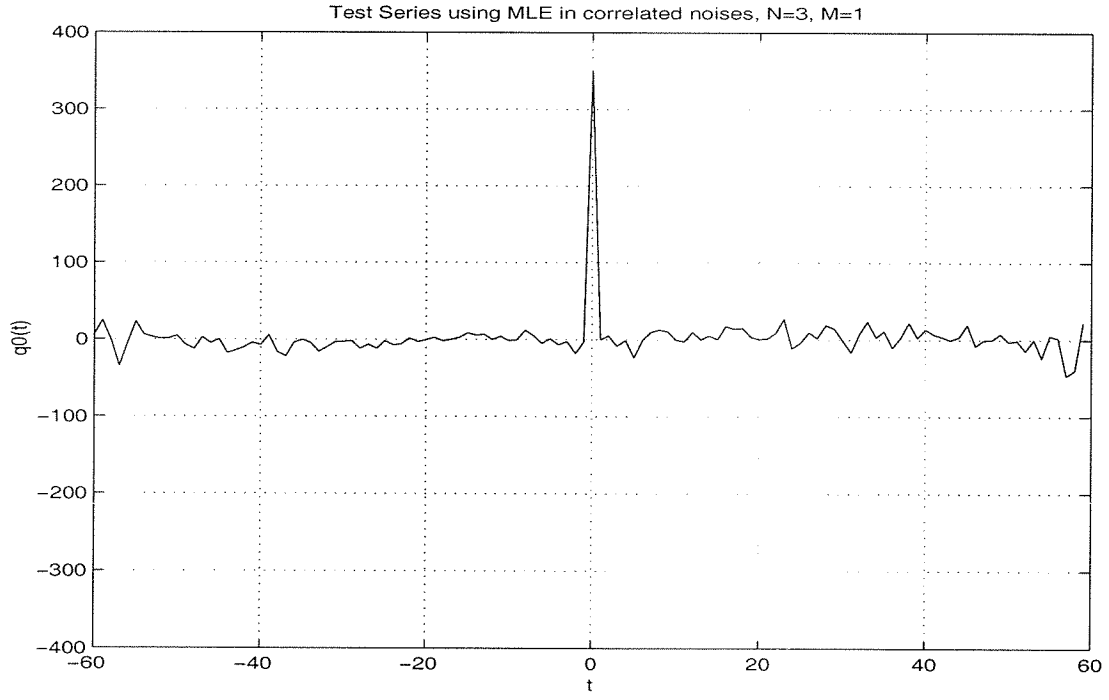

Figure 5.4: MLE result of the impulse source

First, the Maximum Likelihood Estimation method is used. In this case, we take the grid size $\Delta q = 0.5$, the number of iterations $I = 10000$, and initial temperature $T_0 = 5 \times 10^5$. The results are shown as following. The estimation result of the source is shown in figure 5.4.

The standard deviation between the estimation value of the signal and the true signal is $std(p(t) - q(t)) = 11.8752$.

The results of the hydrophone data are shown in figure 5.5.

The MLE result of the bearing is shown in figure 5.6. It's correct, roughly $20°$. The energy is shown in figure 5.7.

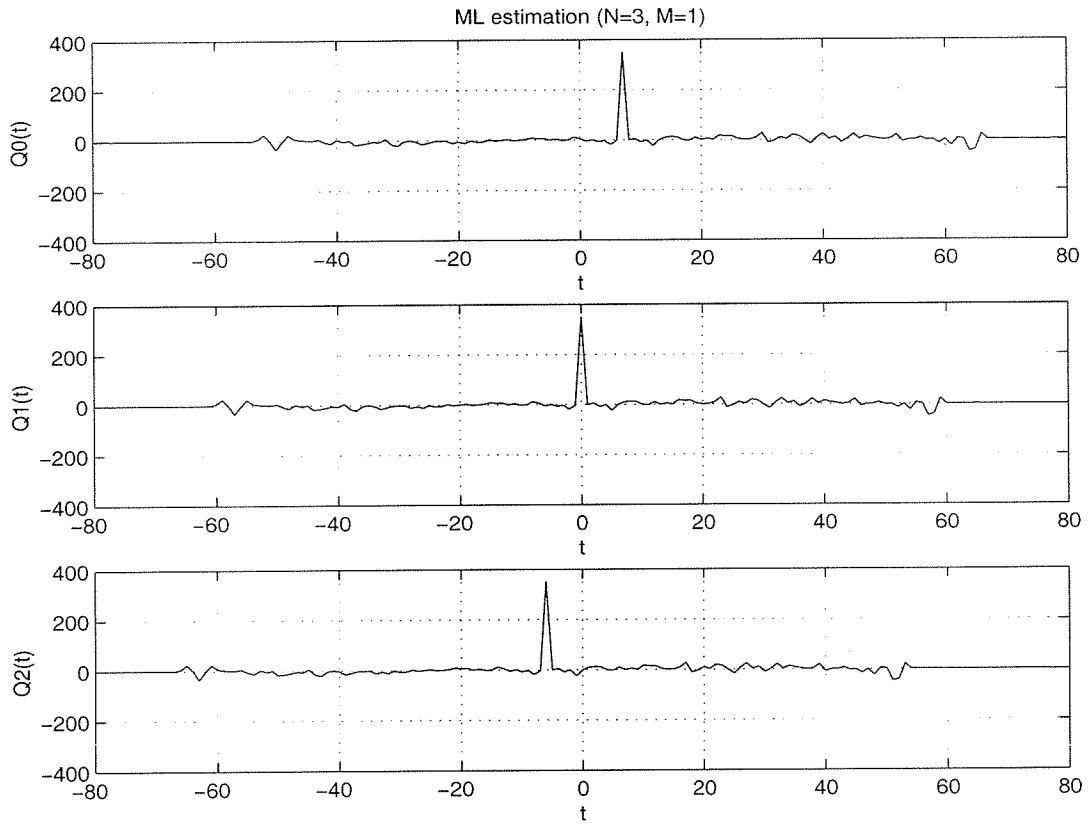

Figure 5.5: MLE result - Hydrophone data

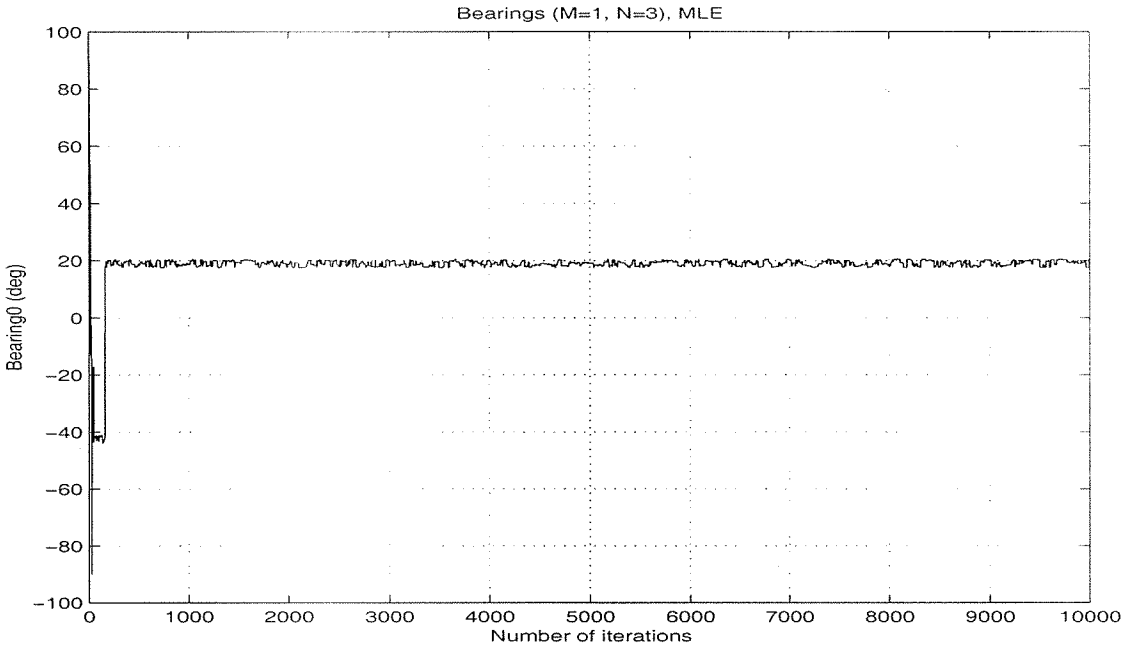

Figure 5.6: MLE result of the bearing

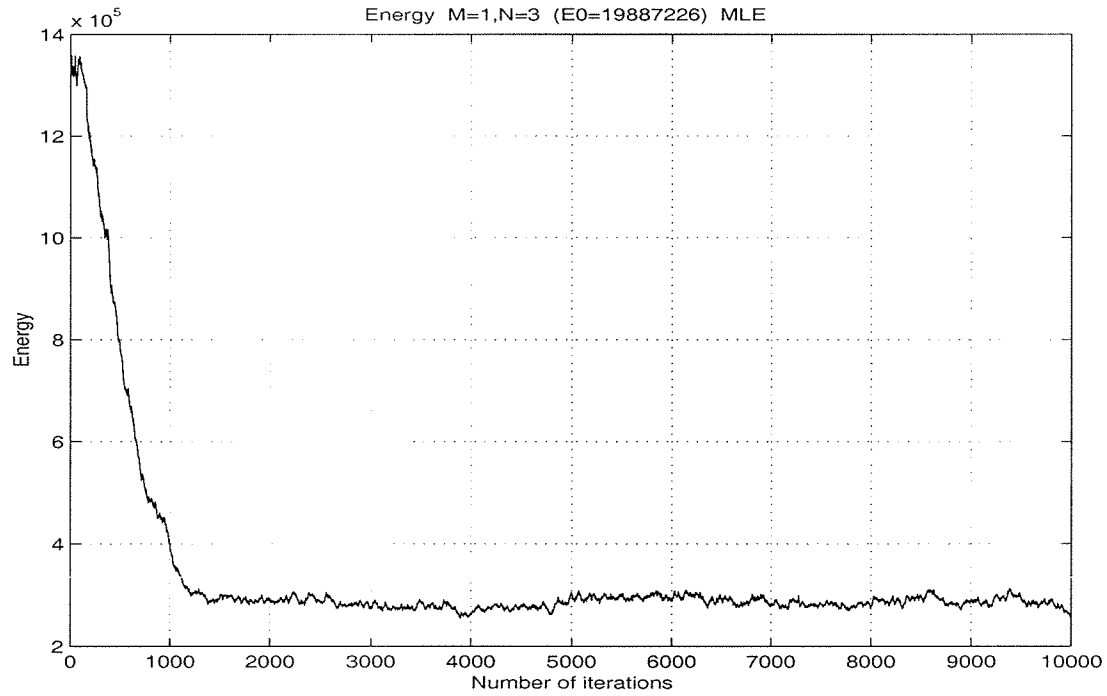

Figure 5.7: Energy

Next, the Least Squares Estimation method is used to work out this problem. Take the grid size $\Delta q = 0.05$, the number of iterations $I = 10000$, the initial temperature $T_0 = 3.75 \times 10^6$. The results are given as followings.

The LSE result of the source is shown in figure 5.8. Unfortunately, the signal can not be found using Least Squares Estimation.

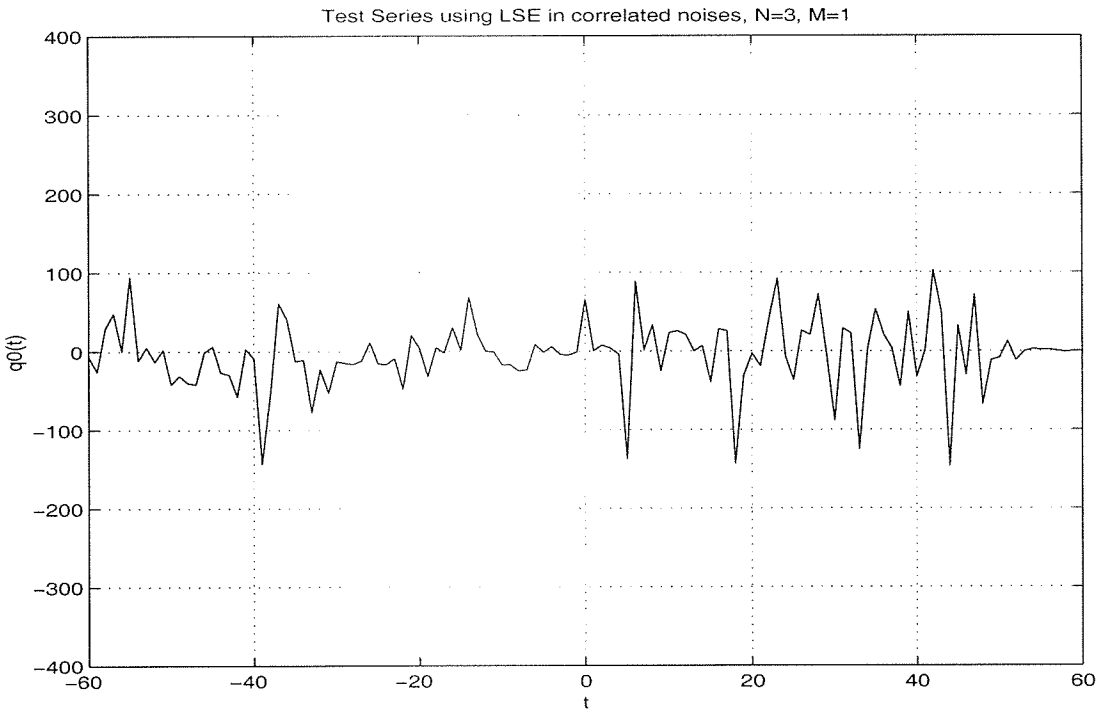

Figure 5.8: LSE result of the impulse signal

The LSE result of the bearing is shown in figure 5.9. The bearing could not be found correctly, either.

5.1.1.2 Source signal is a short pulse

In this case, a short pulse is used as a plane wave signal. It is shown in figure 5.10. The source bearing is $\theta = 20°$. The amplitude is 350. The source equation is

$$p(t) = 350(u(t+10) - u(t-10)) \tag{5.31}$$

The product of the time window interval and the sound velocity is 20, it is less than the length of the array 40, so it is a broadband signal.

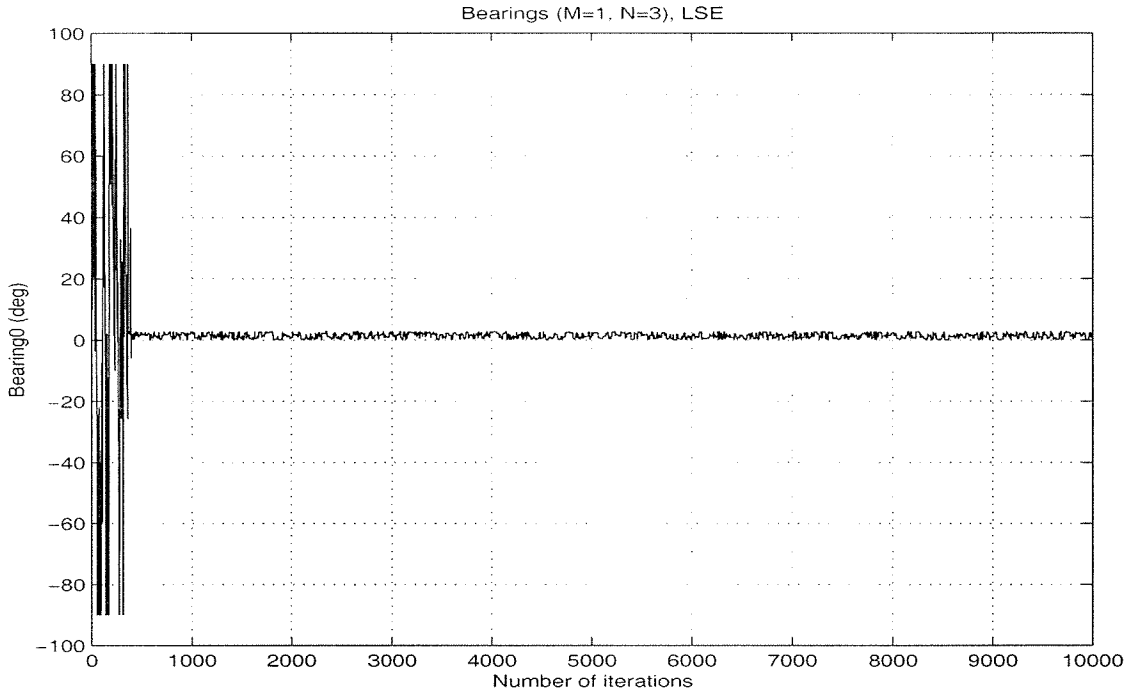

Figure 5.9: LSE result of the bearing

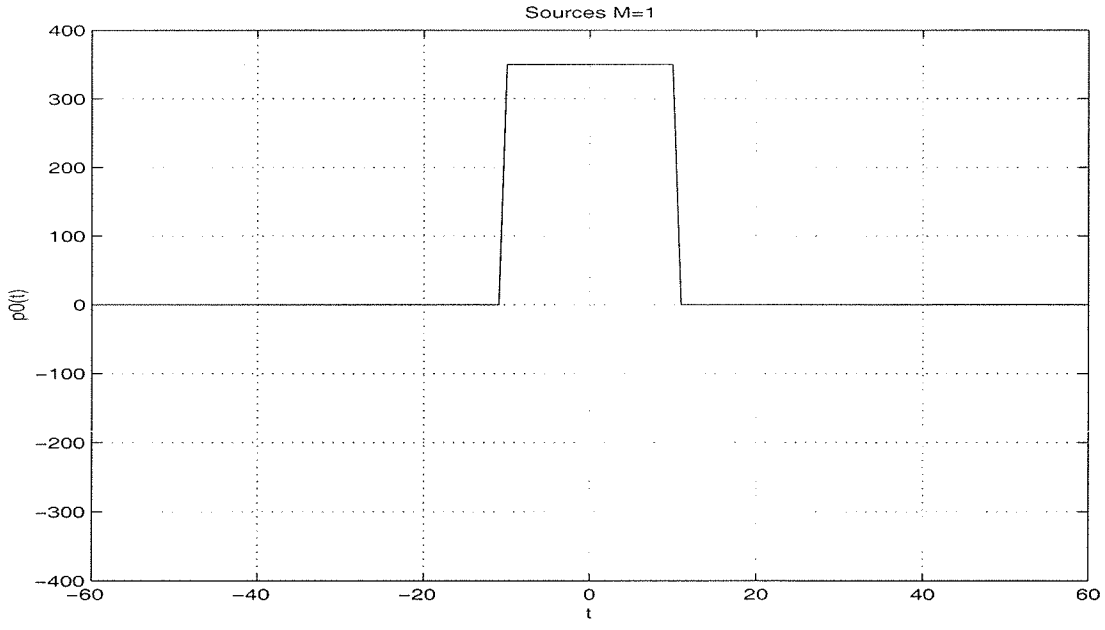

Figure 5.10: Source is a short pulse

The hydrophone data are given in figure 5.11.

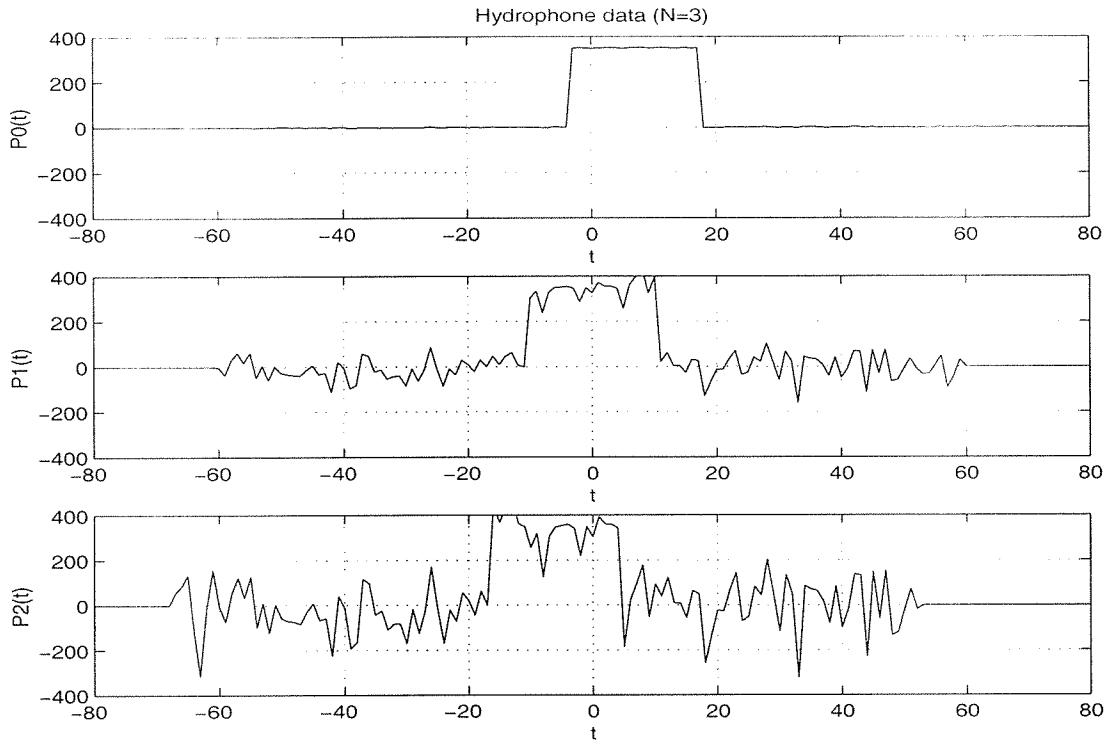

Figure 5.11: Hydrophone data

Both MLE and LSE methods are used to solve this problem. The results are shown in the following figures. For the Maximum Likelihood method, take the grid size $\Delta q = 0.5$, the number of iterations $I = 10000$, initial temperature $T_0 = 5 \times 10^5$. Figure 5.12 shows the MLE result of the source, the standard deviation of the estimated signal is $std(p(t) - q(t)) = 12.4474$. Figure 5.13 shows the MLE result of the bearing, it is around $20°$, which is the true value. For the Least Squares method, take the grid size $\Delta q = 0.075$, the number of iterations $I = 10000$ and the initial temperature $T_0 = 3.75 \times 10^6$. Figure 5.14 shows the LSE results of the source, figure 5.15 shows the LSE result of the bearing. Figure 5.16 shows the energy vs. the iteration. We can see that although the energy is lower than $E_0 = 1610004.5$, and the estimated bearing is very good, but the standard deviation of the estimated signal by LSE is $std(p(t) - q(t)) = 38.3420$, which is much larger than the MLE result.

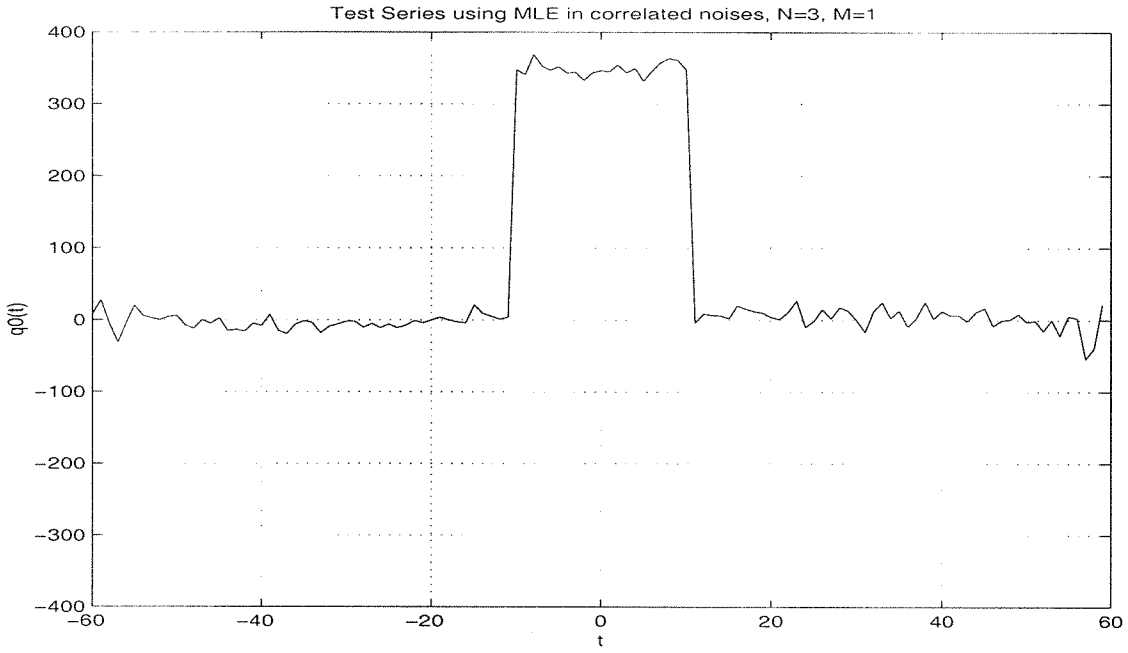

Figure 5.12: MLE result of the source

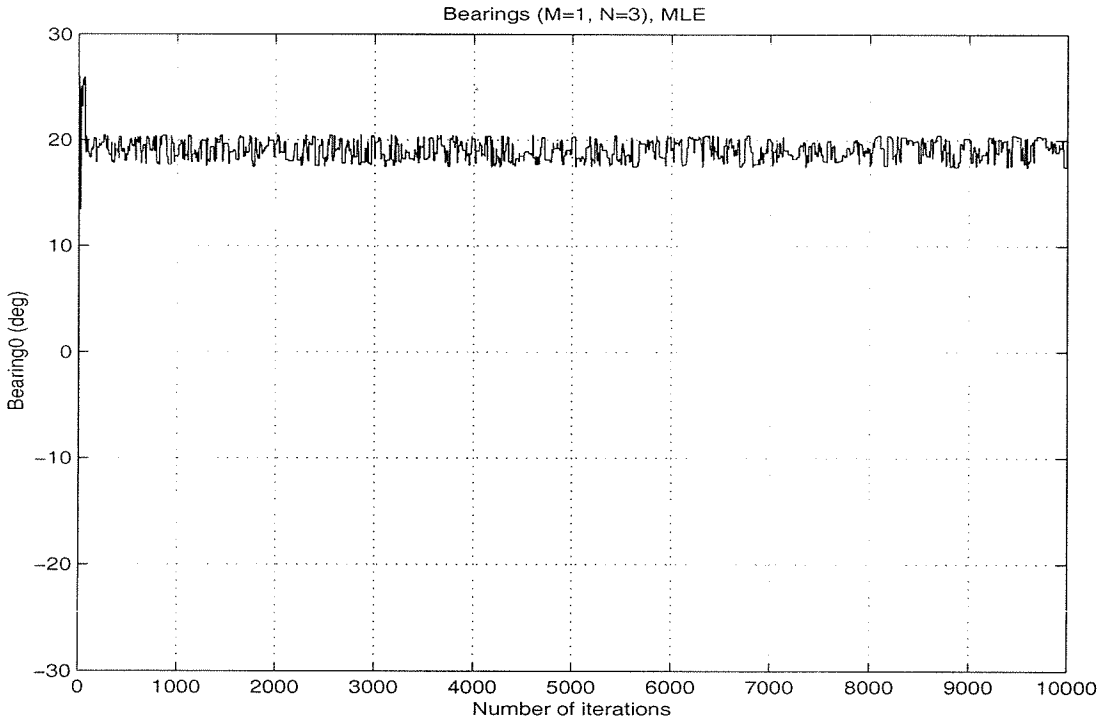

Figure 5.13: MLE result of the bearing

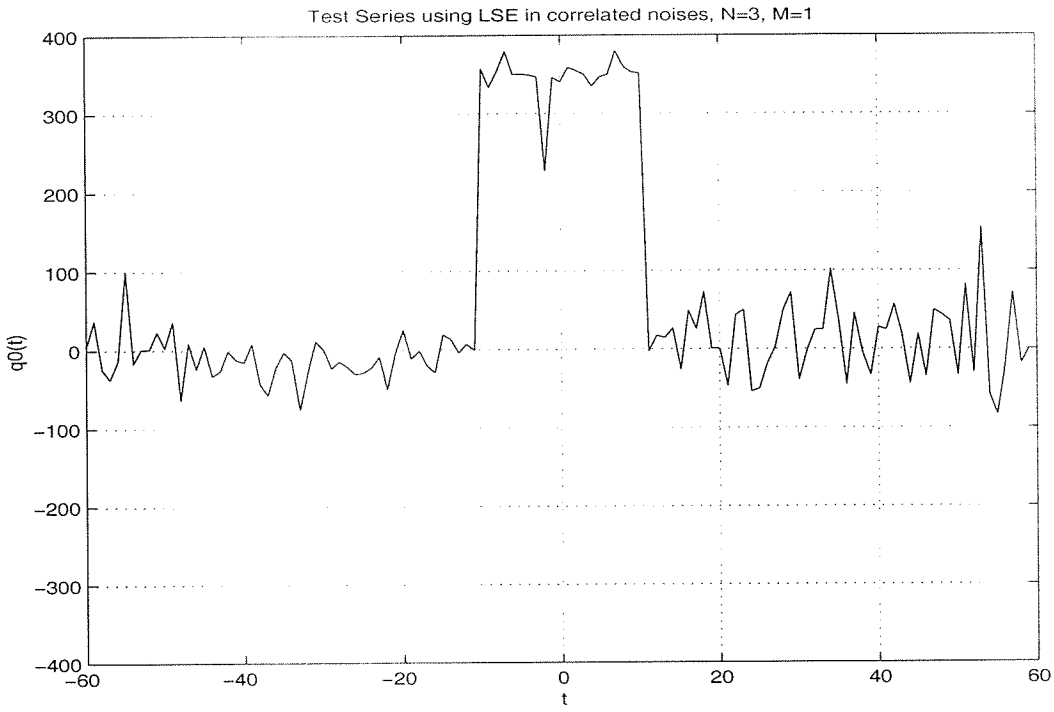

Figure 5.14: LSE result of the signal

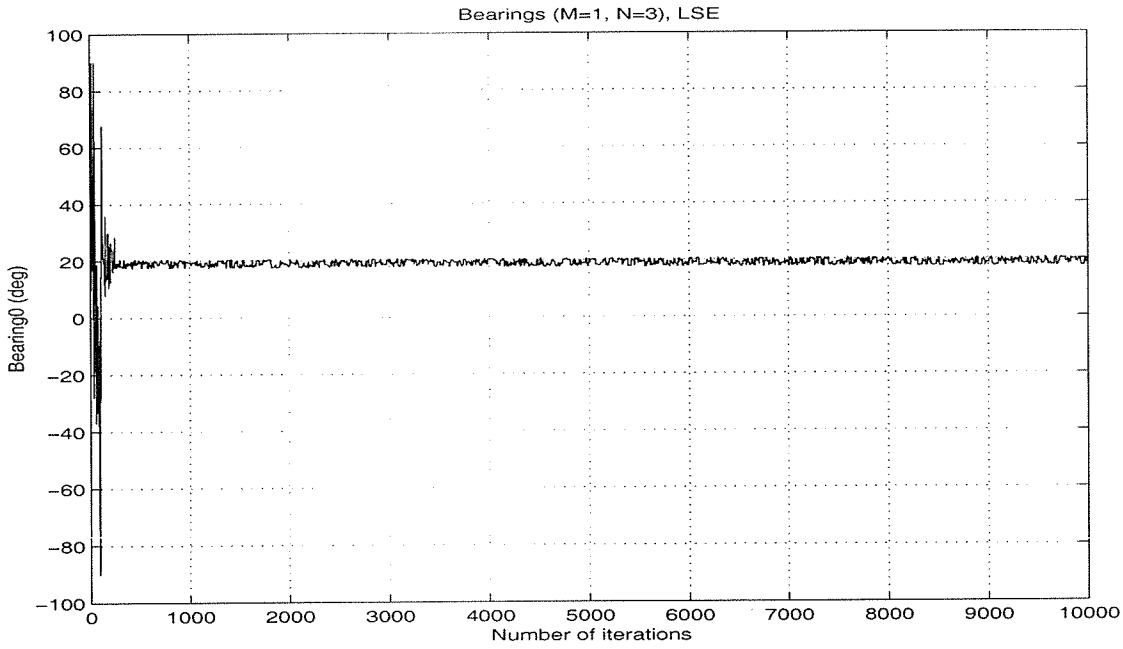

Figure 5.15: LSE result of the bearing

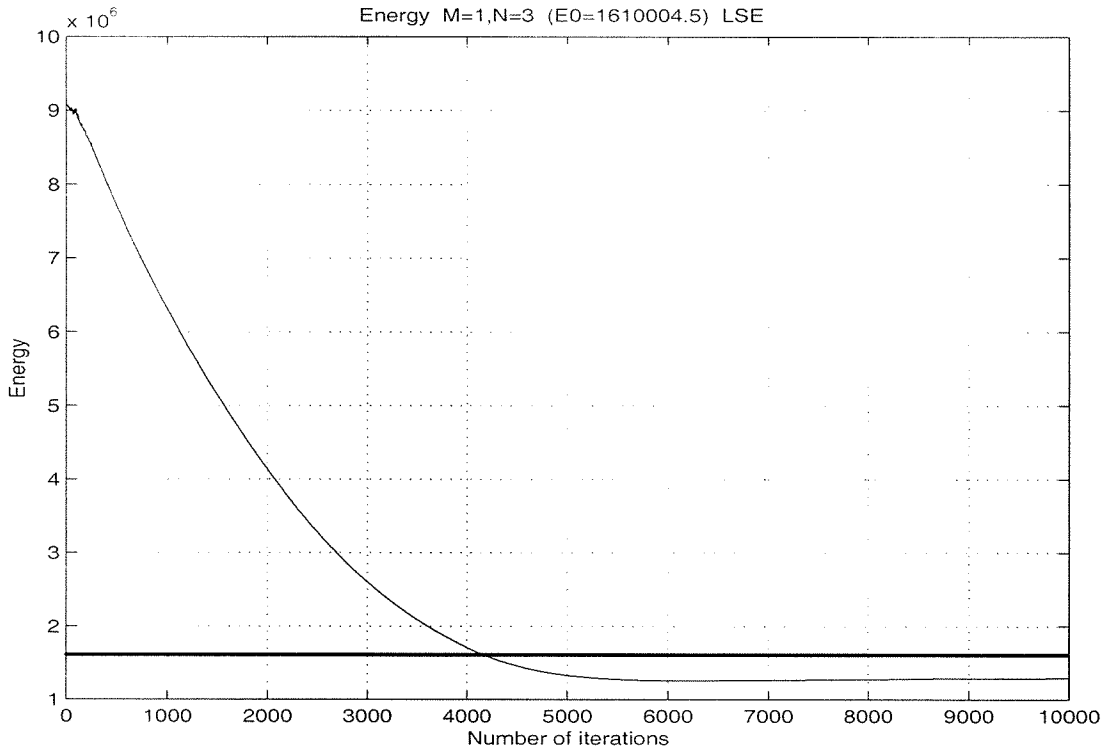

Figure 5.16: LSE Energy

5.1.1.3 Source signal is a long pulse

In this case, a long pulse is used as the source. It is a narrow-band signal. It is shown in figure 5.17. The source bearing is $\theta = 20°$. The amplitude is 350. The source equation is

$$p(t) = 350(u(t+500) - u(t-500)) \tag{5.32}$$

The product of the time window interval is 1000, it is much greater than the length of the hydrophone 40, so it is a narrowband signal.

The hydrophone data is shown in figure 5.18.

Both MLE and LSE methods are used to solve this problem. For the Maximum Likelihood method, take the grid size $\Delta q = 0.25$, the number of iterations $I = 8000$, initial temperature $T_0 = 5 \times 10^7$. Figure 5.19 shows the MLE result of the source, the

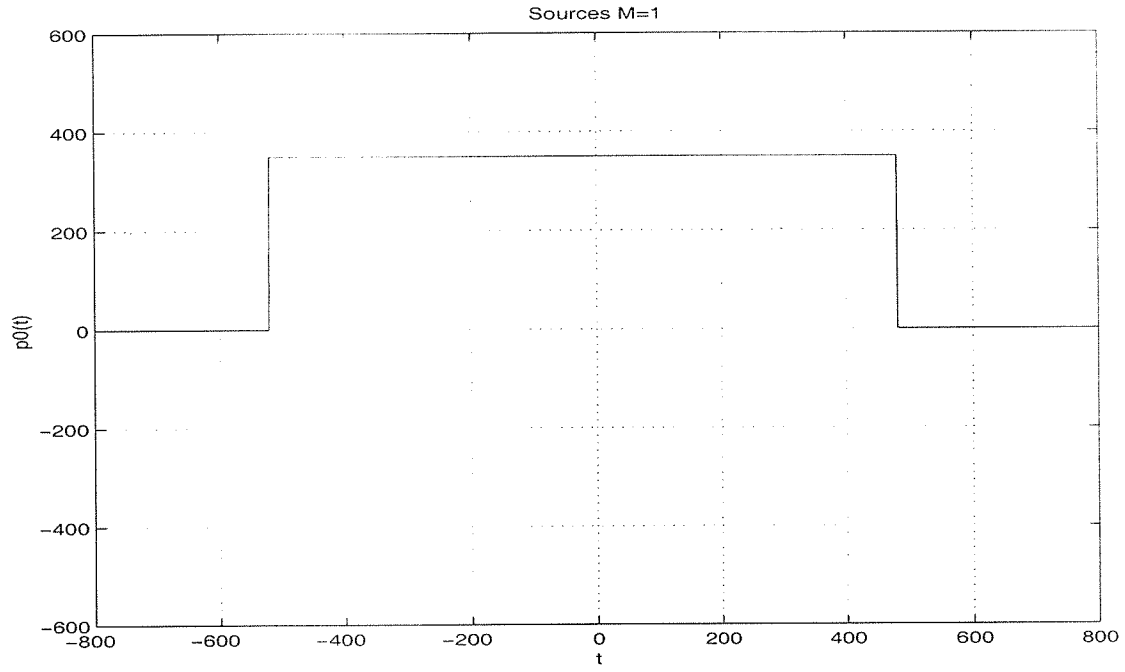

Figure 5.17: Source is a long pulse

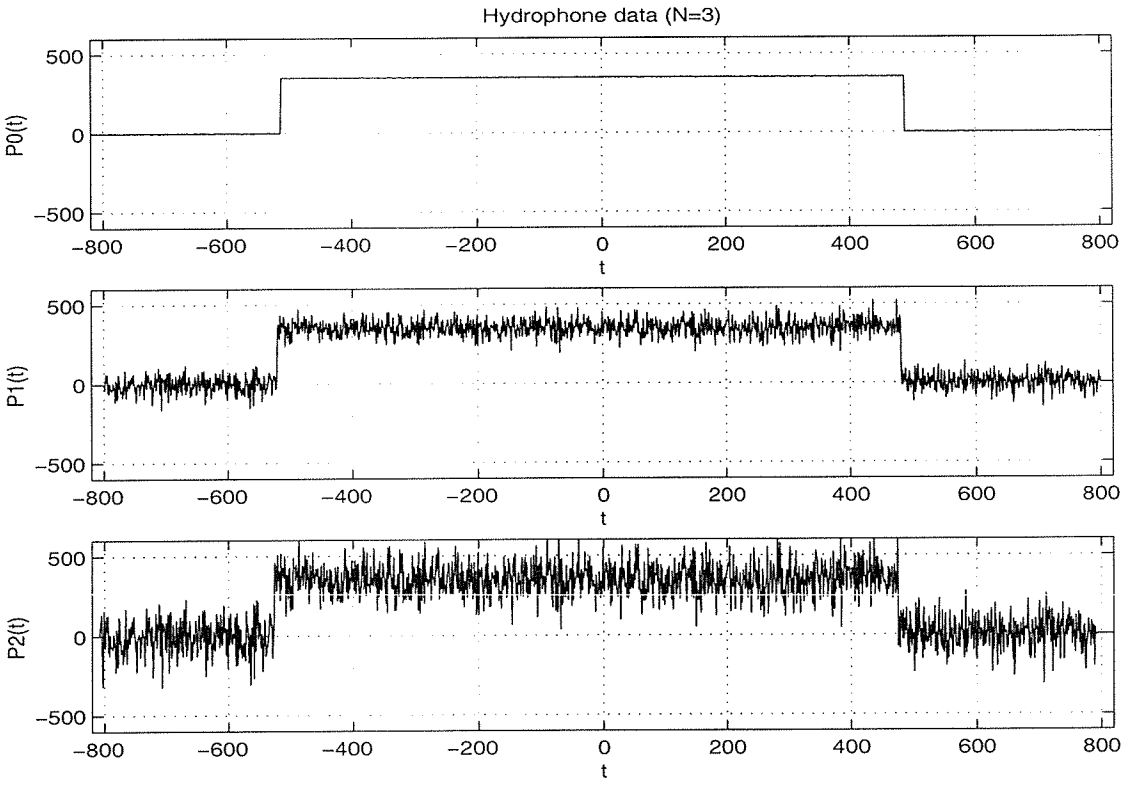

Figure 5.18: Hydrophone data

standard deviation of the estimated signal is $std(p(t)-q(t)) = 11.0596$. Figure 5.20 shows the MLE result of the bearing, it is around $20°$, which is the true value.

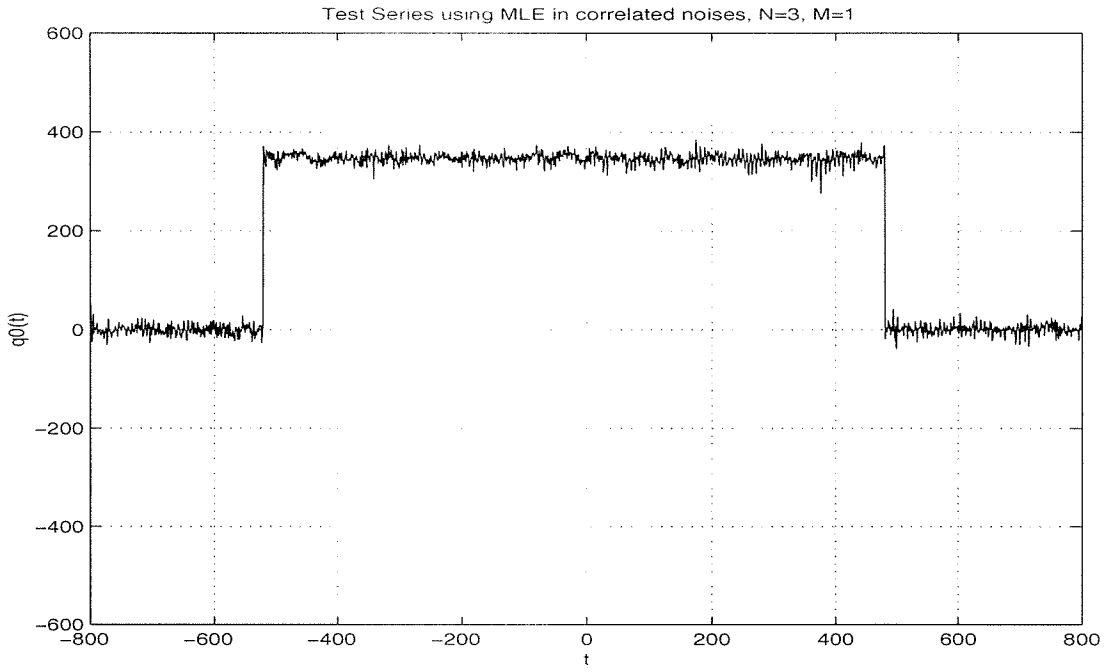

Figure 5.19: MLE result of the source

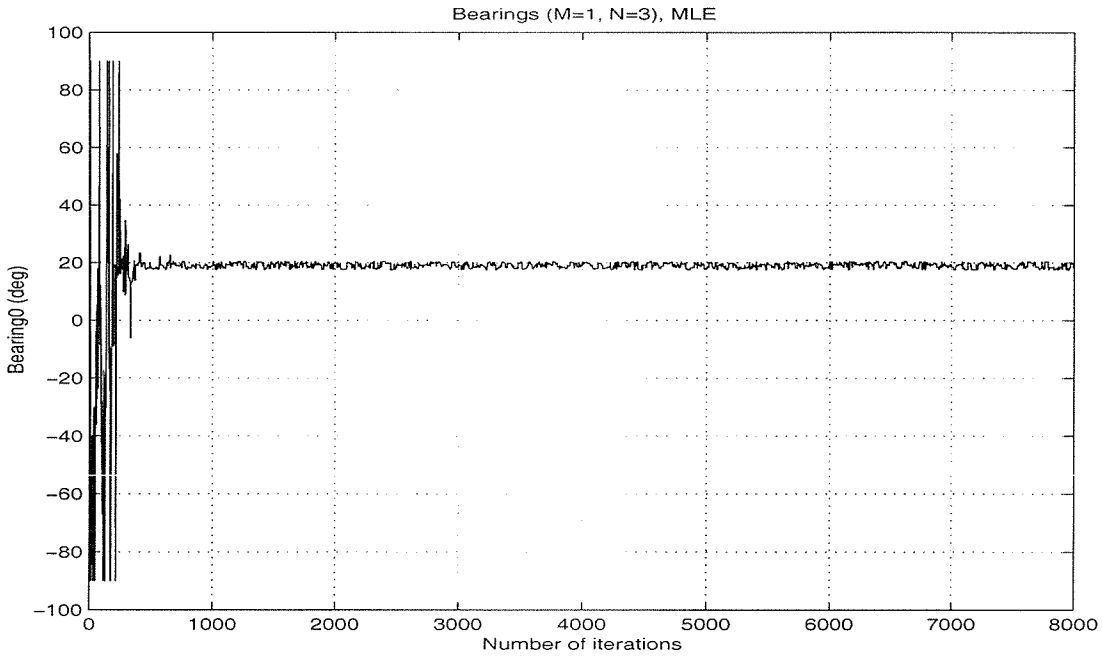

Figure 5.20: MLE result of the bearing

For the Least Squares method, take the grid size $\Delta q = 0.10$, the number of iterations $I = 8000$ and the initial temperature $T_0 = 3.75 \times 10^5$. Figure 5.21 shows the LSE results of the source, figure 5.22 shows the LSE result of the bearing. We can see that although the estimated bearing is good, but the standard deviation of the estimated signal by LSE is $std(p(t) - q(t)) = 33.3887$, which is much larger than the MLE result.

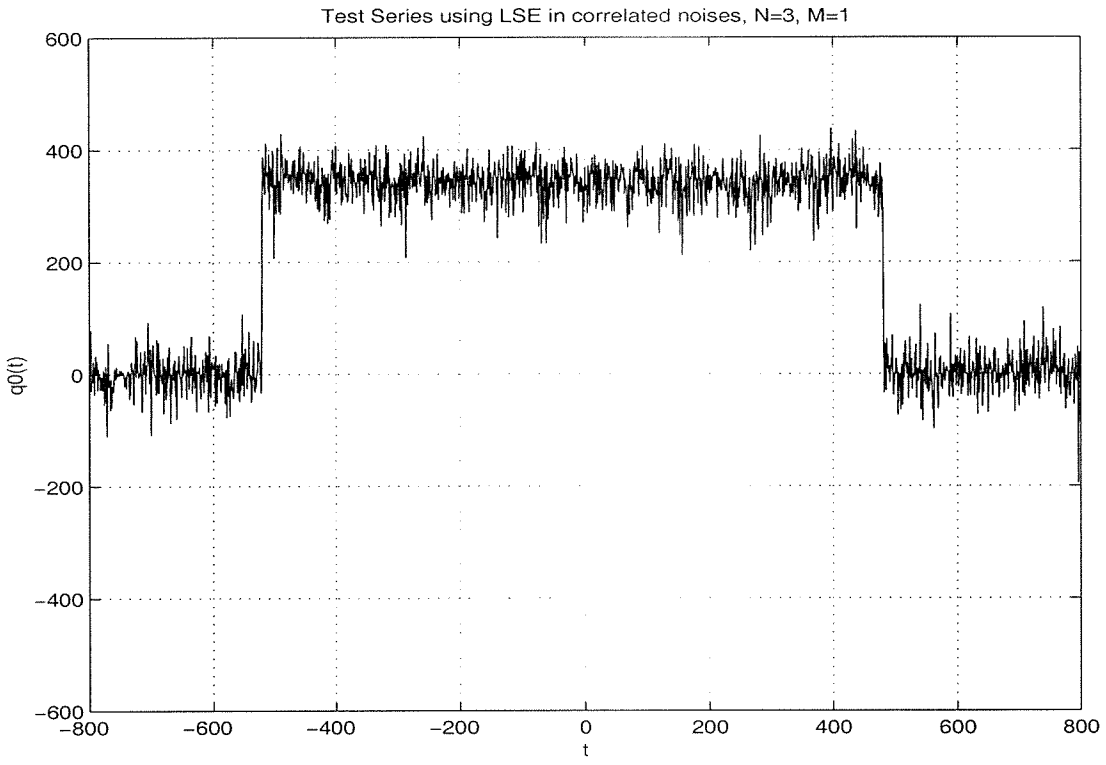

Figure 5.21: LSE result of the time series

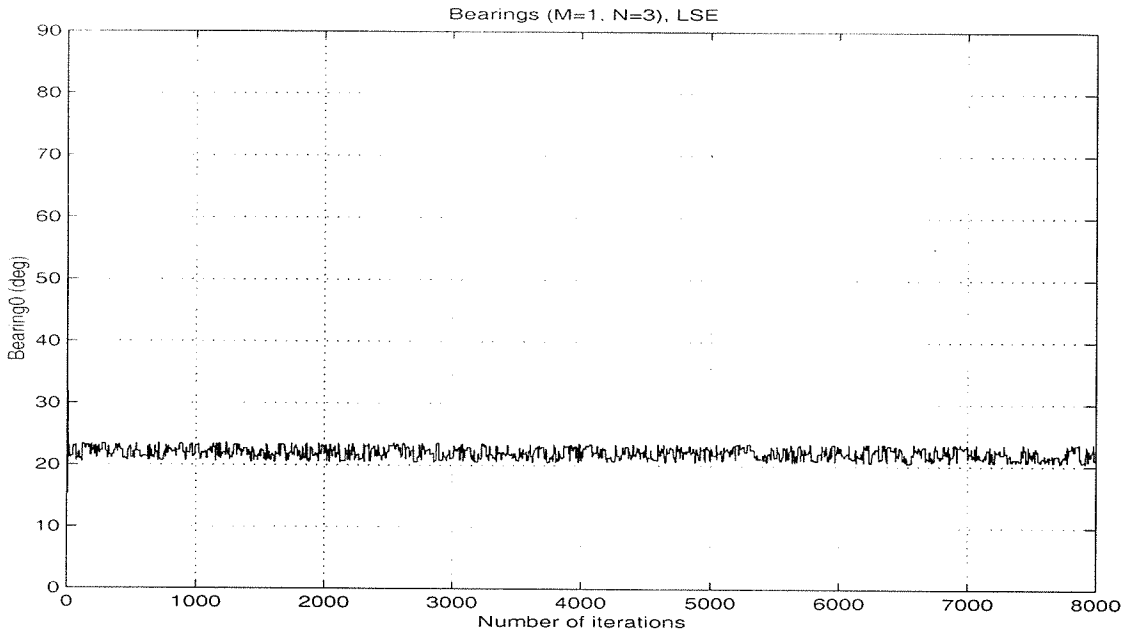

Figure 5.22: LSE result of the bearing

5.1.1.4 Source is a sinusoidal signal

Sinusoidal signals with different frequencies are used as sources. In this case, the results by suing Maximum Likelihood Estimation are also better than those by using Least Squares Estimation.

5.1.1.4.1 Source is a low frequency sinusoidal signal

The source is a low frequency sinusoidal signal with a bearing of $\theta = 20°$. The time series is given by the equation:

$$p(t) = \begin{cases} 350\sin\left(\dfrac{\pi(t+500)}{250}\right) & -500 \le t \le 500 \\ 0 & otherwise \end{cases} \tag{5.33}$$

It is shown in figure 5.23. Its frequency is $f = 1/500$, which is much smaller than the ratio of the sound velocity and the length of the array $c/L = 1/40$, thus, it is a broad-band signal. The hydrophone data is shown in figure 5.24.

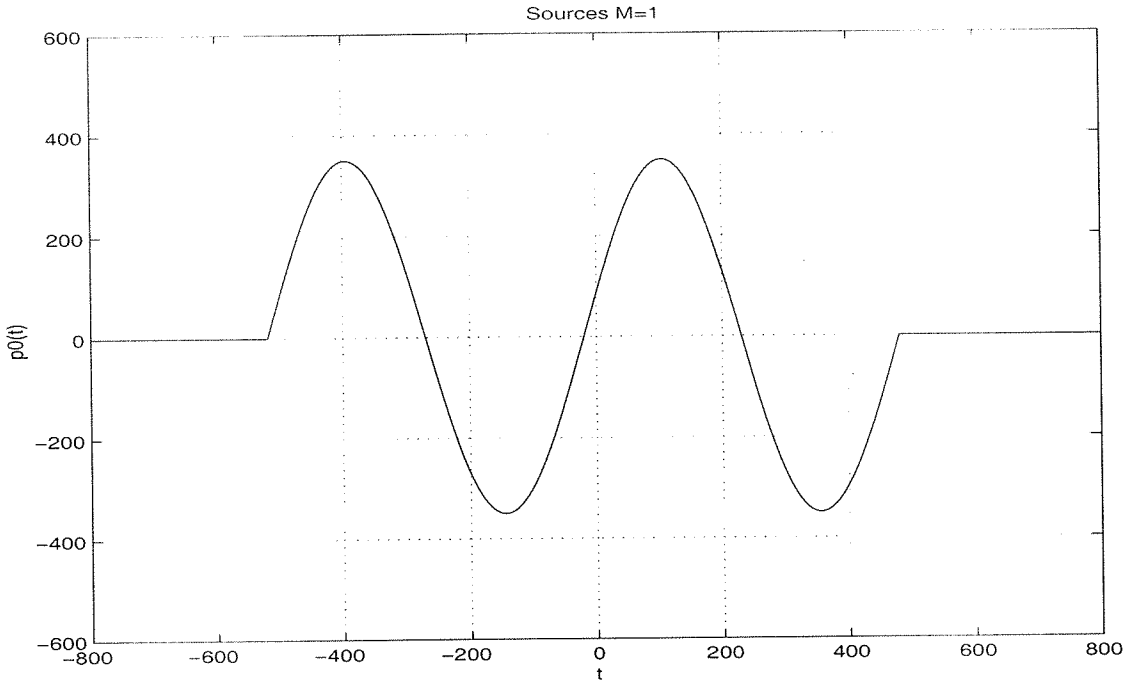

Figure 5.23: Sinusoidal signal with a low frequency

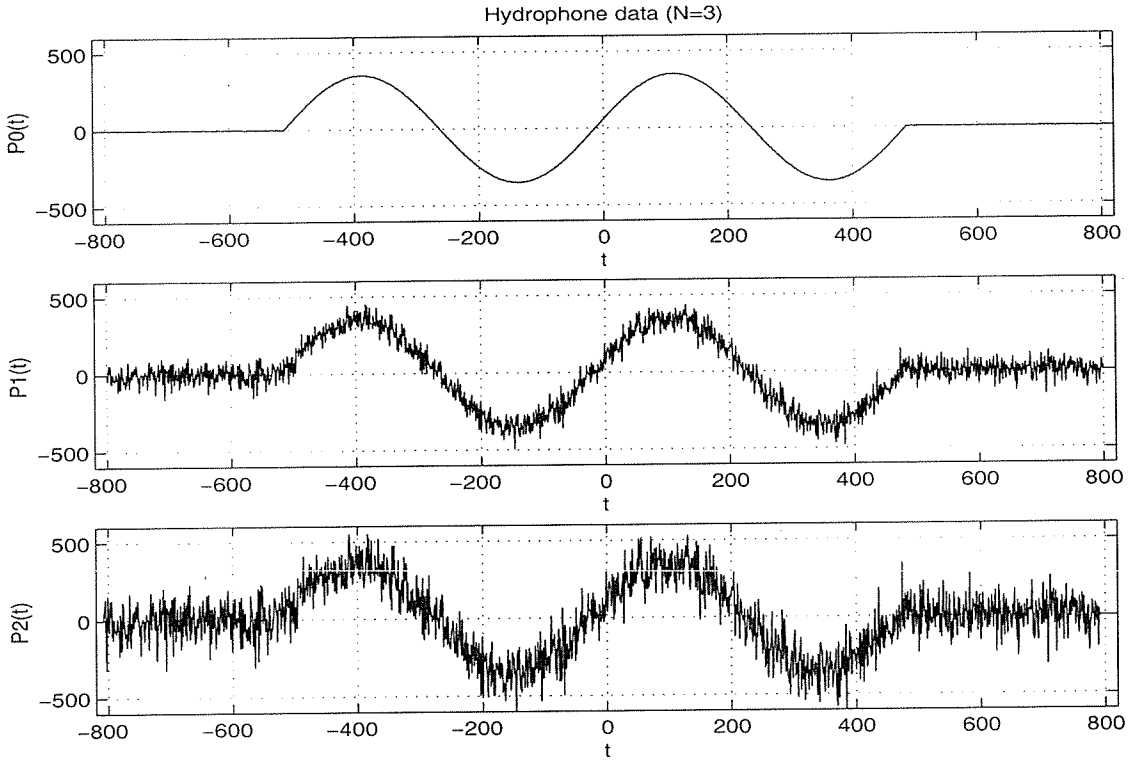

Figure 5.24: Hydrophone data when the source is a low frequency sine signal

Once more both MLE and LSE methods are used to solve this problem. For the Maximum Likelihood method, take the grid size $\Delta q = 0.5$, the number of iterations $I = 8000$, initial temperature $T_0 = 1.0 \times 10^9$. Figure 5.25 shows the MLE result of the source, the standard deviation of the estimated signal is $std(p(t) - q(t)) = 11.6573$. Figure 5.26 shows the MLE result of the bearing, it is around $20°$, which is the true value.

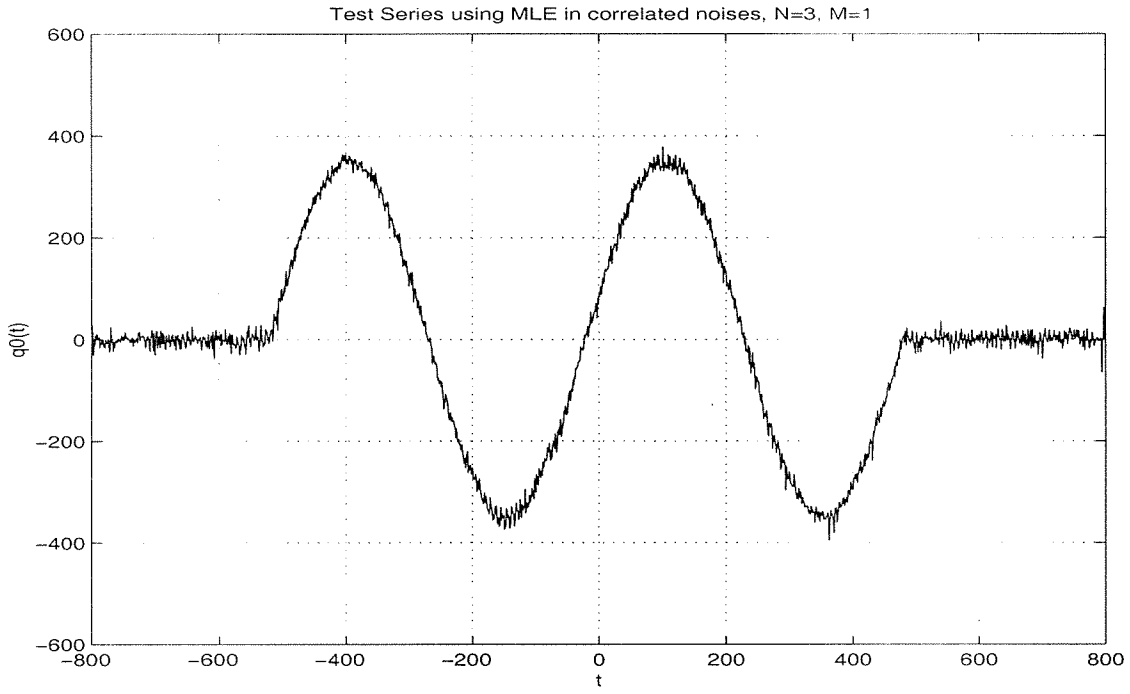

Figure 5.25: MLE result of the time series

For the Least Squares method, take the grid size $\Delta q = 0.50$, the number of iterations $I = 8000$ and the initial temperature $T_0 = 5 \times 10^6$. Figure 5.27 shows the LSE results of the source, figure 5.28 shows the LSE result of the bearing. We can see that the estimated bearing is a little bit higher than the true value, also the standard deviation of the estimated signal by LSE is $std(p(t) - q(t)) = 34.4685$, which is much larger than the MLE result.

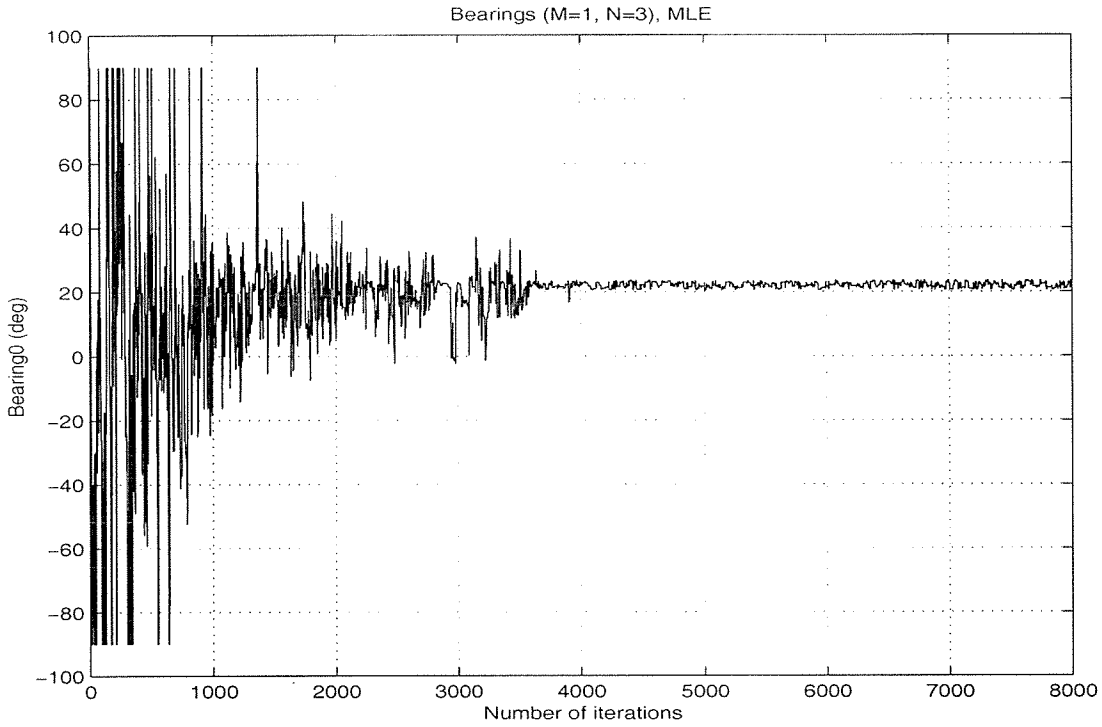

Figure 5.26: MLE result of the bearing

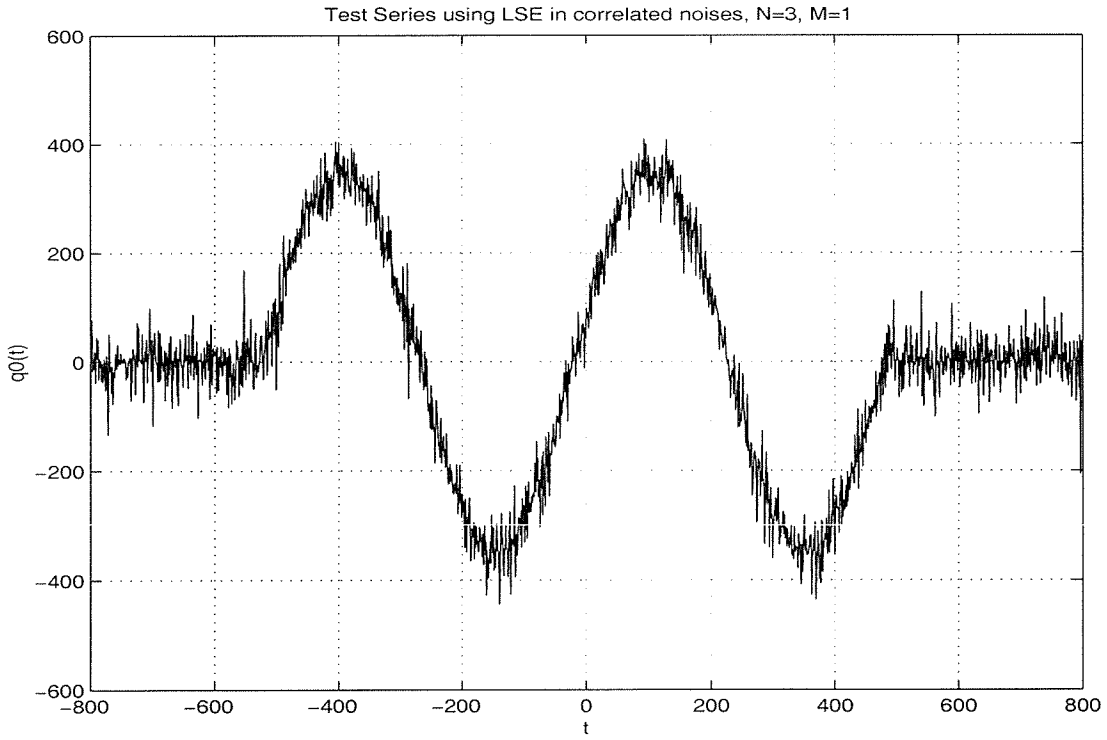

Figure 5.27: LSE result of the time series

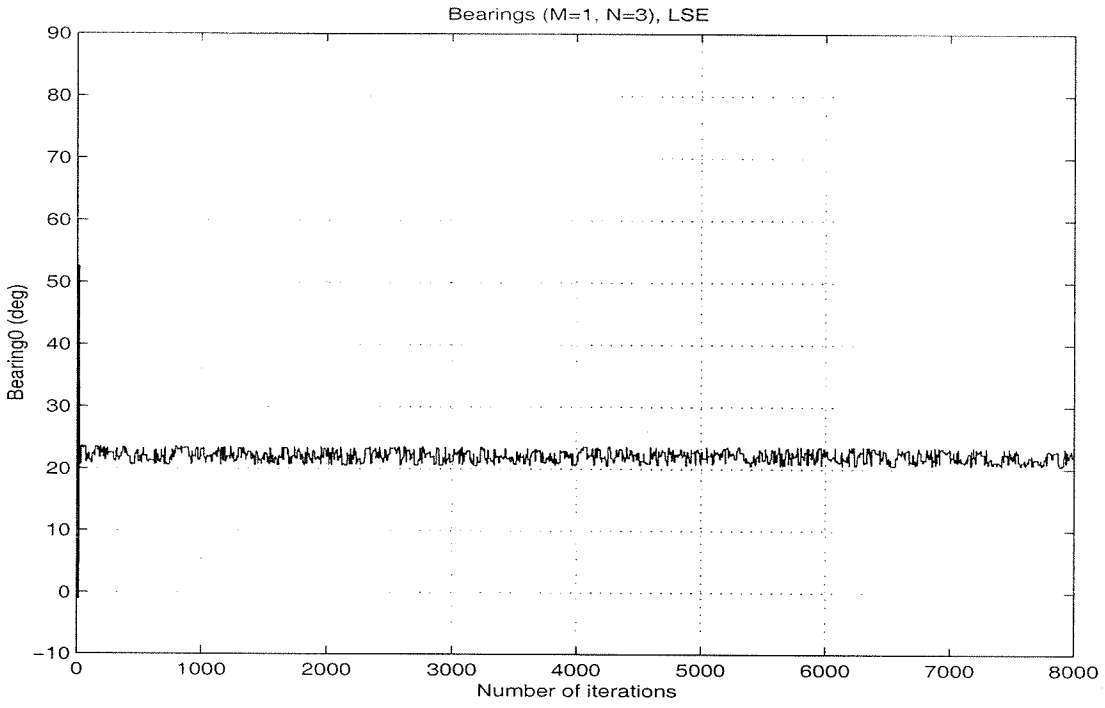

Figure 5.28: LSE result of the bearing

5.1.1.4.2 Source is a higher frequency sinusoidal signal

The source is a higher frequency sinusoidal signal with a bearing of $\theta = 20°$. The time series is given by the equation:

$$p(t) = \begin{cases} 350\sin\left(\dfrac{\pi(t+500)}{25}\right) & -500 \le t \le 500 \\ 0 & otherwise \end{cases} \tag{5.34}$$

It is shown in figure 5.29. Its frequency is $f = \frac{1}{50}$, which is smaller than the ratio of the sound velocity and the length of the array $\frac{c}{L} = \frac{1}{40}$, thus, it is also a broadband signal.

The hydrophone data is shown in figure 5.30.

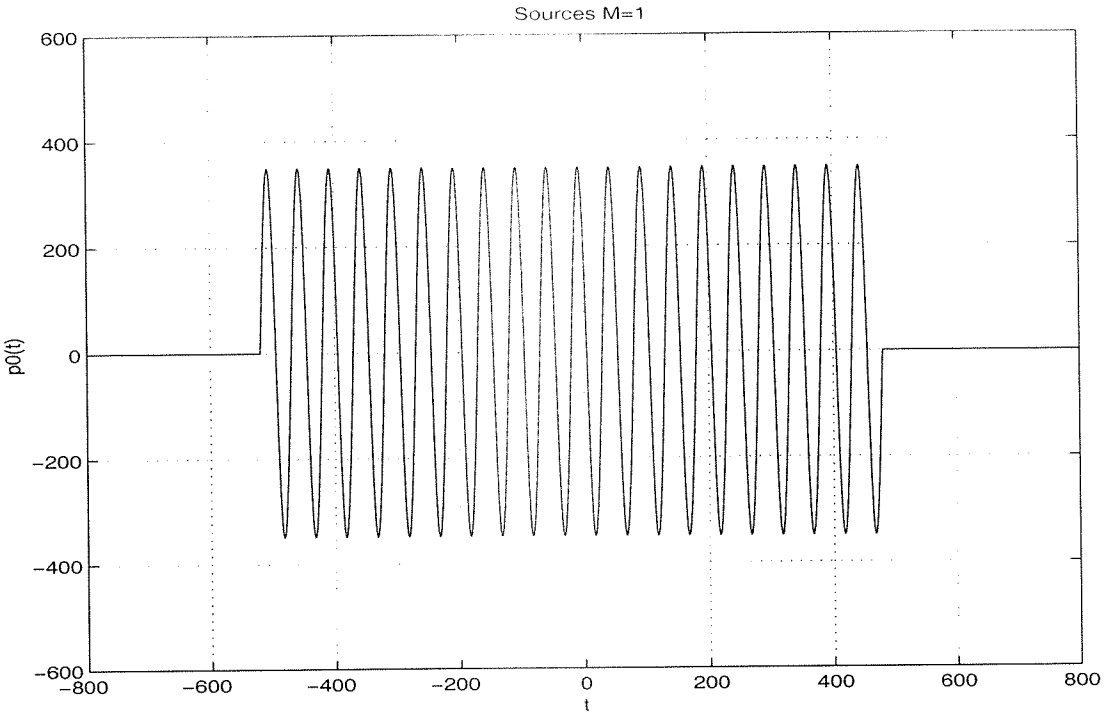

Figure 5.29: Sinusoidal signal with a higher frequency

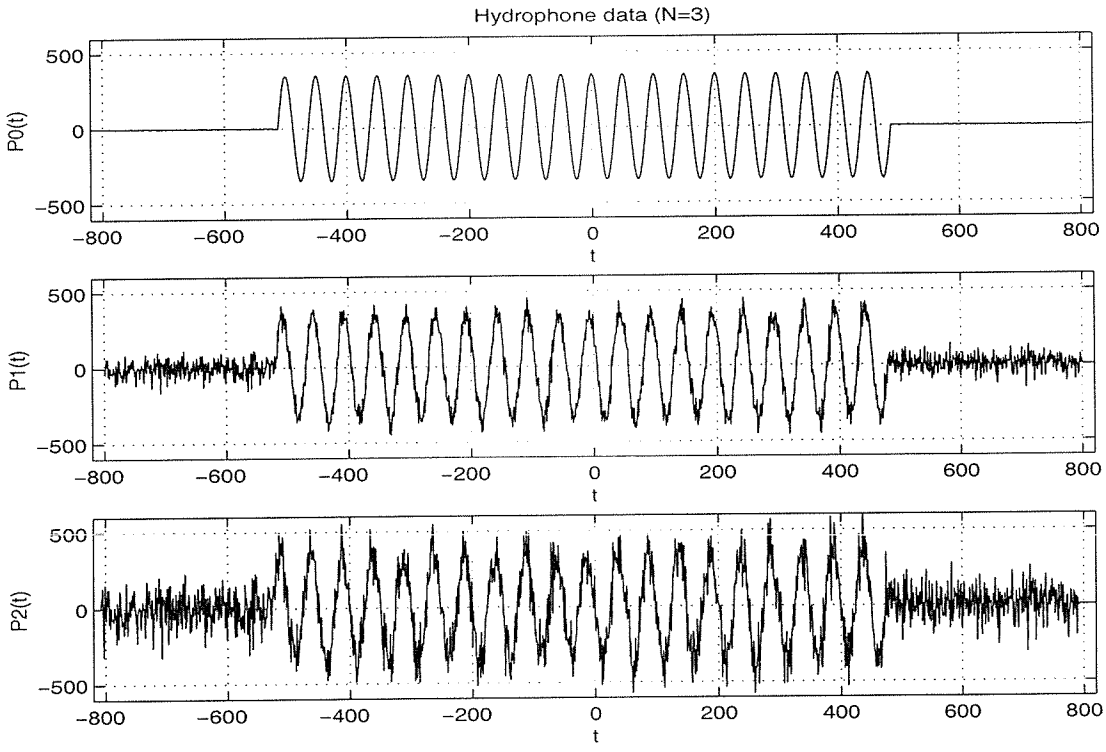

Figure 5.30: Hydrophone data when the source is a higher frequency sine signal

Both MLE and LSE methods are used to solve this problem. For the Maximum Likelihood method, take the grid size $\Delta q = 0.5$, the number of iterations $I = 8000$, initial temperature $T_0 = 5.0 \times 10^8$. Figure 5.31 shows the MLE result of the source, the standard deviation of the estimated signal is $std(p(t) - q(t)) = 12.1417$. Figure 5.32 shows the MLE result of the bearing, it is around $20°$, which is the true value.

For the Least Squares method, take the grid size $\Delta q = 0.50$, the number of iterations $I = 8000$ and the initial temperature $T_0 = 5 \times 10^5$. Figure 5.33 shows the LSE results of the source, figure 5.34 shows the LSE result of the bearing. We can see that although the estimated bearing is good, but the standard deviation of the estimated signal by LSE is $std(p(t) - q(t)) = 34.8488$, which is much larger than the MLE result.

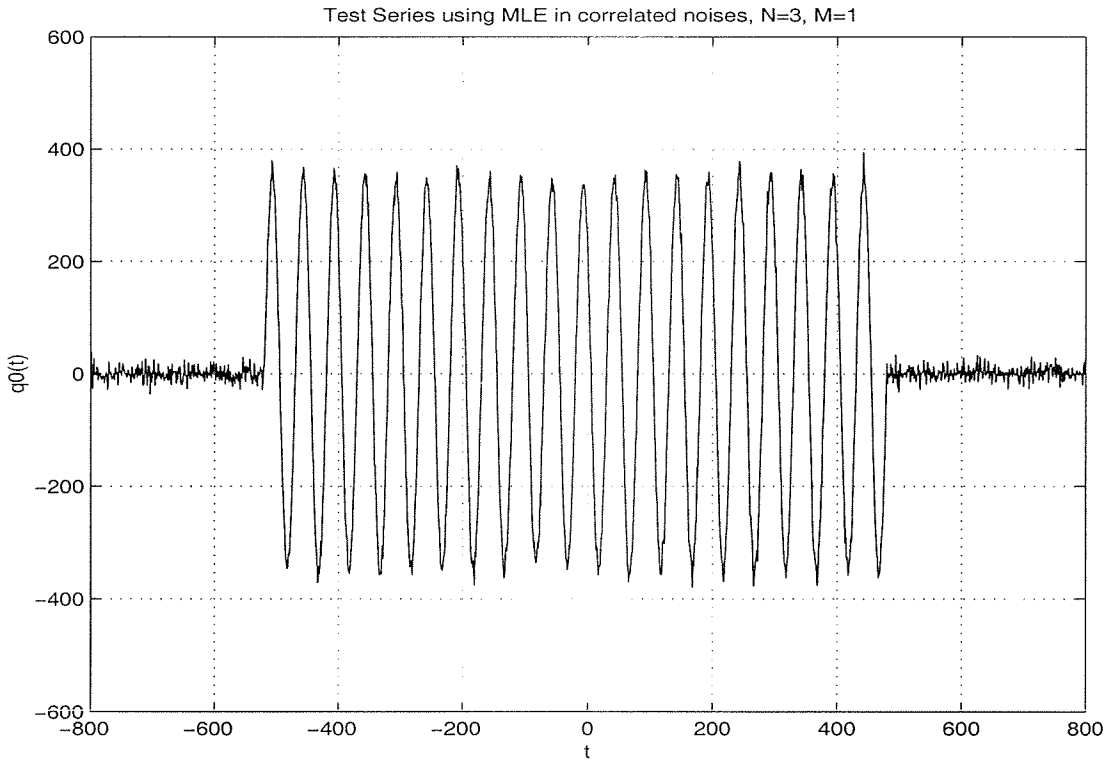

Figure 5.31: MLE result of the time series

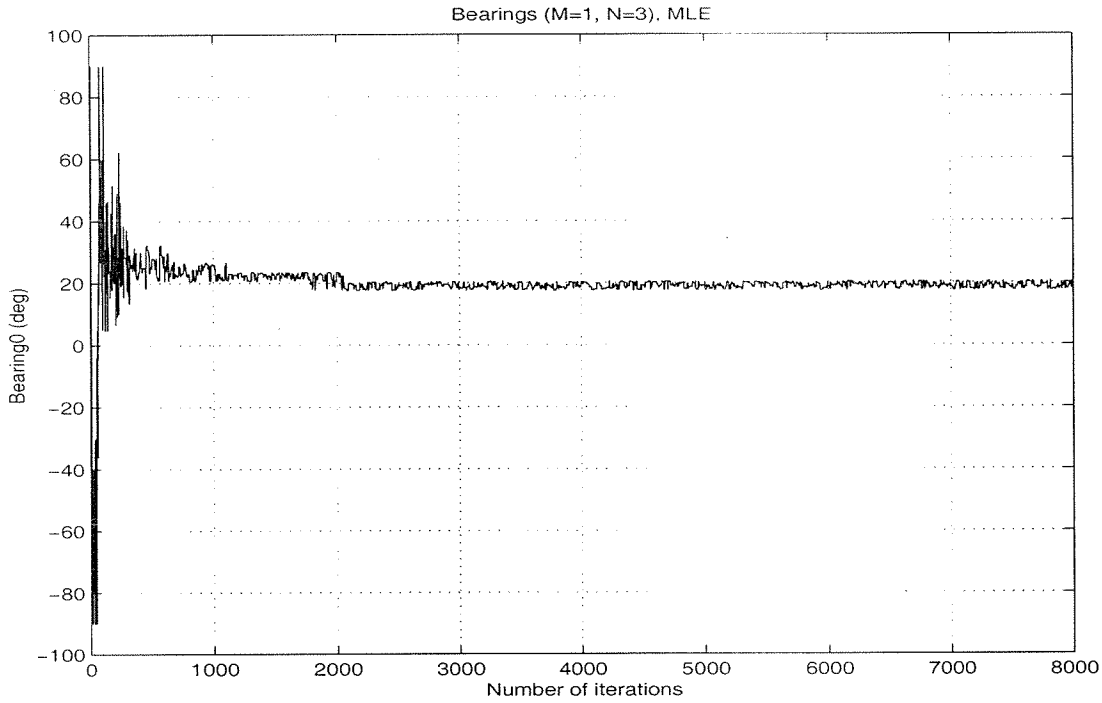

Figure 5.32: MLE result of the bearing

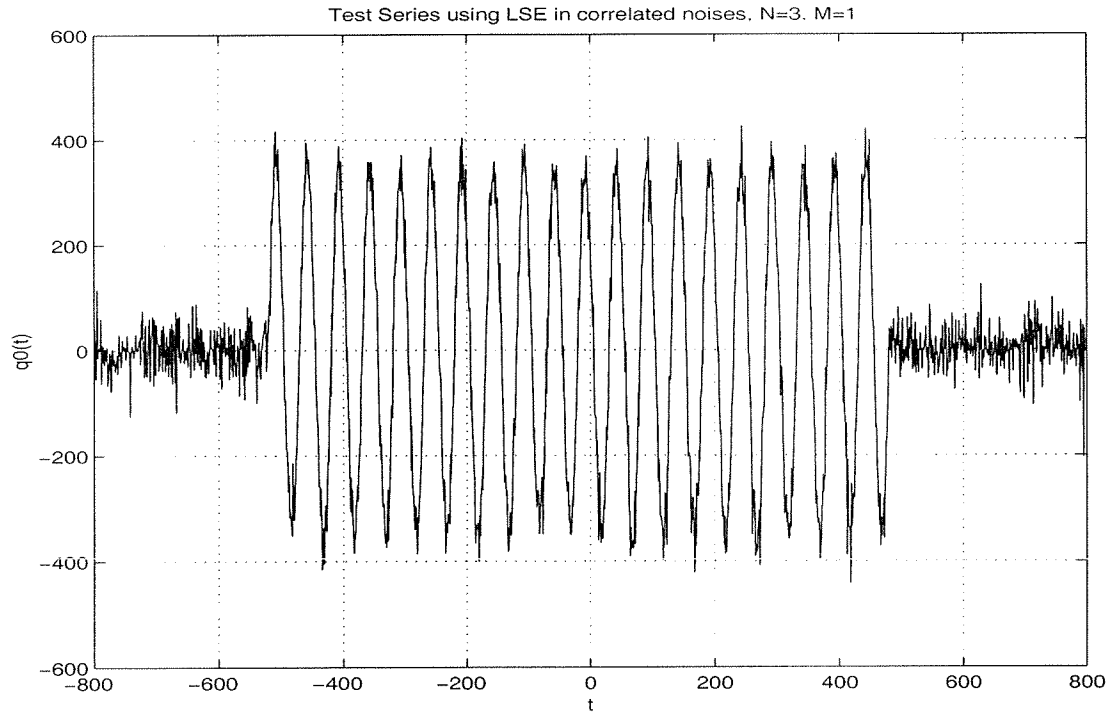

Figure 5.33: LSE result of the time series

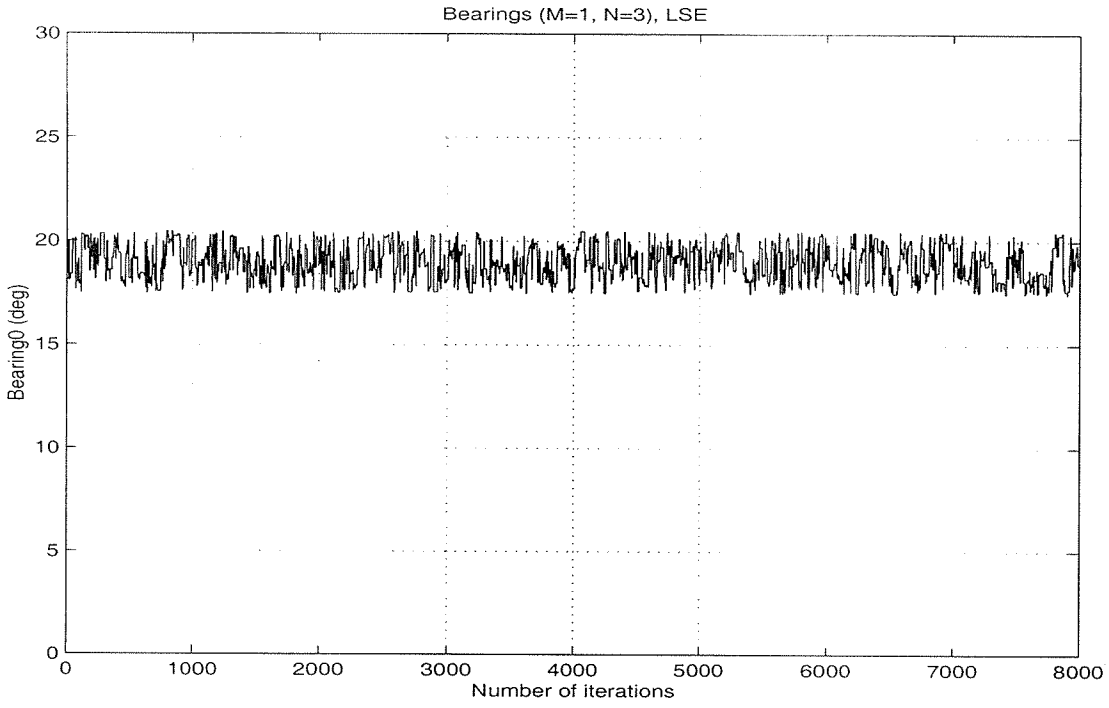

Figure 5.34: LSE result of the bearing

5.1.1.4.3 Source is a general broadband signal

The source is a broadband signal with a bearing of $\theta = 20°$. The time series is given by the equation:

$$p(t) = \exp\left\{-\left[\frac{t+10}{20}\right]^2\right\}\cos\left[\frac{2\pi(t+10)}{30}\right] \tag{5.35}$$

it is shown in figure 5.35. This signal is a broadband signal because of the exponential term, it makes the carrier waveform much narrower in time domain, so it is broad in frequency domain.

The hydrophone data is shown in figure 5.36.

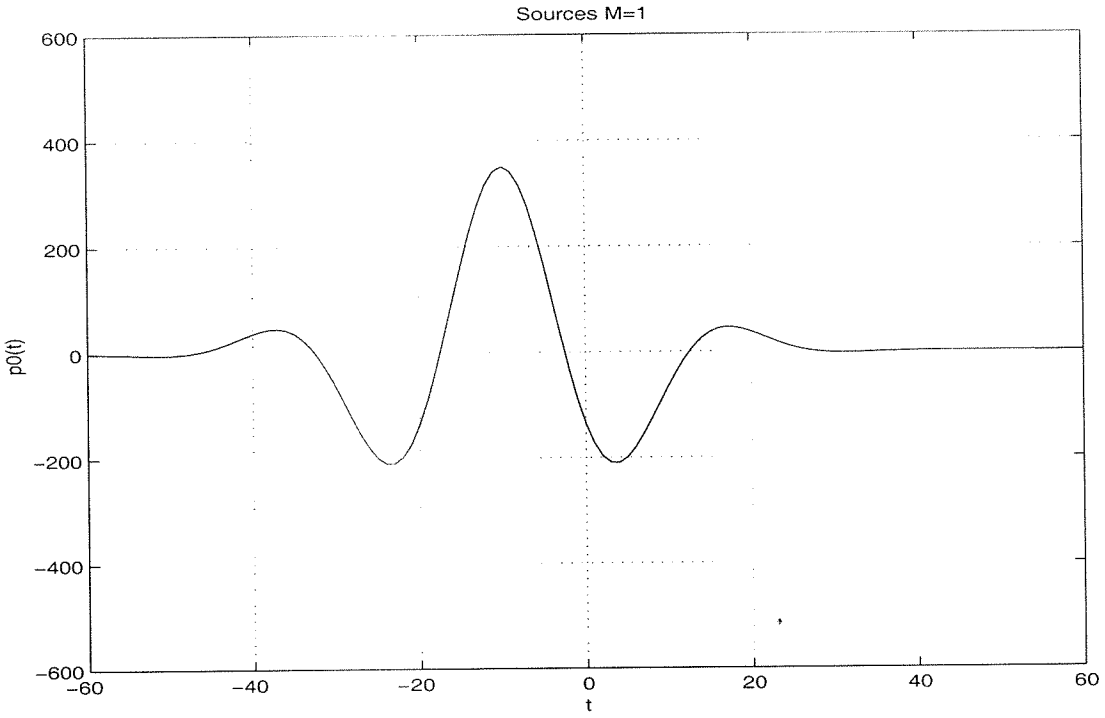

Figure 5.35: Source is a broadband signal

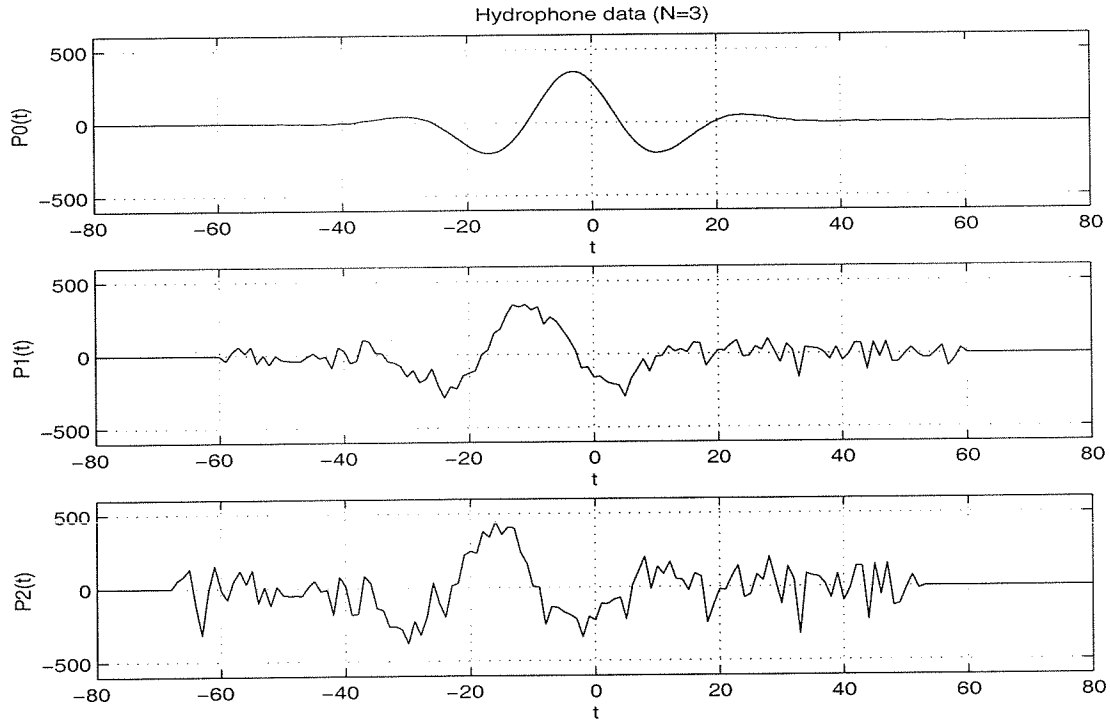

Figure 5.36: Hydrophone data when the source is a broadband signal

Both MLE and LSE methods are used to solve this problem. For the Maximum Likelihood method, take the grid size $\Delta q = 0.5$, the number of iterations $I = 8000$, initial temperature $T_0 = 3.75 \times 10^5$. Figure 5.37 shows the MLE result of the source, the standard deviation of the estimated signal is $std(p(t) - q(t)) = 13.0113$. Figure 5.38 shows the MLE result of the bearing, it is around $20°$, which is the true value.

For the Least Squares method, take the grid size $\Delta q = 0.05$, the number of iterations $I = 8000$ and the initial temperature $T_0 = 2.5 \times 10^5$. Figure 5.39 shows the LSE results of the source, figure 5.40 shows the LSE result of the bearing. We can see that although the estimated bearing is good, but the standard deviation of the estimated signal by LSE is $std(p(t) - q(t)) = 34.3556$, which is much larger than the MLE result.

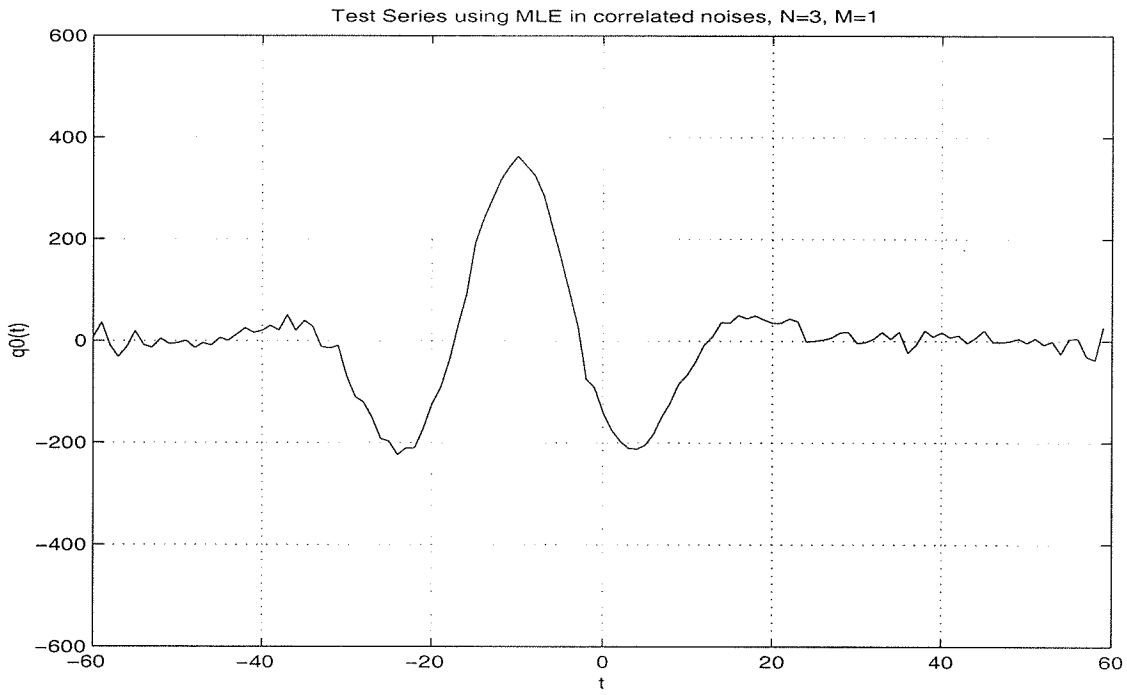

Figure 5.37: MLE result of the time series

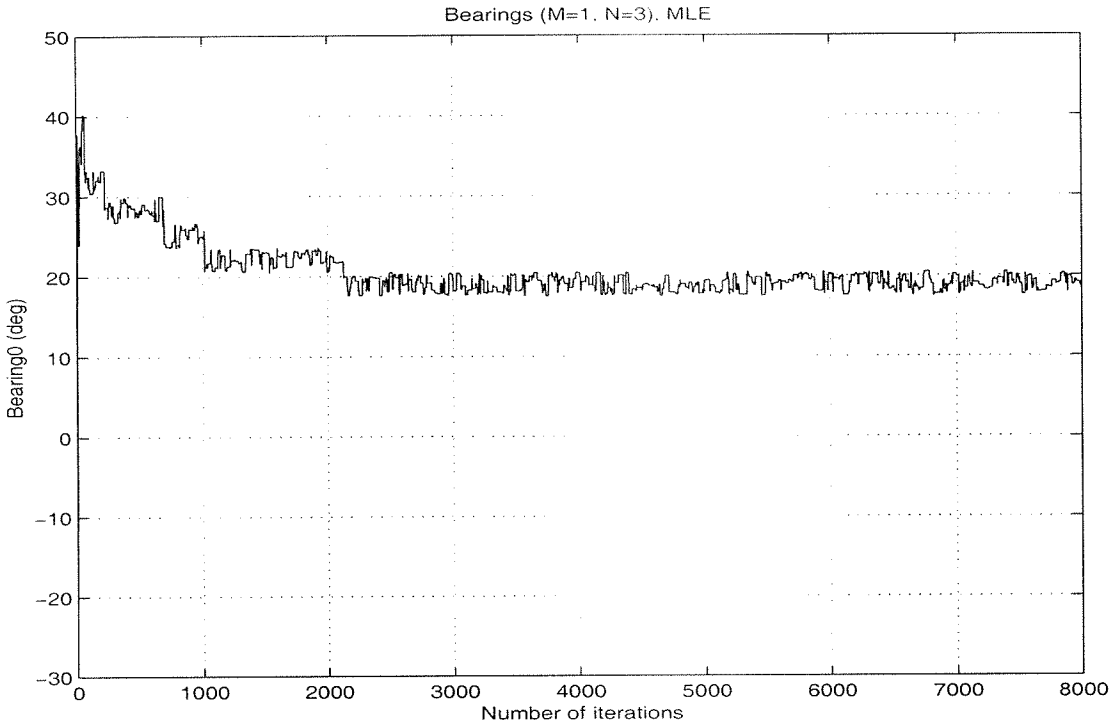

Figure 5.38: MLE result of the bearing

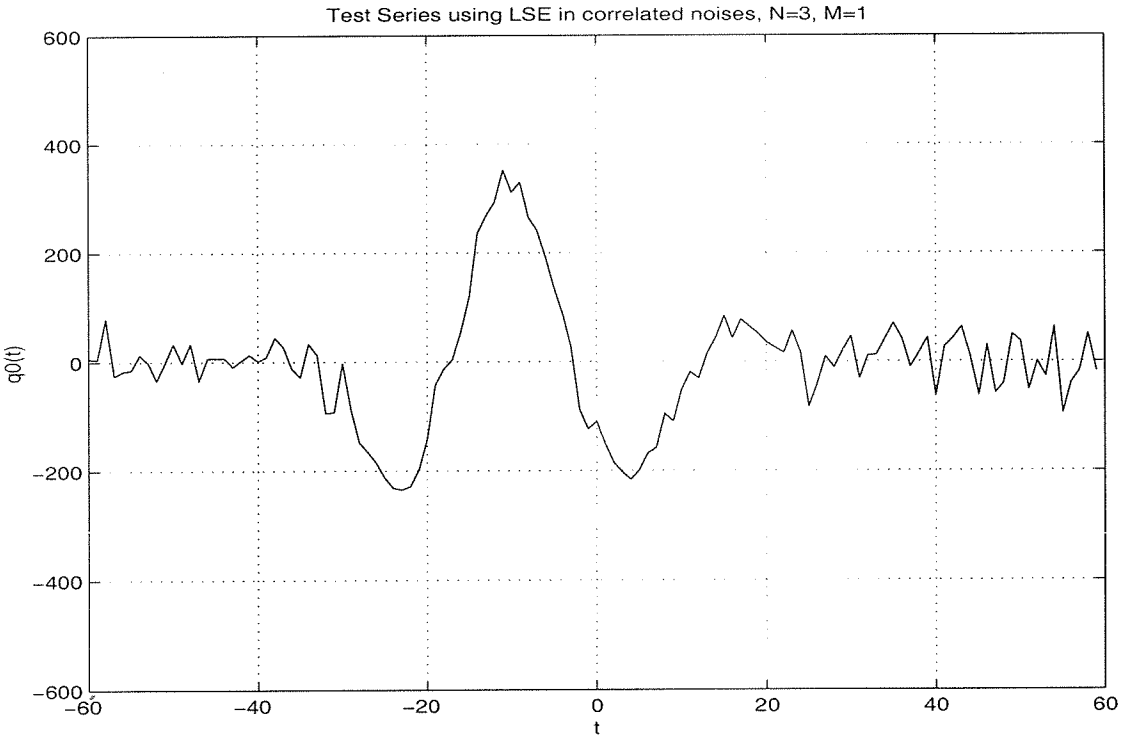

Figure 5.39: LSE result of the time series

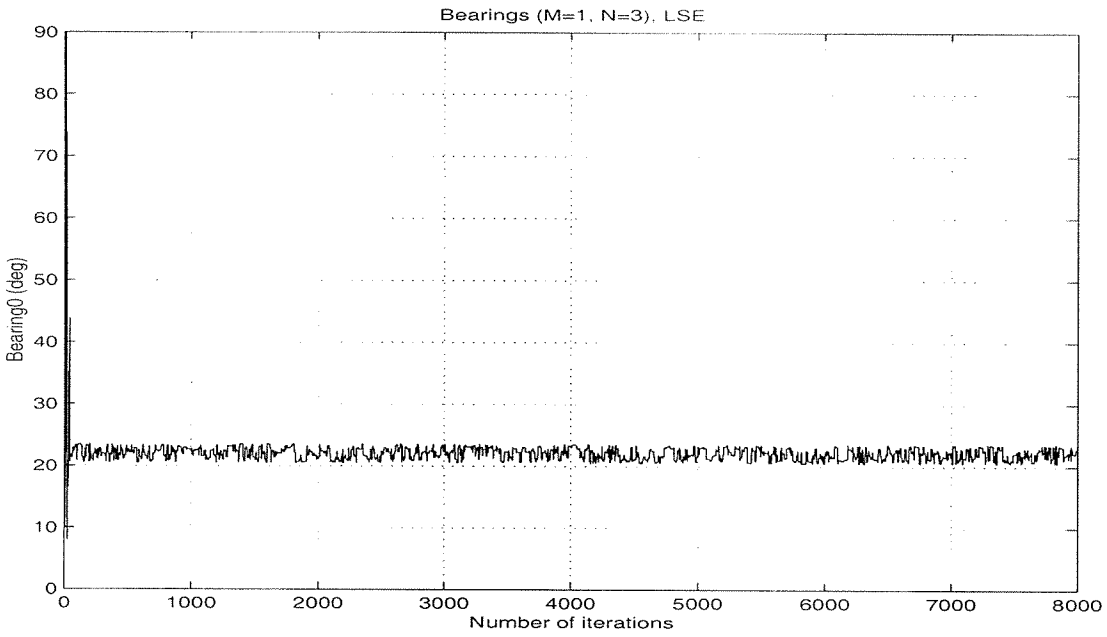

Figure 5.40: LSE result of the bearing

5.1.2 The diagonal elements of the covariance matrix are homogeneous

In this case the diagonal elements of the covariance are homogeneous. The noise at every hydrophone has the same variance, and is zero-mean Gaussian noise, and it is spatially correlated.

The noise generation process is as same as that in 5.1.1, however, in this case, $x_1(t) \sim N(0, 2500)$, $x_2(t) \sim N(0, 2500)$, $x_3(t) \sim N(0, 2500)$.

$y_1(t)$, $y_2(t)$ and $y_3(t)$ are linear combinations of $x_1(t)$, $x_2(t)$ and $x_3(t)$, therefore, they also have Gaussian distribution. Because $x_1(t)$, $x_2(t)$ and $x_3(t)$ are independent random processes, we have the mean values

$$\mu_{y_1} = a\mu_{x_1} + b\mu_{x_2} + d\mu_{x_3} = 0 \tag{5.36}$$

$$\mu_{y_2} = b\mu_{x_1} + a\mu_{x_2} + b\mu_{x_3} = 0 \tag{5.37}$$

$$\mu_{y_3} = d\mu_{x_1} + b\mu_{x_2} + a\mu_{x_3} = 0 \tag{5.38}$$

and the variance

$$\sigma_{y_1}^2 = a^2\sigma_{x_1}^2 + b^2\sigma_{x_2}^2 + d^2\sigma_{x_3}^2 = 2500(a^2 + b^2 + d^2) \tag{5.39}$$

$$\sigma_{y_2}^2 = b^2\sigma_{x_1}^2 + a^2\sigma_{x_2}^2 + b^2\sigma_{x_3}^2 = 2500(b^2 + a^2 + b^2) \tag{5.40}$$

$$\sigma_{y_3}^2 = d^2\sigma_{x_1}^2 + b^2\sigma_{x_2}^2 + a^2\sigma_{x_3}^2 = 2500(d^2 + b^2 + a^2) \tag{5.41}$$

and the covariance

$$\sigma_{y_1y_2}^2 = ab\sigma_{x_1}^2 + ab\sigma_{x_2}^2 + bd\sigma_{x_3}^2 \tag{5.42}$$

$$\sigma_{y_2y_3}^2 = bd\sigma_{x_1}^2 + ab\sigma_{x_2}^2 + ab\sigma_{x_3}^2 \tag{5.43}$$

$$\sigma_{y_1y_3}^2 = ad\sigma_{x_1}^2 + b^2\sigma_{x_2}^2 + ad\sigma_{x_3}^2 \tag{5.44}$$

Take $a = 1$, $b = 0.5$ and $d = 0.01$, we have

$$\underline{C} = \begin{bmatrix} 3125.25 & 2512.50 & 675 \\ 2512.50 & 3750 & 2512.50 \\ 675 & 2512.50 & 3125.25 \end{bmatrix} \tag{5.45}$$

This is the theoretical value. Its inverse matrix is

$$\underline{C}^{-1} = \begin{bmatrix} 0.0014 & -0.0015 & 0.0009 \\ -0.0015 & 0.0023 & -0.0015 \\ 0.0009 & -0.0015 & 0.0014 \end{bmatrix} \tag{5.46}$$

The generated noise is shown in figure 5.41. The correlation matrix is:

$$\underline{Cor} = \begin{bmatrix} 1.0000 & 0.7179 & 0.2115 \\ 0.7179 & 1.0000 & 0.7438 \\ 0.2115 & 0.7438 & 1.0000 \end{bmatrix}. \tag{5.47}$$

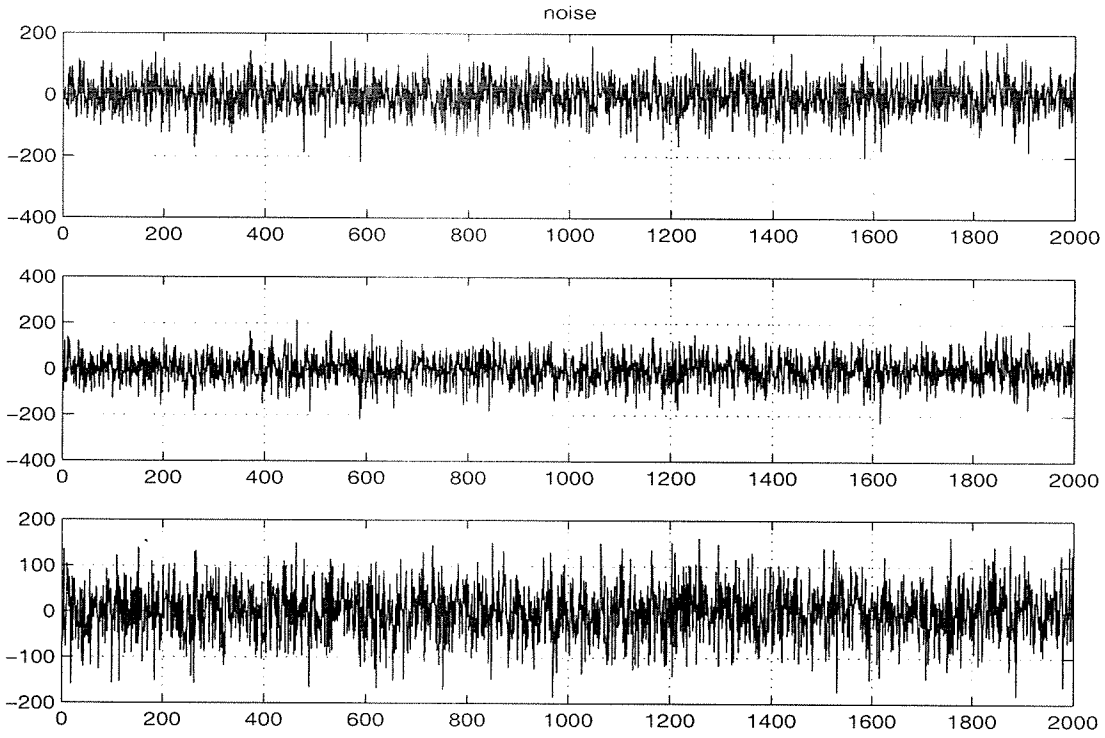

Figure 5.41: The spatially correlated Gaussian noise with same variance

5.1.2.1 Source is a broadband signal

The source is a broadband signal with a bearing of $20°$. The time series is given by the equation:

$$p(t) = \exp\left\{-\left[\frac{t+10}{20}\right]^2\right\}\cos\left[\frac{2\pi(t+10)}{30}\right] \tag{5.48}$$

it is the same broadband signal as in 5.1.1.4.3, as shown in figure 5.35.

The hydrophone data is shown in figure 5.42. First, MLE is used. Take the grid size $\Delta q = 0.25$, the number of iterations $I = 8000$, initial temperature $T_0 = 2.5 \times 10^6$. The MLE result of the time series is shown in figure 5.43, the standard deviation of the estimated signal is $std(p(t) - q(t)) = 22.7044$, and the MLE result of the bearing is shown in figure 5.44, it's around the true value, $20°$.

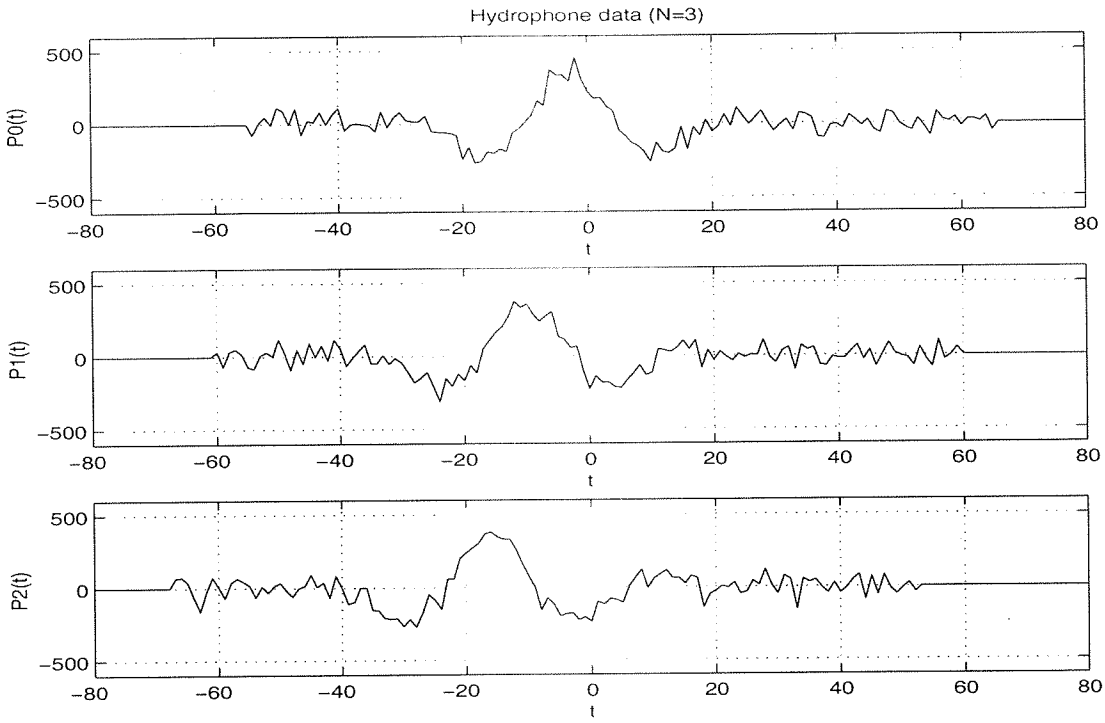

Figure 5.42: Hydrophone data when source is a broadband signal in correlated noise

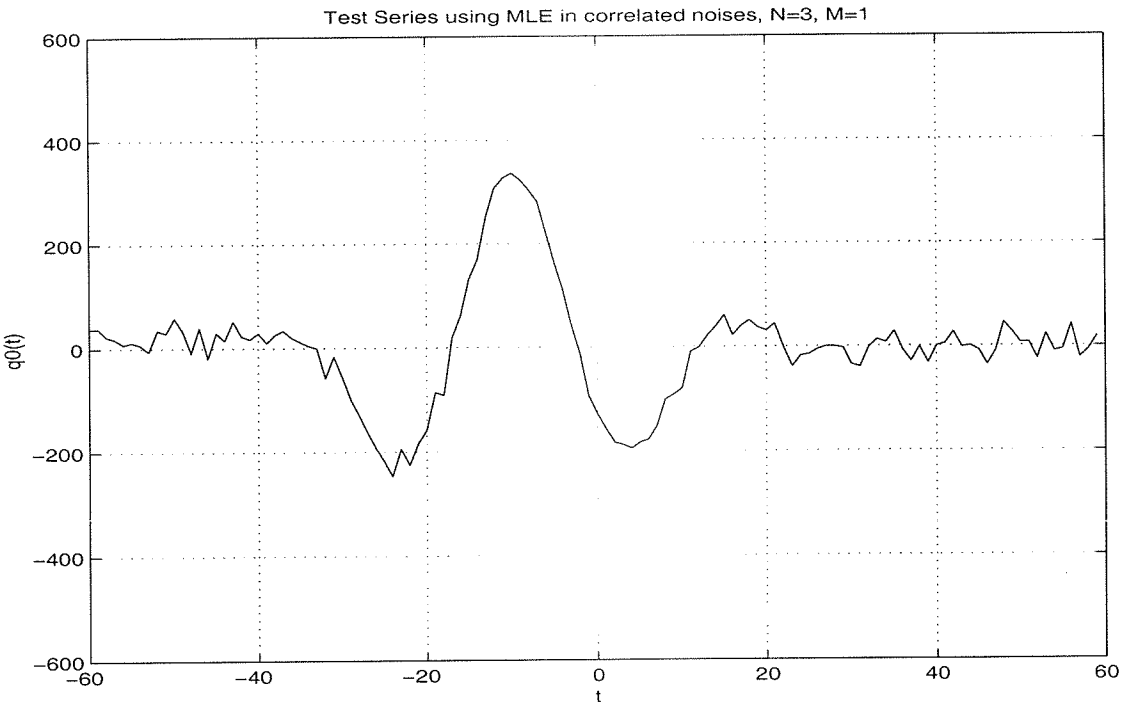

Figure 5.43: MLE result of the time series

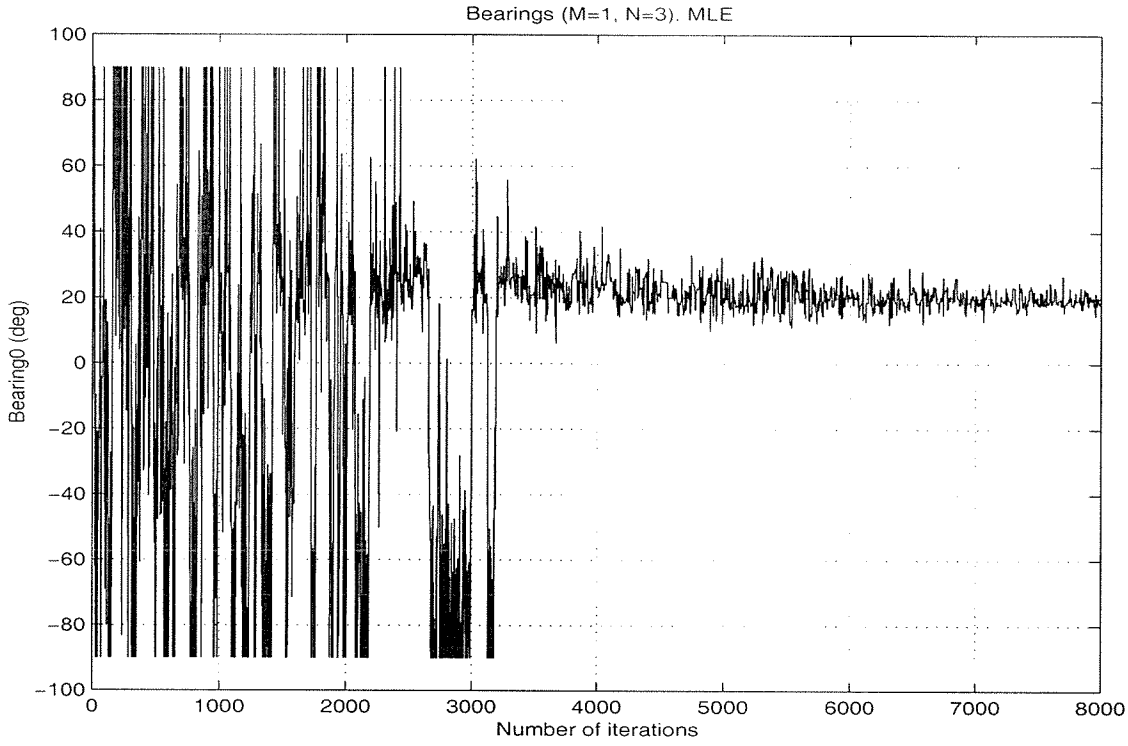

Figure 5.44: MLE result of the bearing

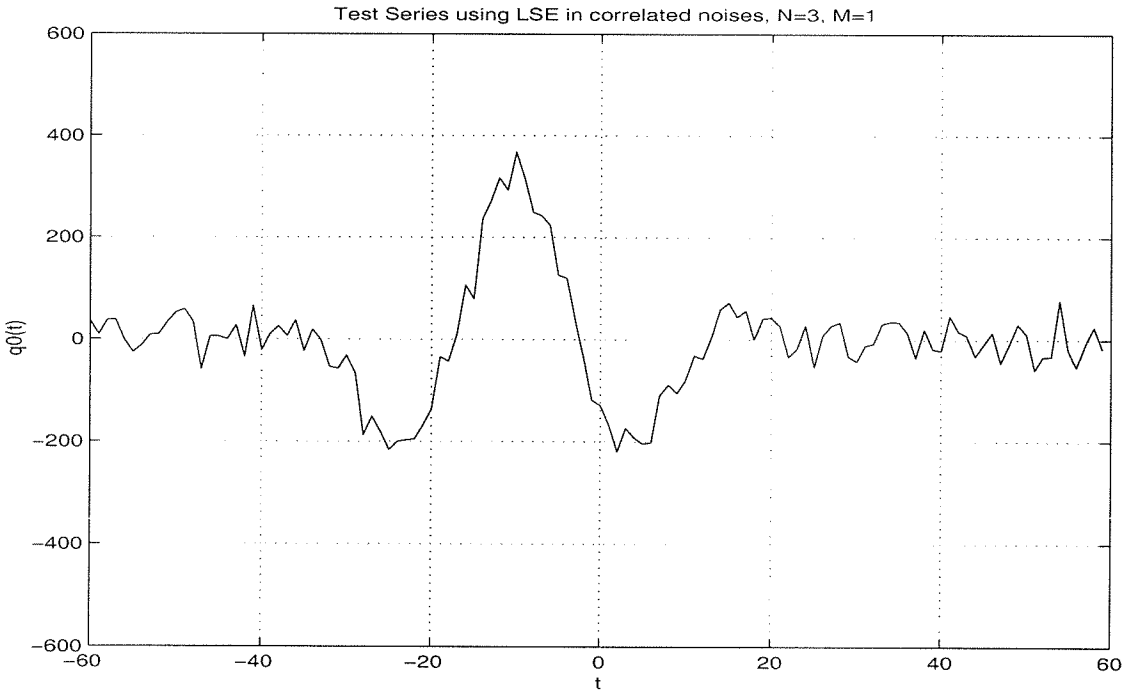

Figure 5.45: LSE result of the time series

Next the LSE is used. Take the grid size $\Delta q = 0.05$, the number of iterations $I = 8000$, initial temperature $T_0 = 2.5 \times 10^5$. The LSE result of the time series is shown in figure 5.45, the standard deviation of the estimated signal is $std(p(t) - q(t)) = 31.5055$. which is greater than that of the MLE result. And the LSE result of the bearing is shown in figure 5.46.

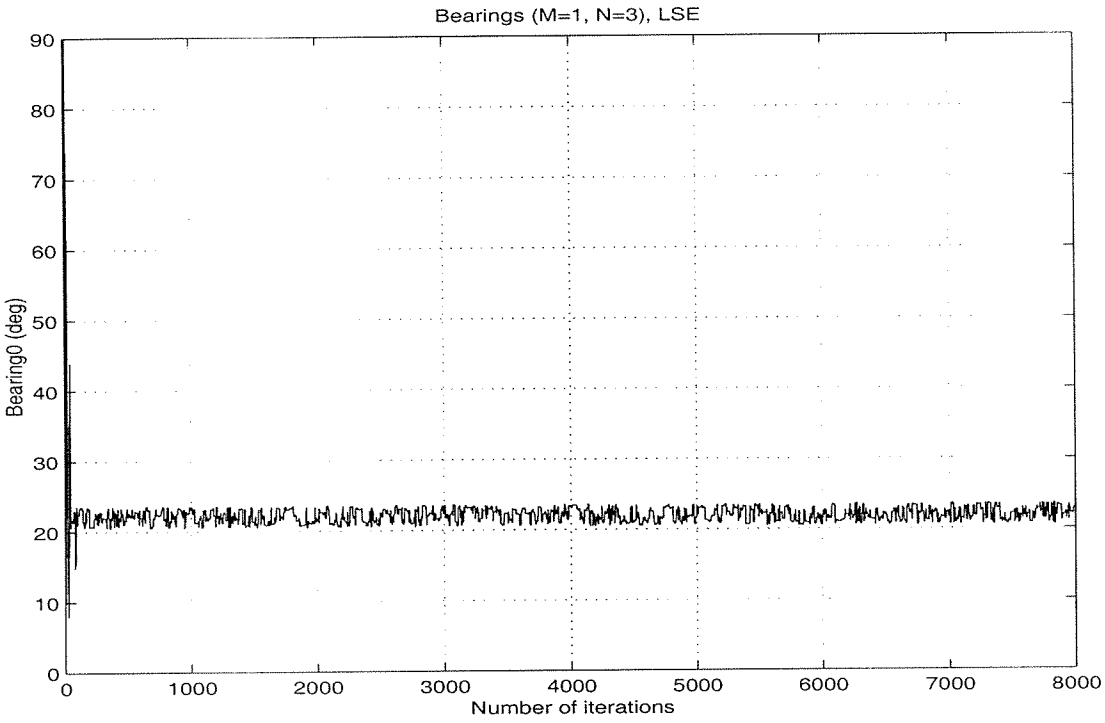

Figure 5.46: LSE result of the bearing

5.1.2.2 Source is multi-impulse

The source is a multi-impulse signal with a bearing of $\theta = 20°$. The time series is given by the equation:

$$p(t) = 350 \sum_{k=-4}^{4} \delta(t + 10k) \tag{5.49}$$

It is shown in figure 5.47. This signal is the sum of the time delayed pulses, is a broad-band signal. The hydrophone data is shown in figure 5.48.

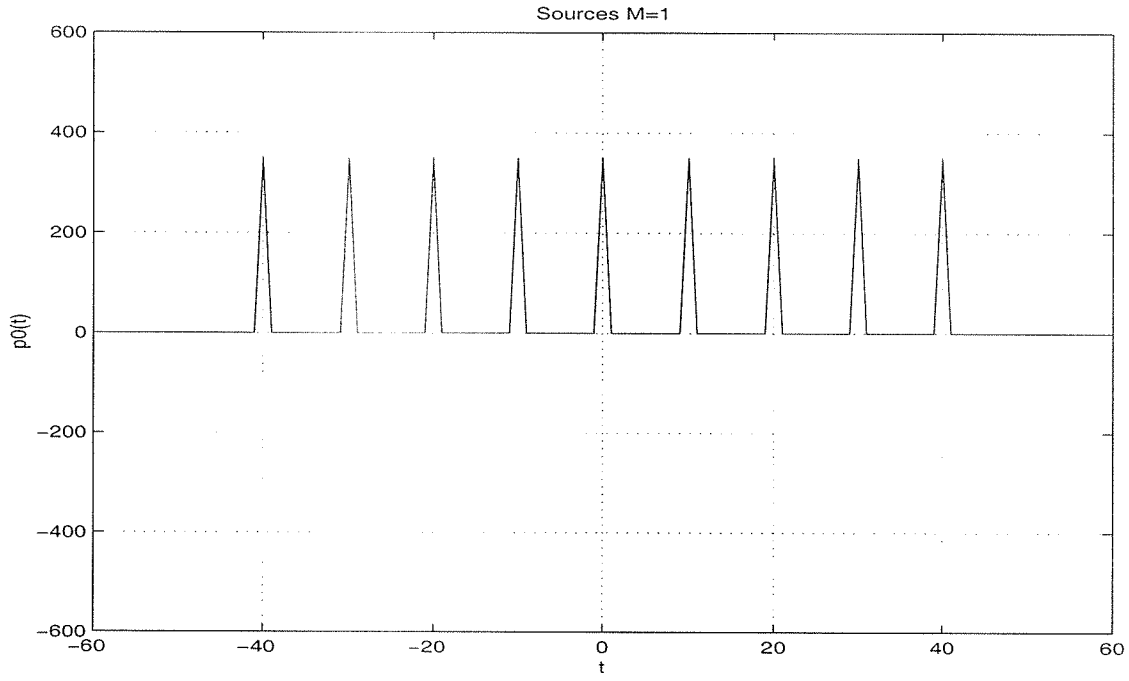

Figure 5.47: Source is multi-impulse

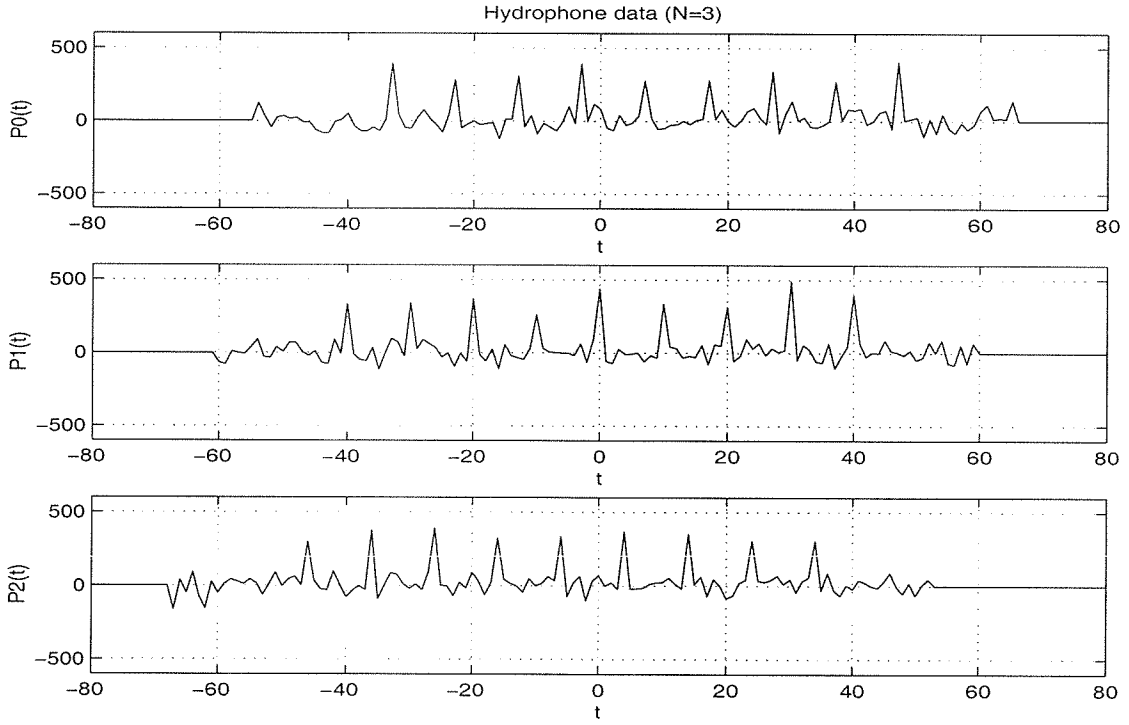

Figure 5.48: Hydrophone data when the source is multi-impulse

Both MLE and LSE are used to estimated the signal. When using MLE, take the grid size $\Delta q = 0.5$, the number of iterations $I = 8000$, initial temperature $T_0 = 5.0 \times 10^4$. The MLE result of the time series is shown in figure 5.49, the standard deviation of the estimated signal is $std(p(t) - q(t)) = 26.7640$, and the MLE result of the bearing is shown in figure 5.50, it's around the true value, $20°$.

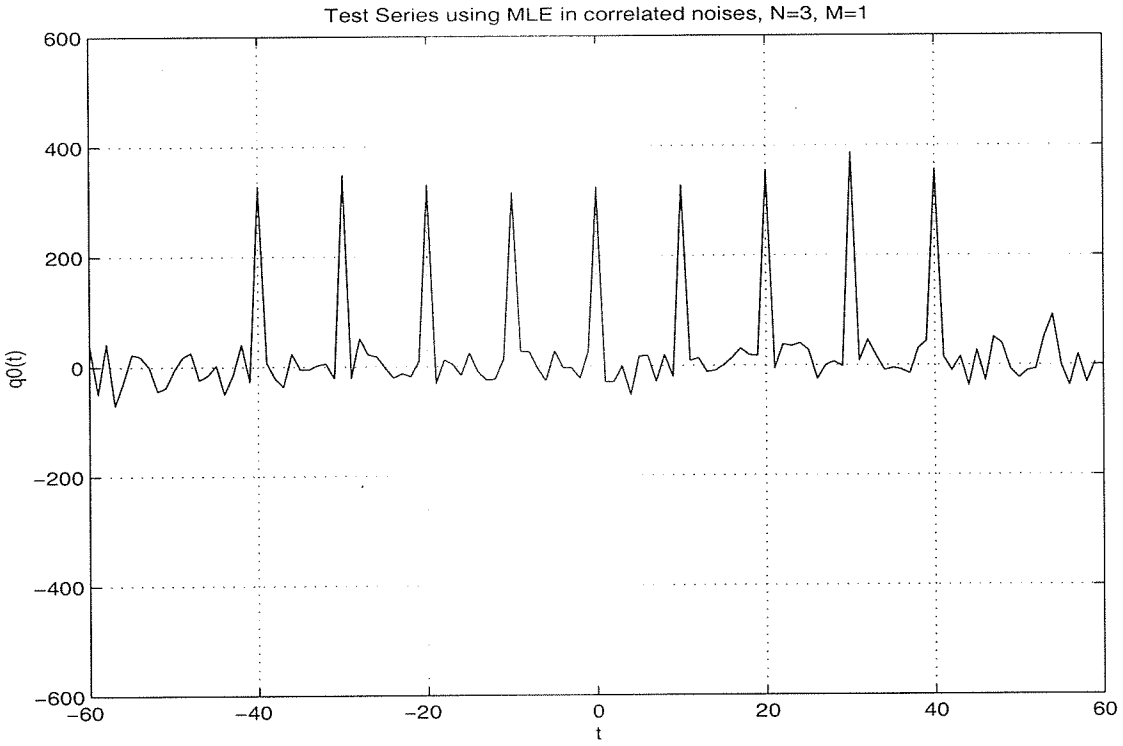

Figure 5.49: MLE result of the time series

For the LSE case, take the grid size $\Delta q = 0.5$, the number of iterations $I = 8000$, initial temperature $T_0 = 5.0 \times 10^6$. The LSE result of the time series is shown in figure 5.51. The standard deviation of the estimated signal is $std(p(t) - q(t)) = 33.5828$, which is greater than that of the MLE result. And the LSE result of the bearing is shown in figure 5.52.

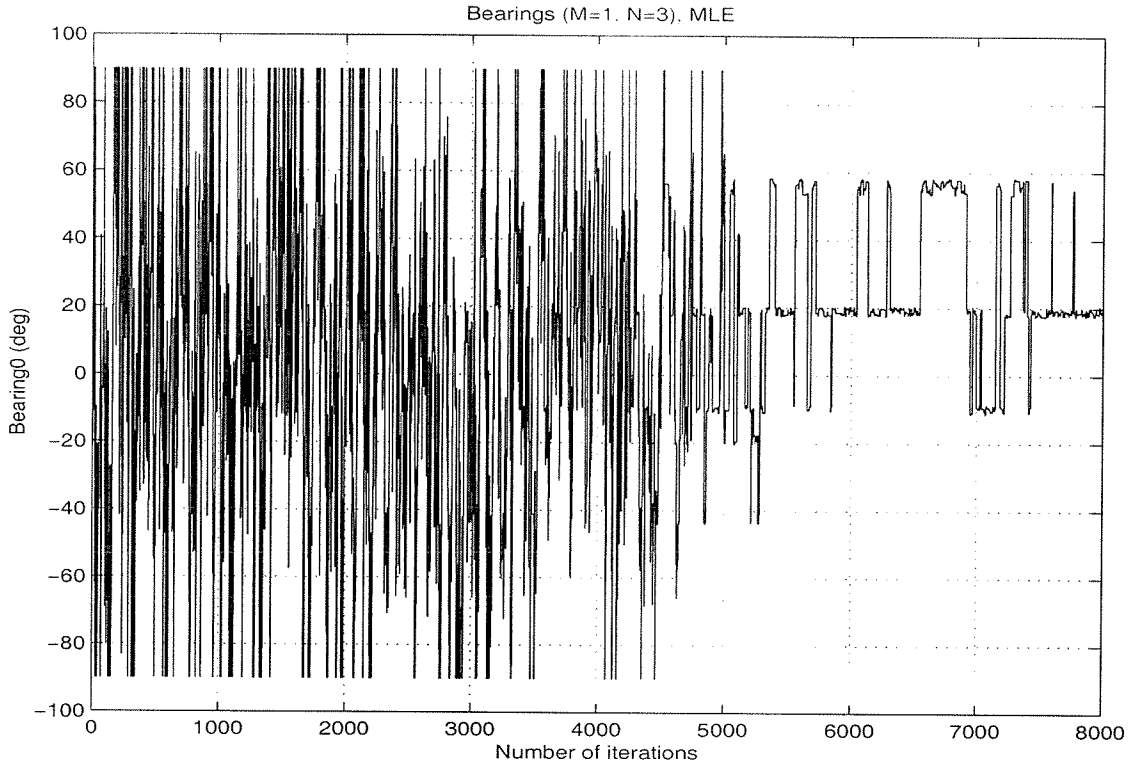

Figure 5.50: MLE result of the bearing

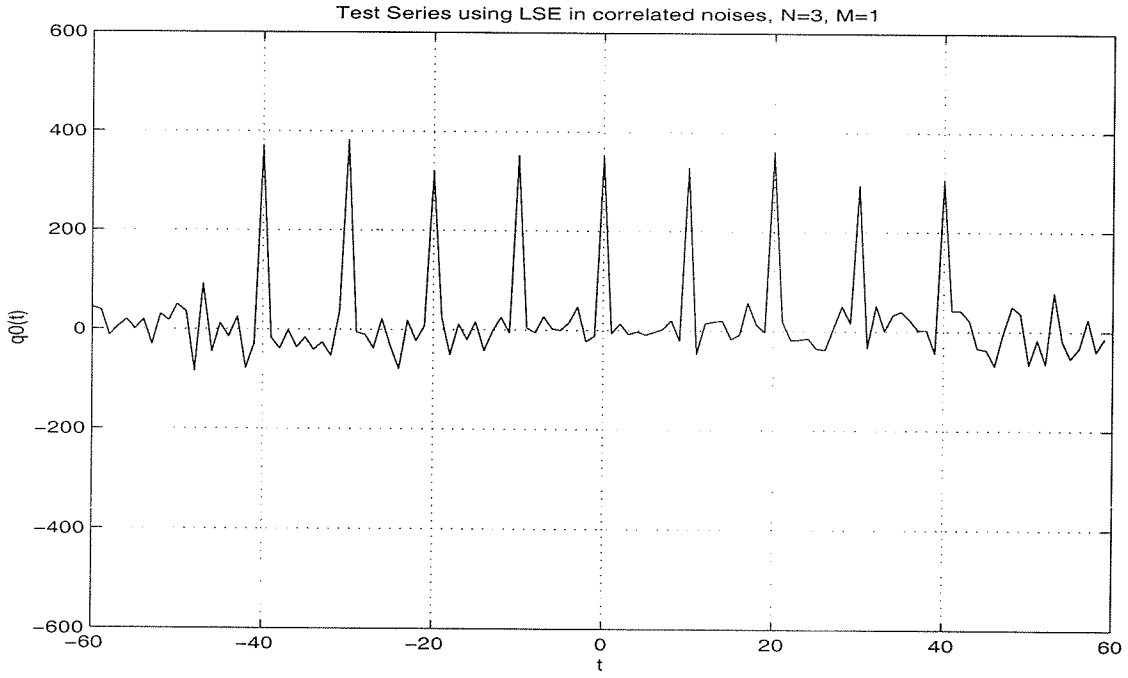

Figure 5.51: LSE result of the time series

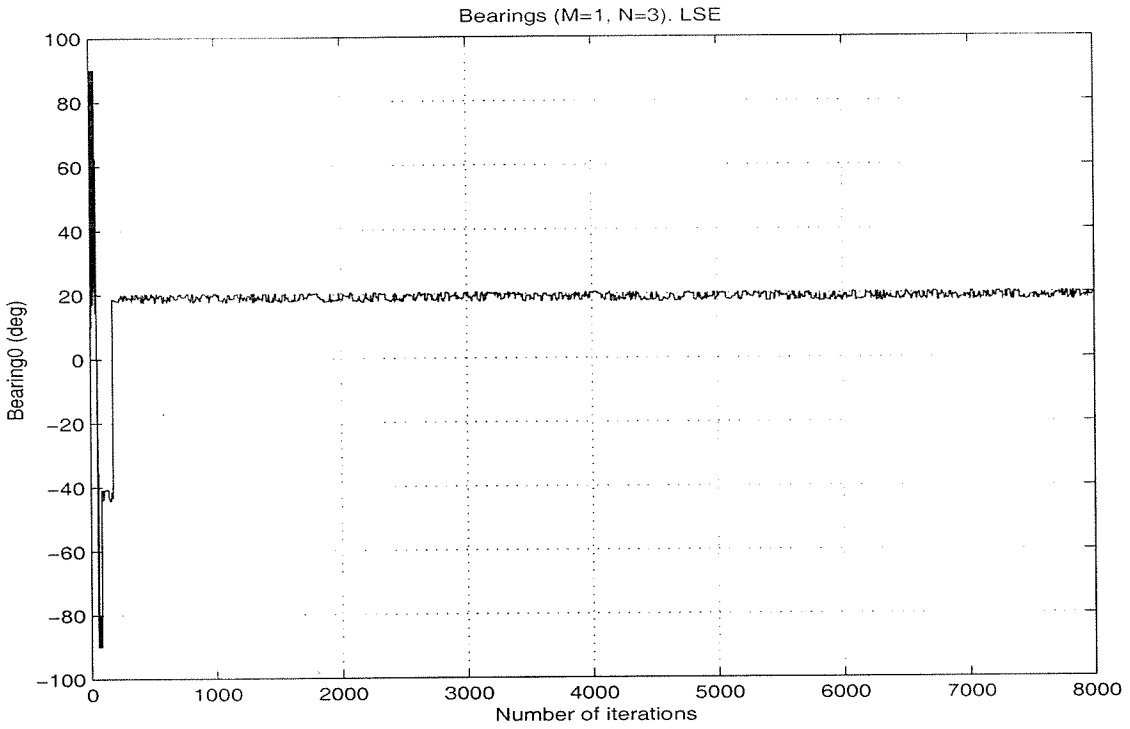

Figure 5.52: LSE result of the bearing

5.1.2.3 Multi-source

For various different sources from different directions, based on the array data, both Least Squares Estimation and Maximum Likelihood Estimation are used to find out the signals.

Several examples dealing with different cases are simulated.

Suppose there are 3 plane wave sources, $M = 3$. The 3 signals are shown in figure 5.53. The time series are broadband signals. They are given by

$$p_0(t) = \exp\left\{-\left[\frac{t+10}{20}\right]^2\right\}\cos\left[\frac{2\pi(t+10)}{30}\right] \tag{5.50}$$

$$p_1(t) = -\exp\left\{-\left[\frac{t}{20}\right]^2\right\}\cos\left[\frac{2\pi t}{20}\right] \tag{5.51}$$

$$p_2(t) = \exp\left\{-\left[\frac{t-10}{20}\right]^2\right\}\cos\left[\frac{2\pi(t-10)}{15}\right] \tag{5.52}$$

Signal 0 comes with an angle of $\theta_0 = 20°$, signal 1comes with an angle of $\theta_1 = -30°$, signal 2 comes with an angle at $\theta_2 = 45°$. The amplitude of the signals is normalized to 1.

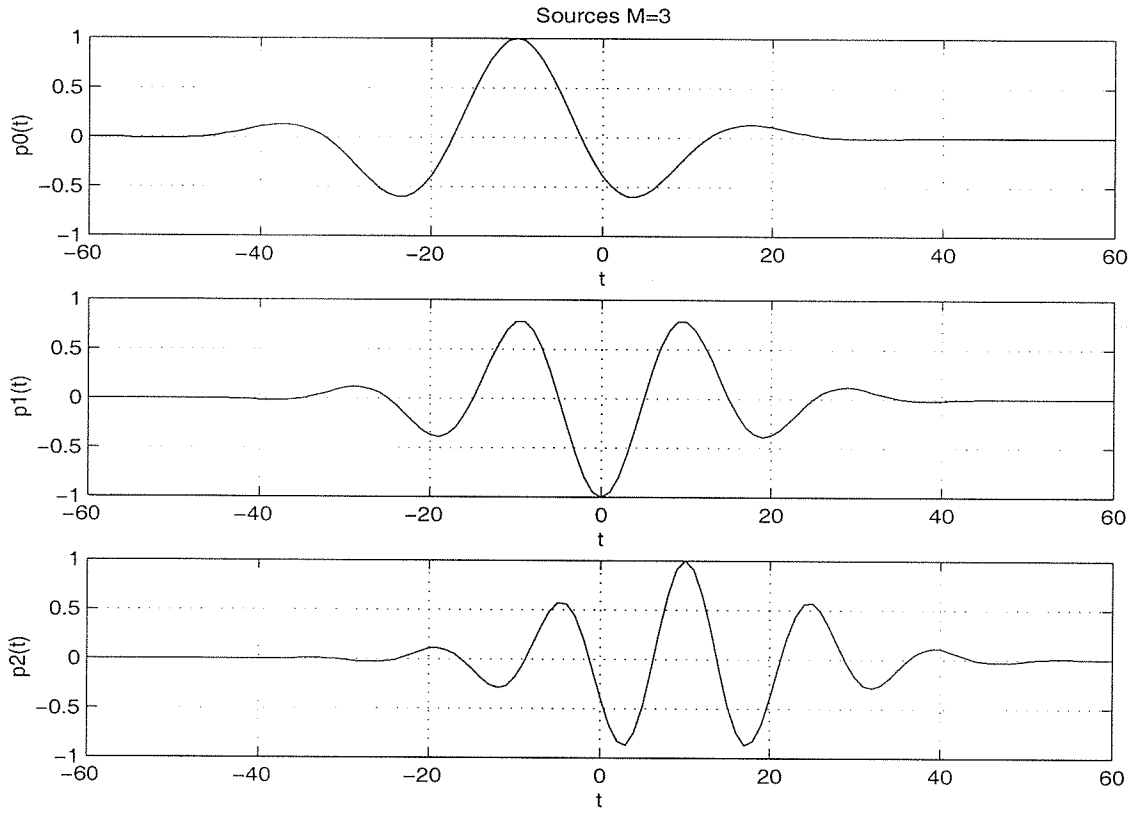

Figure 5.53: Broadband sources

The variance of the noise at each hydrophone is at the same level. Two single arrays are used to solve this problem. First, an array of 5 hydrophones is employed. Second, an array of 25 hydrophones is used.

5.1.2.3.1 An array of 5 hydrophones is used

For this case, the noise is shown in figure 5.54. The hydrophone data is shown in figure 5.55.

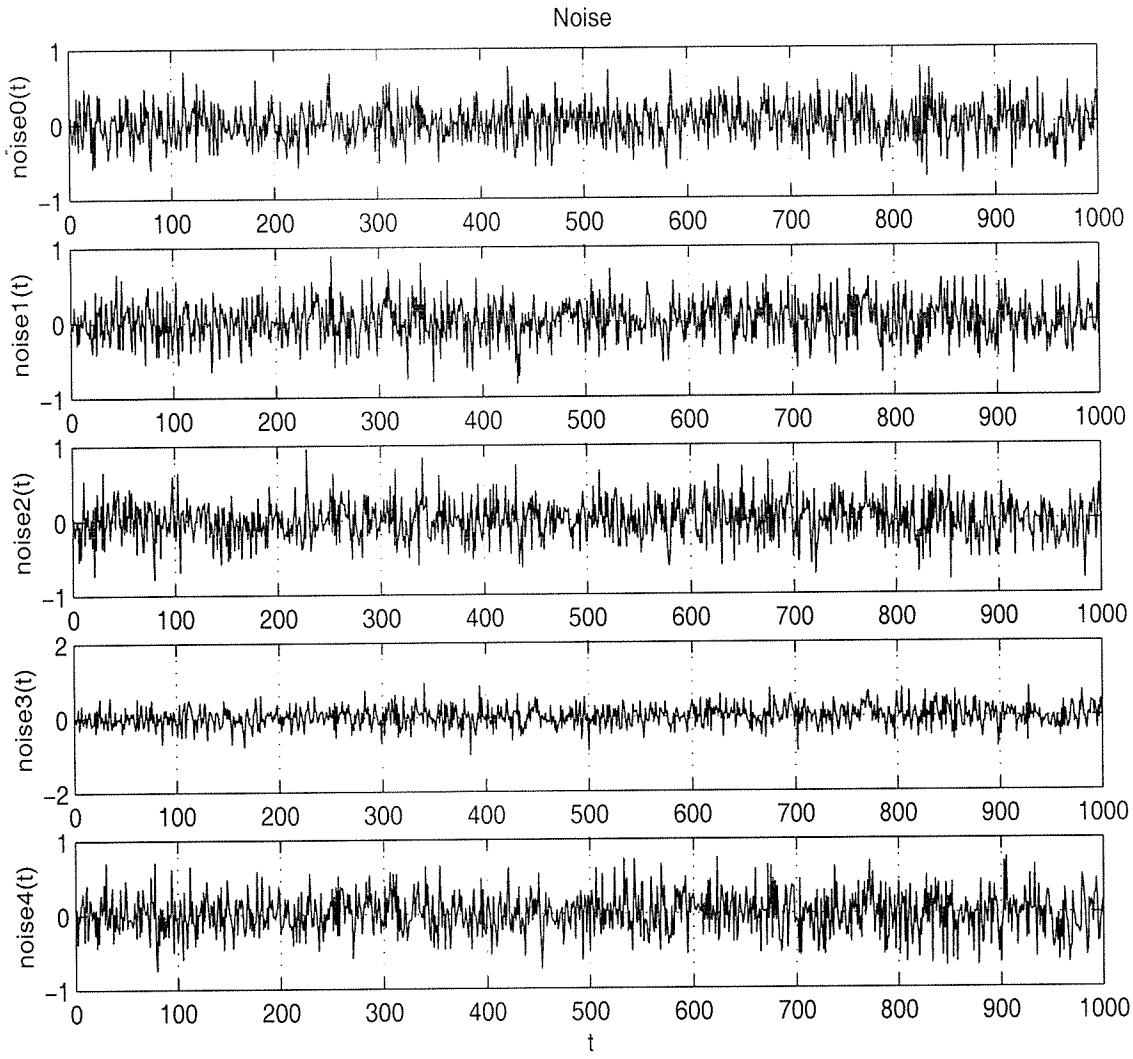

Figure 5.54: Spatially correlated noise (N=5)

Both MLE and LSE are employed to estimate the signal time series and their bearings. When using MLE, take the grid size $\Delta q = 0.0015$, the number of iterations $I = 10000$, initial temperature $T_0 = 37500$. The MLE result of the time series is shown in figure 5.56. The standard deviation of the estimated signals is $std(p_0(t) - q_0(t)) = 0.0936$, $std(p_1(t) - q_1(t)) = 0.0988$, and $std(p_2(t) - q_2(t)) = 0.1025$ respectively. The MLE result of the bearings is shown in figure 5.57, the estimated bearings are roughly the real value: $\hat{\theta}_0 = 20°$, $\hat{\theta}_1 = -30°$, and $\hat{\theta}_2 = 45°$ respectively.

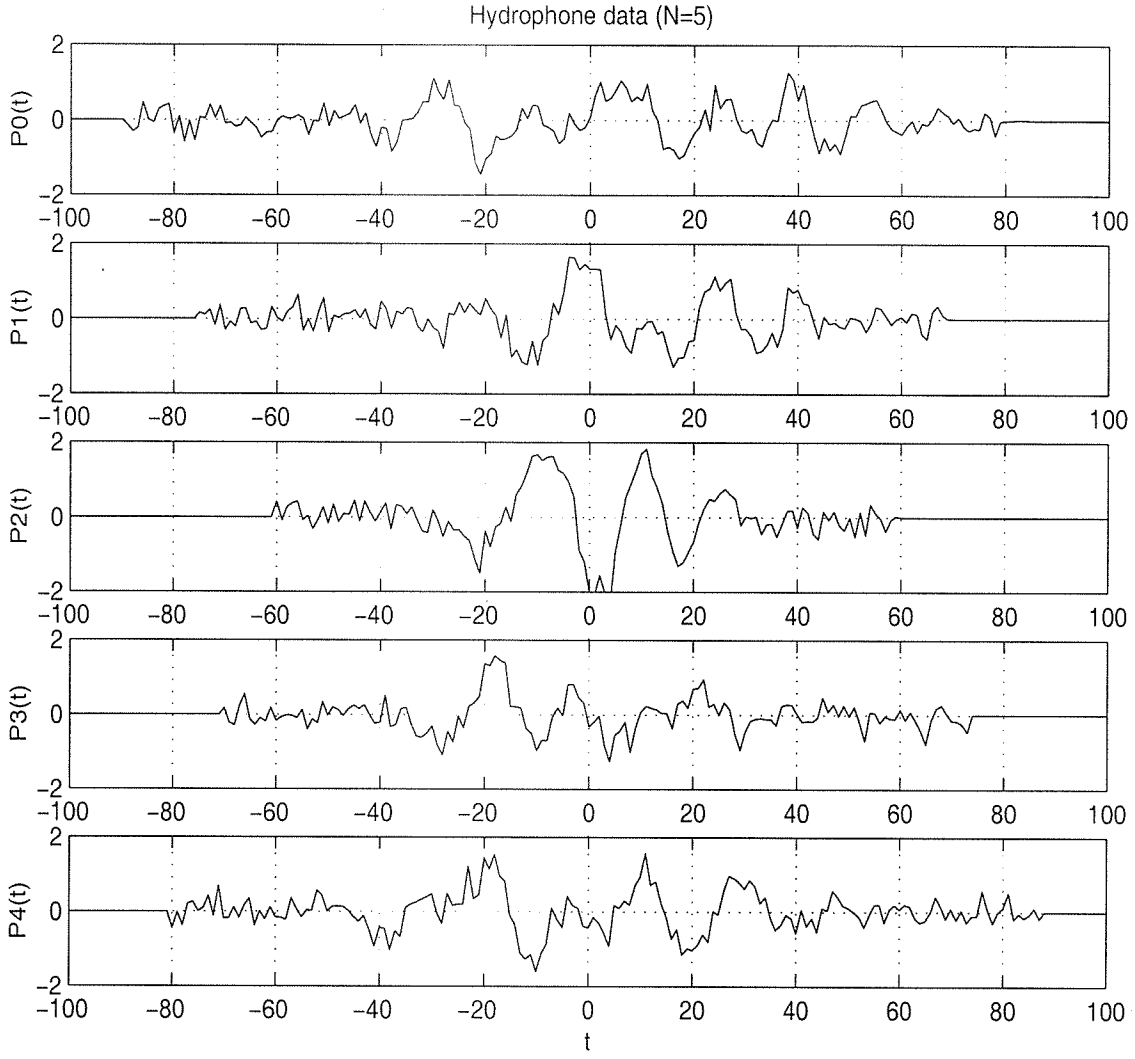

Figure 5.55: Hydrophone data (N=5)

When using the LSE, take the grid size $\Delta q = 0.002$, the number of iterations $I = 10000$, the initial temperature $T_0 = 3.75 \times 10^4$. The LSE result of the time series is shown in figure 5.58, the standard deviation of the estimated signals is $std(p_0(t) - q_0(t)) = 0.1557$, $std(p_1(t) - q_1(t)) = 0.1507$, and $std(p_2(t) - q_2(t)) = 0.1206$ respectively. They are larger than those of the MLE result. This means that the MLE is better than the LSE, the standard deviation of the estimated signals is smaller, closer to the true value. The LSE result of the bearings is shown in figure 5.59.

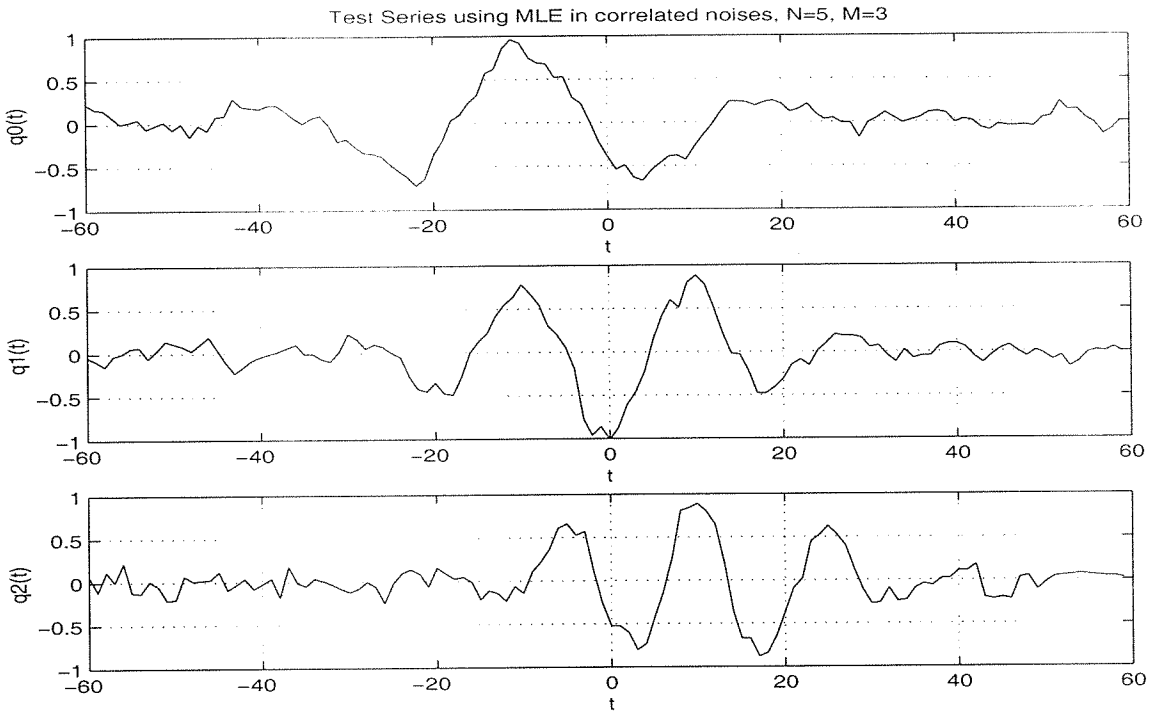

Figure 5.56: MLE result of the time series (N=5)

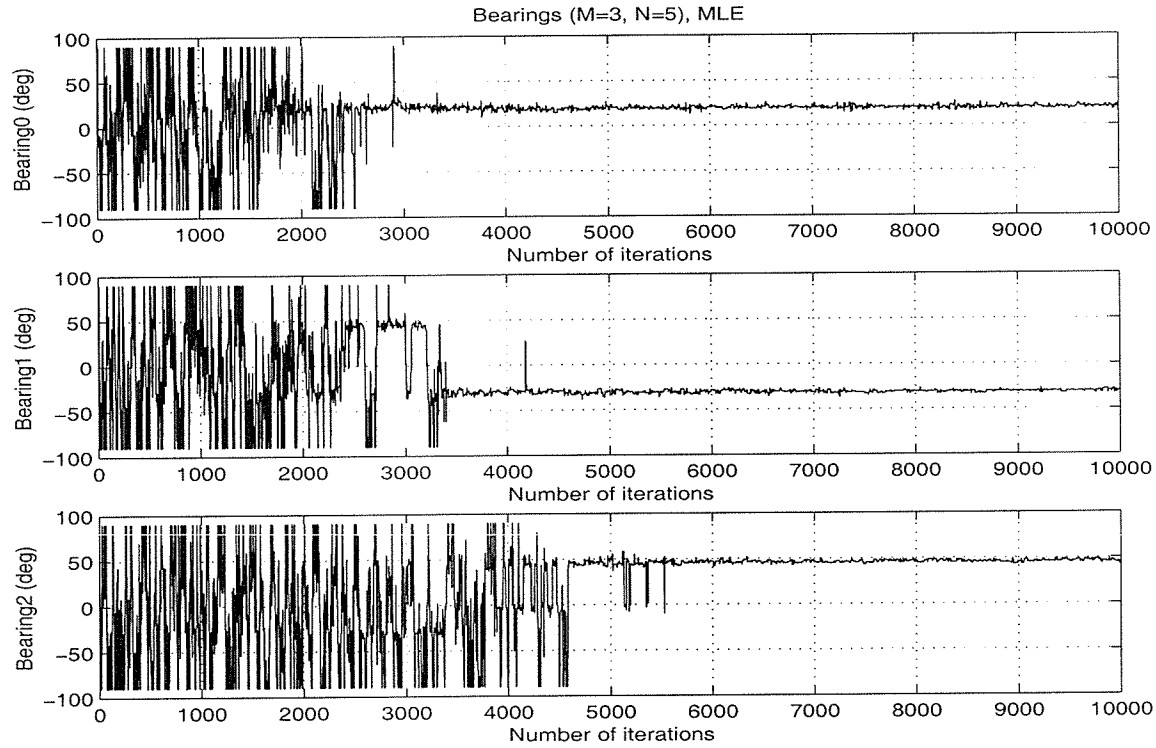

Figure 5.57: MLE result of the bearings (N=5)

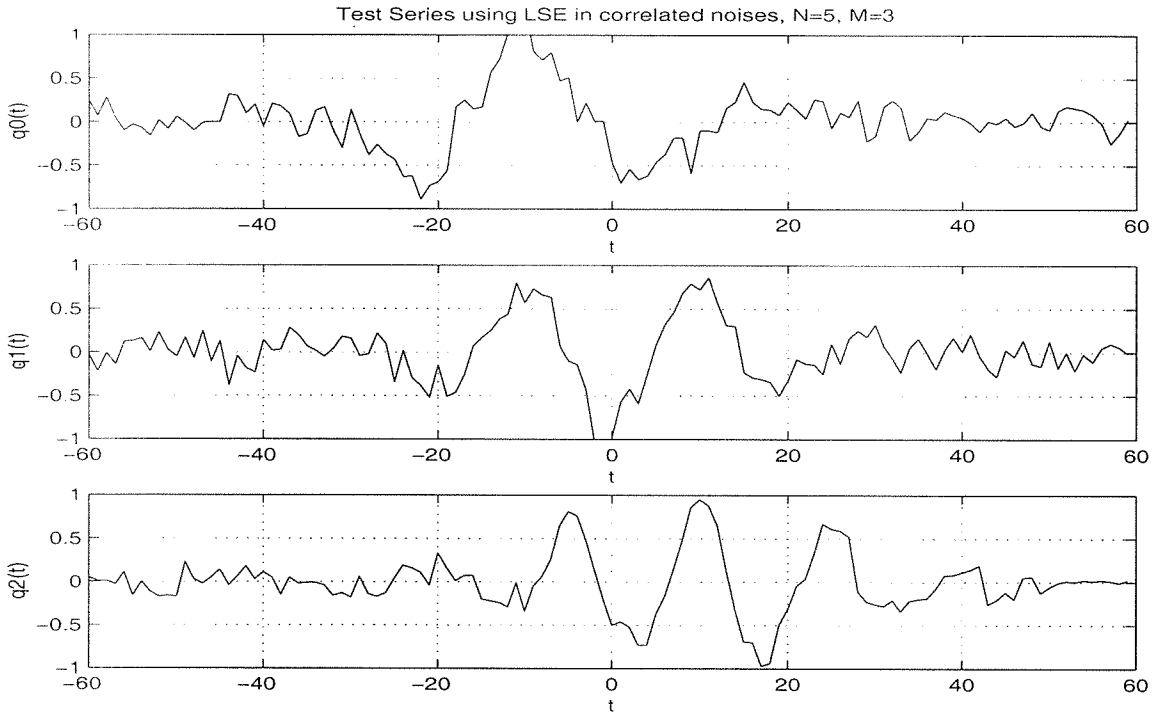

Figure 5.58: LSE result of the time series (N=5)

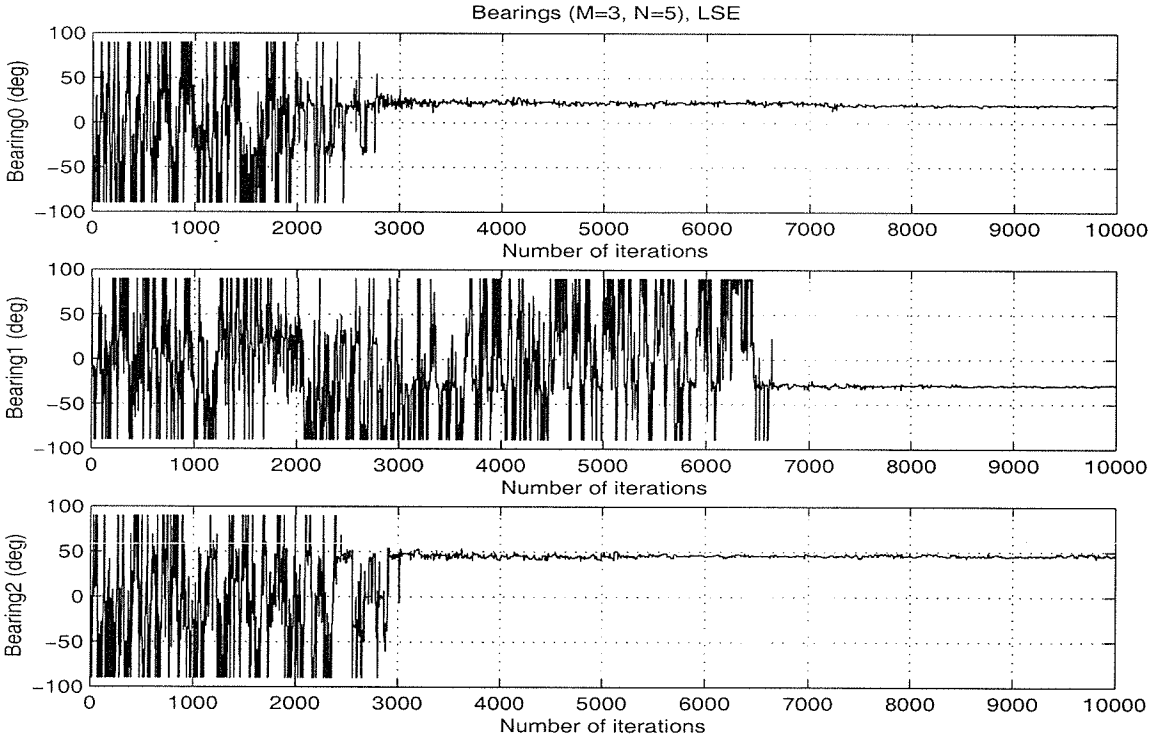

Figure 5.59: LSE result of the bearings (N=5)

5.1.2.3.2 An array of 25 hydrophones is used

For this case, the noise is shown in figure 5.60, 5.61, and 5.62. The hydrophone data is shown in figure 5.63, 5.64, and 5.65.

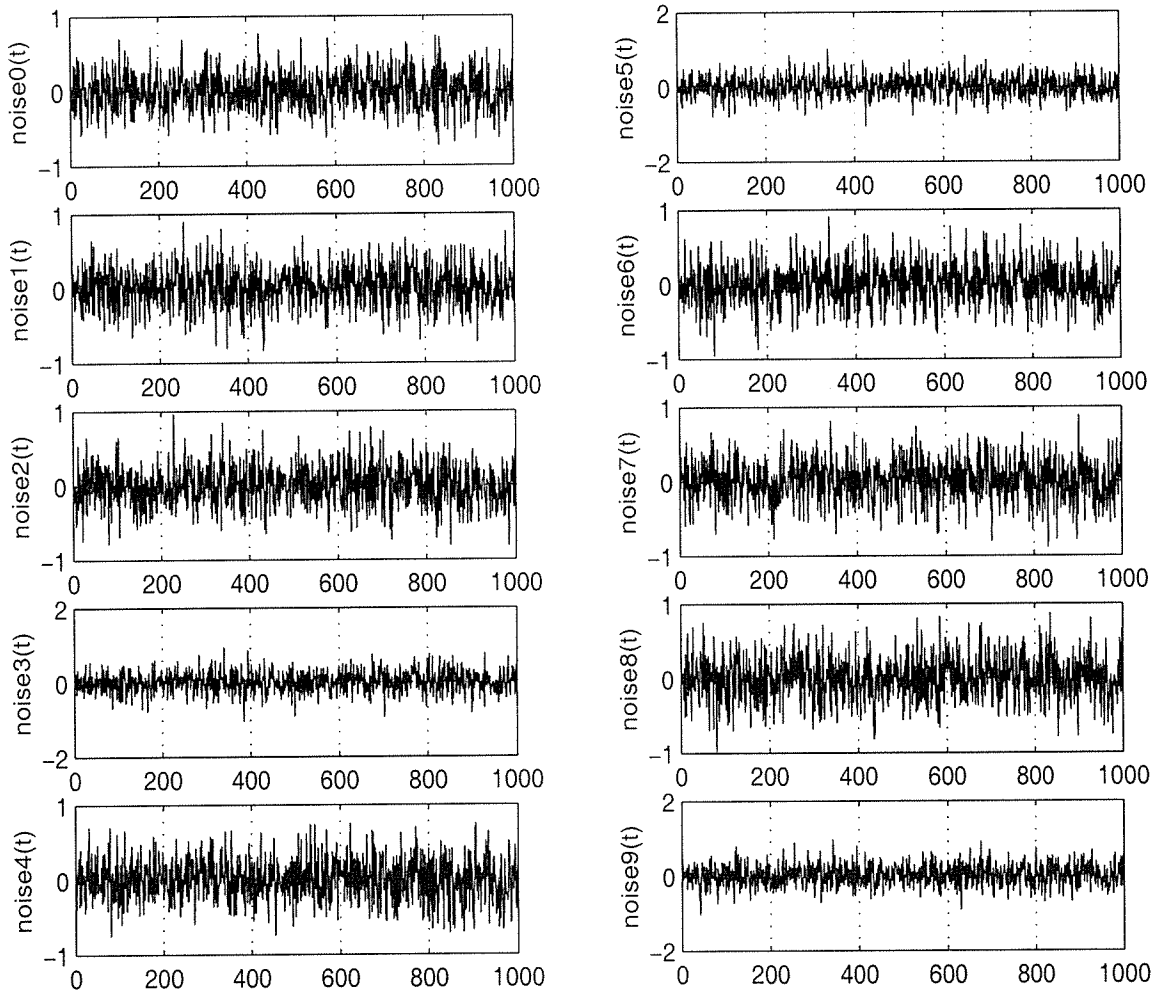

Figure 5.60: Spatially correlated noise (N=25)

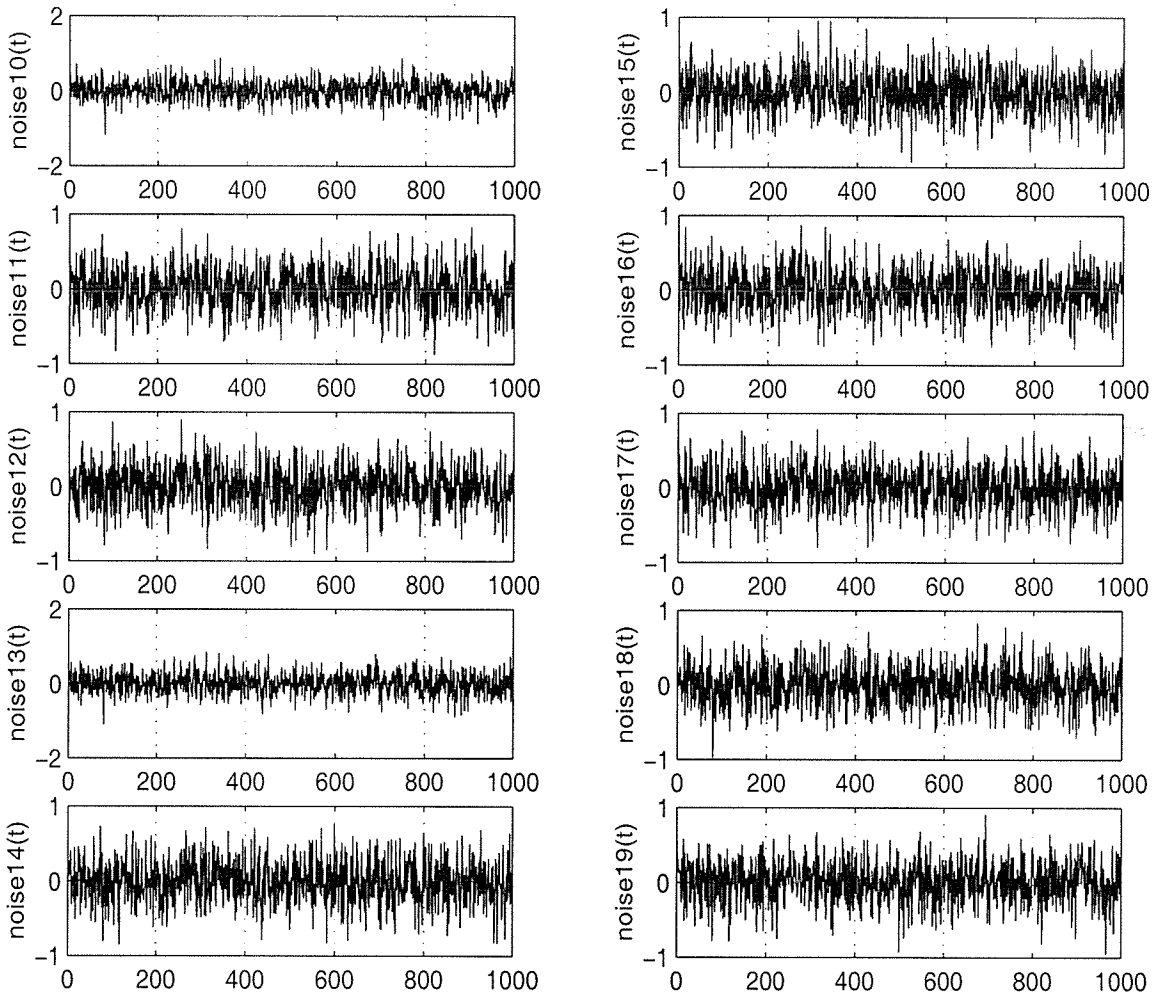

Figure 5.61: Spatially correlated noise (Cont.) (N=25)

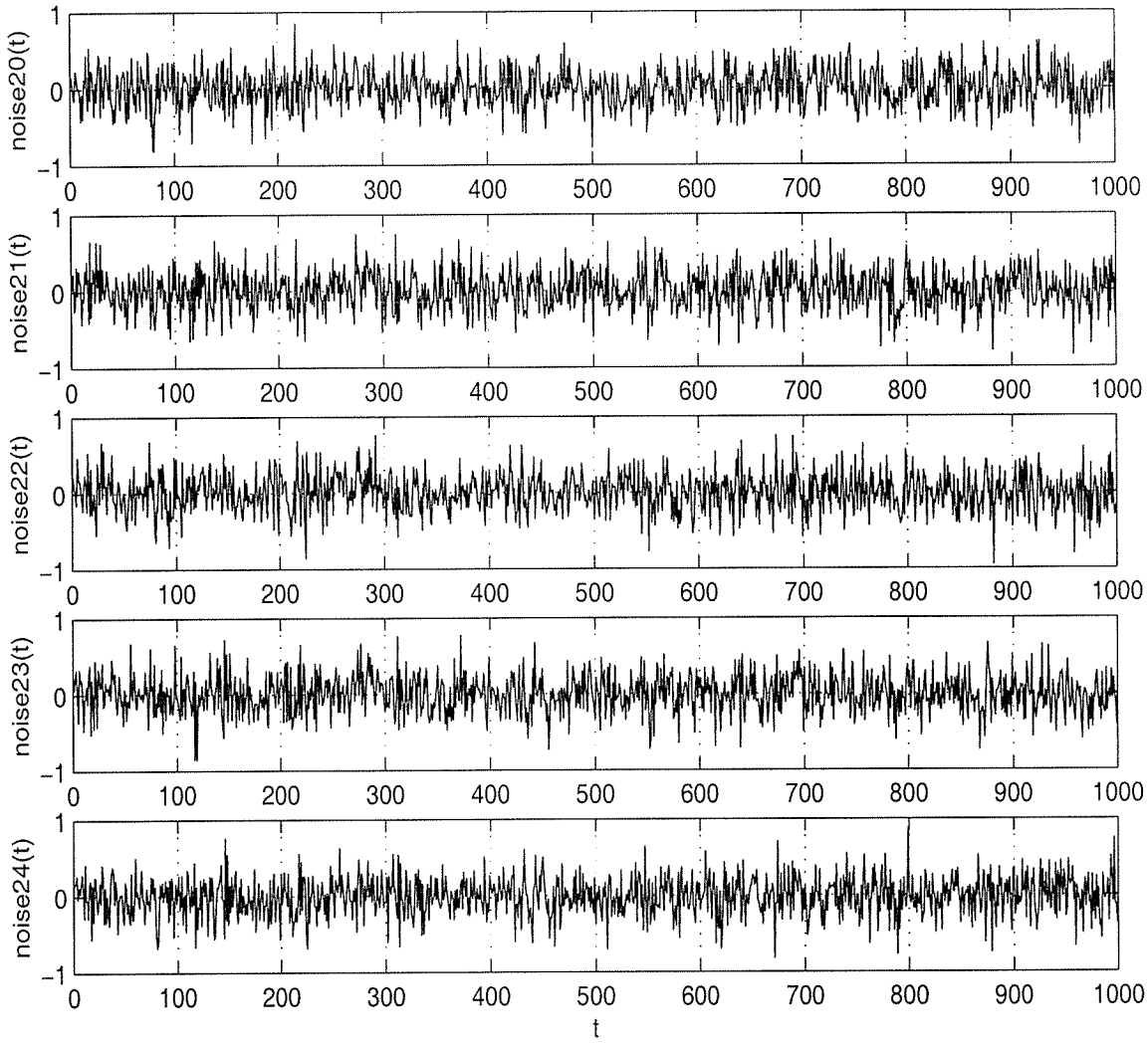

Figure 5.62: Spatially correlated noise (Cont.) (N=25)

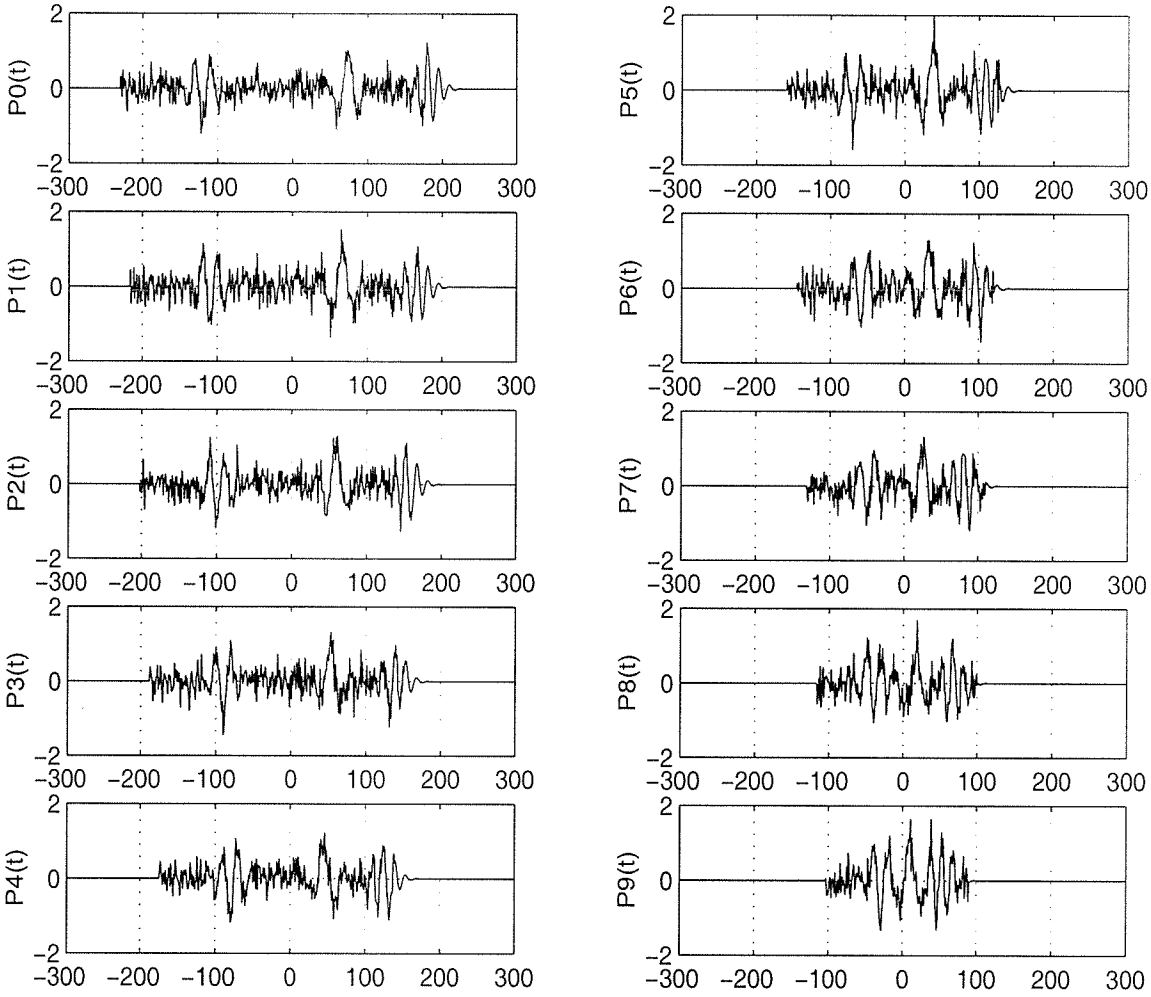

Figure 5.63: Hydrophone data (N=25)

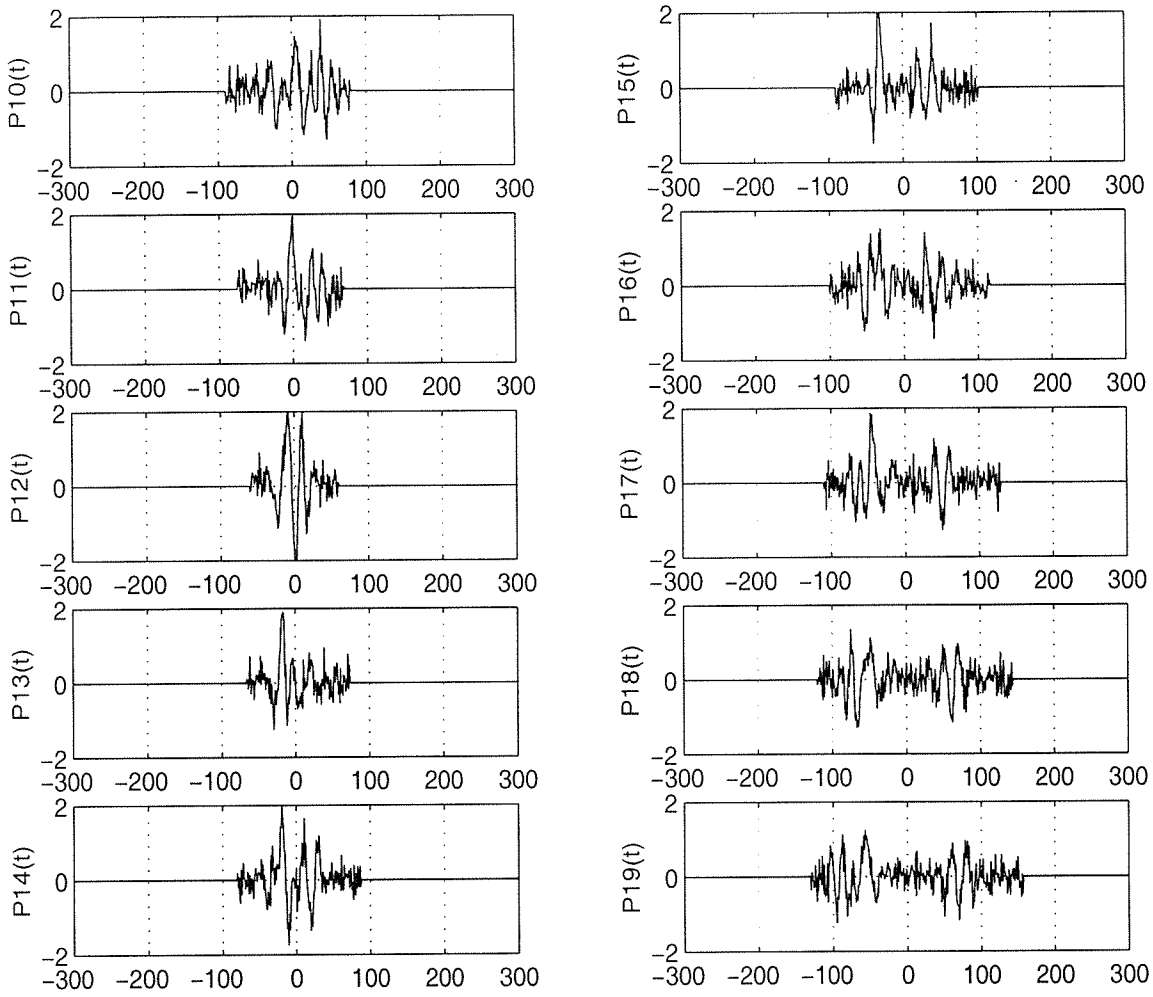

Figure 5.64: Hydrophone data (Cont.) (N=25)

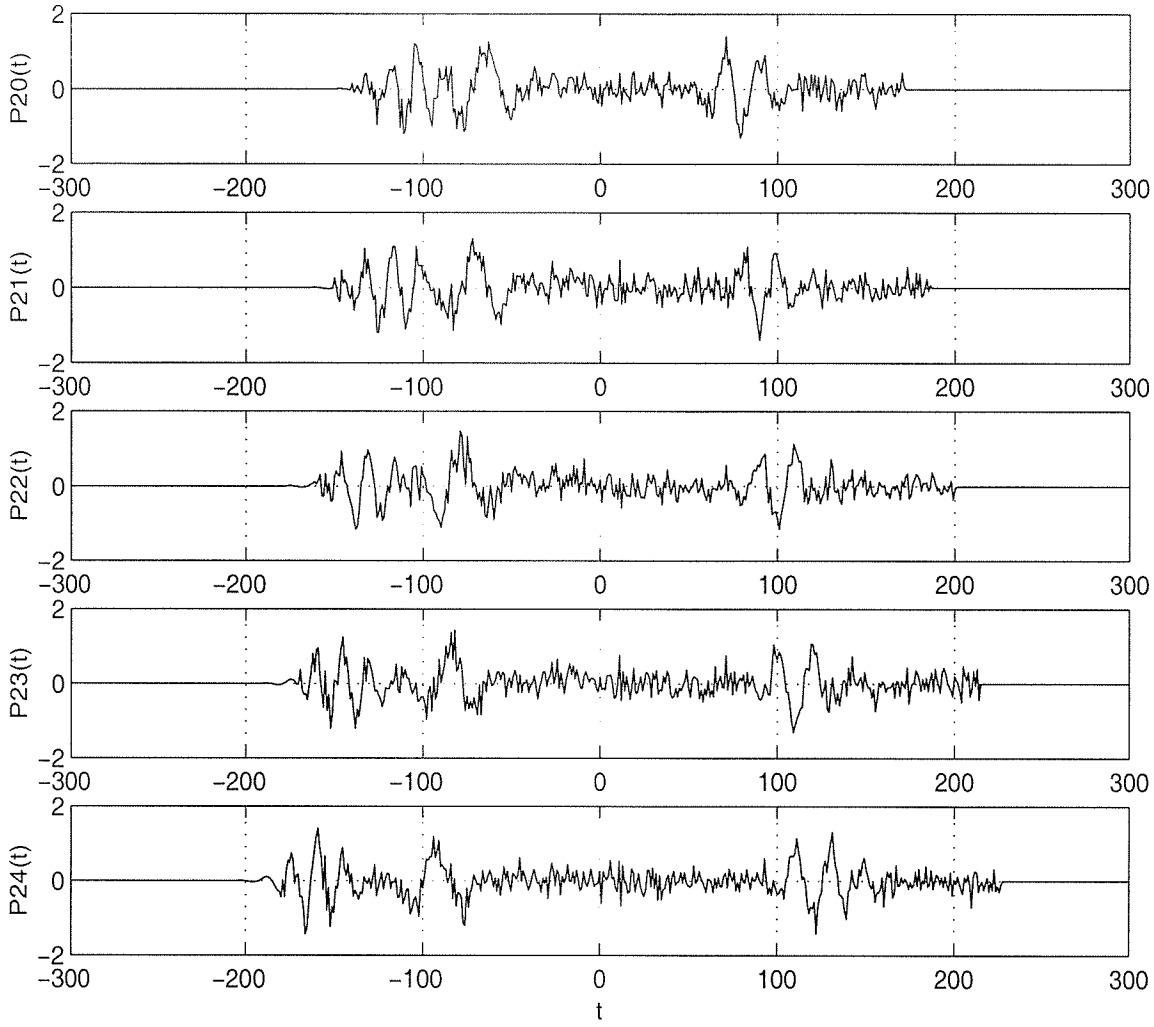

Figure 5.65: Hydrophone data (Cont.) (N=25)

Both MLE and LSE are used to estimate the signal time series and their bearings. When using MLE, take the grid size $\Delta q = 0.001$, the number of iterations $I = 10000$, the initial temperature $T_0 = 2.5 \times 10^4$. The MLE result of the time series is shown in figure 5.66. The standard deviation of the estimated signals is $std(p_0(t) - q_0(t)) = 0.0433$, $std(p_1(t) - q_1(t)) = 0.0650$, and $std(p_2(t) - q_2(t)) = 0.0434$ respectively. The MLE result of the bearings is shown in figure 5.67.

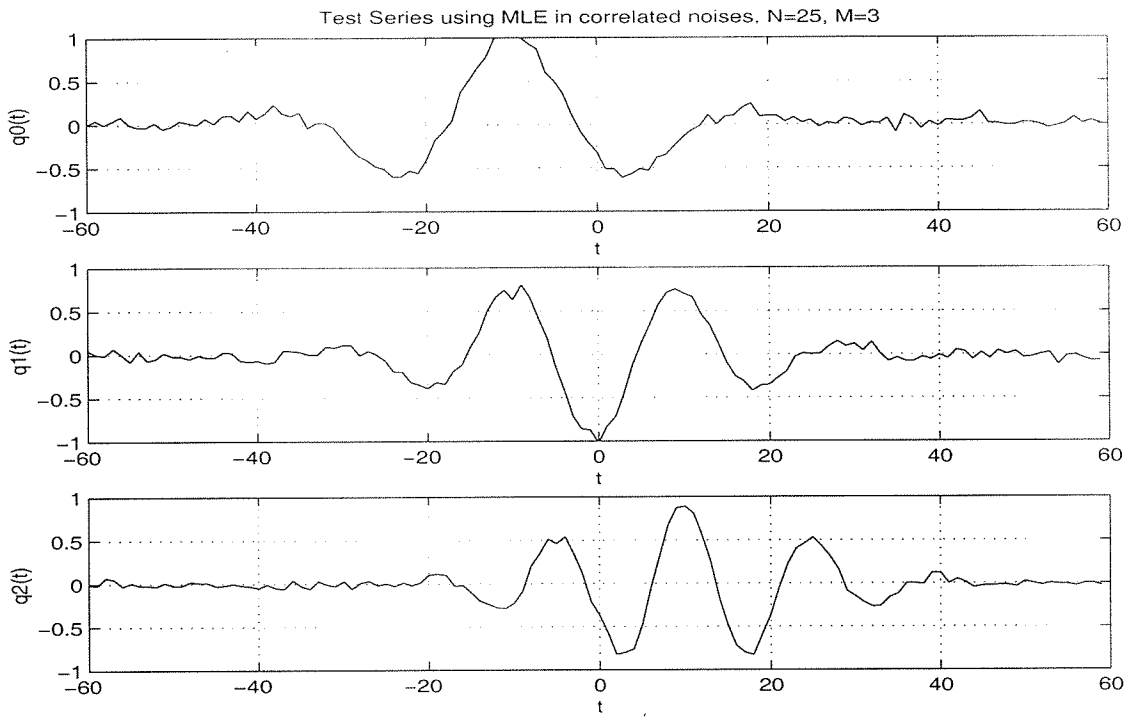

Figure 5.66: MLE result of the time series (N=25)

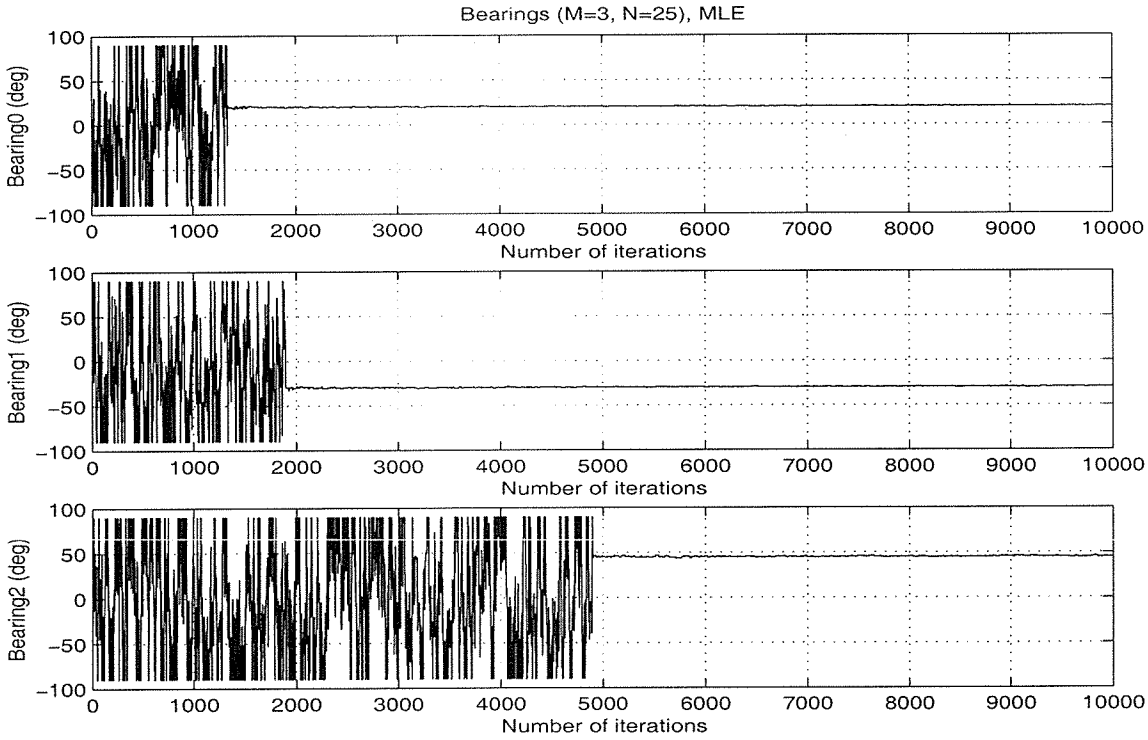

Figure 5.67: MLE result of the bearings (N=25)

When using LSE, take the grid size $\Delta q = 0.002$, the number of iterations $I = 10000$, the initial temperature $T_0 = 3.75 \times 10^4$. The LSE result of the time series is shown in figure 5.68, the standard deviation of the estimated signals is $std(p_0(t) - q_0(t)) = 0.0526$, $std(p_1(t) - q_1(t)) = 0.0786$, and $std(p_2(t) - q_2(t)) = 0.0526$, respectively. They are greater than those of the MLE result. This means that the estimated values by using MLE is closer to the true values, thus MLE is better than LSE in time series estimation. The LSE result of the bearings is shown in figure 5.69.

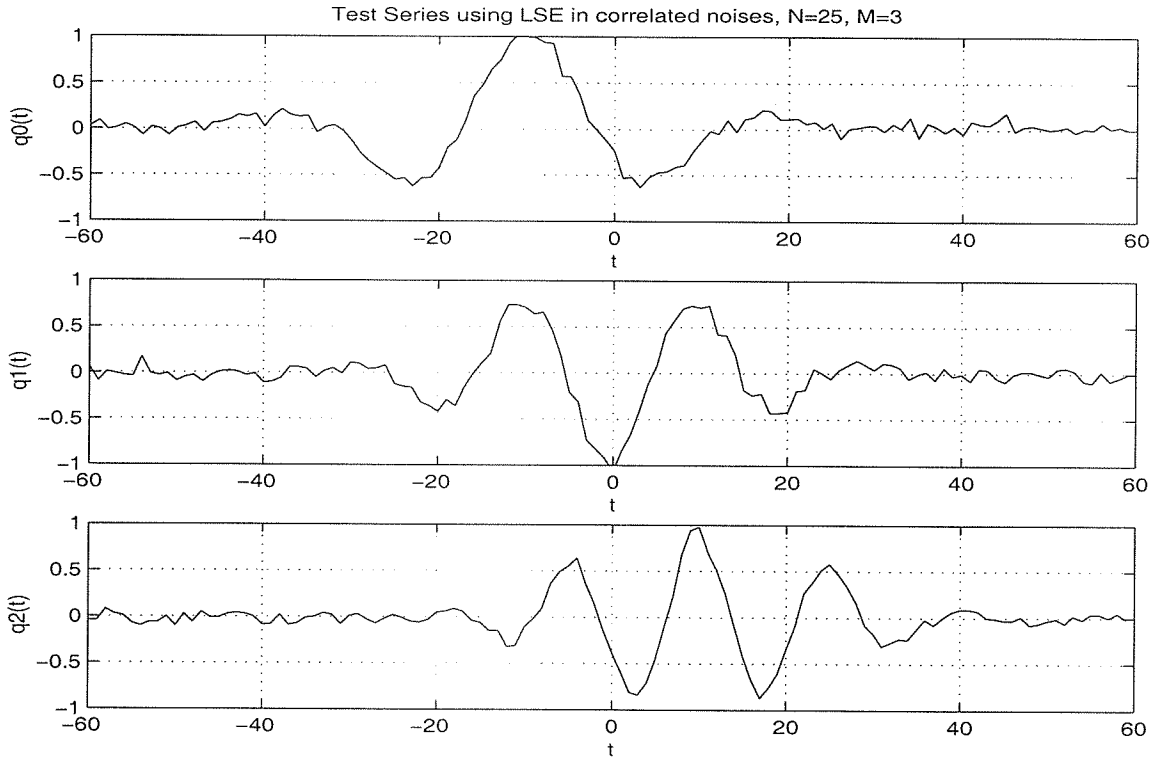

Figure 5.68: LSE result of the time series (N=25)

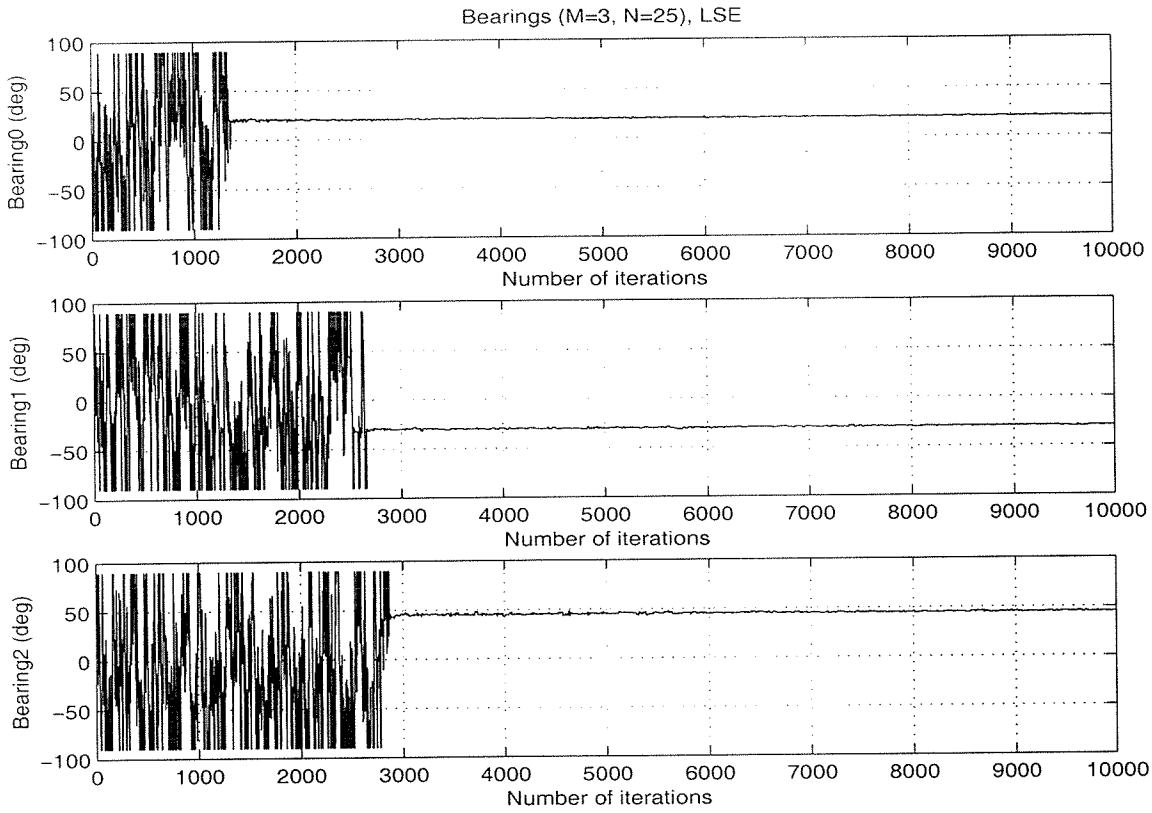

Figure 5.69: LSE result of the bearings (N=25)

5.2 Surface generated noise in a waveguide

Surface generated noise is the major ocean ambient noise in our beamforming problem, especially in shallow water case. Assume that the sources are located in a infinite plane parallel to the ocean surface, the plane is below the surface at depth z'. Suppose the sources are uncorrelated, but when they propagate to the array, the hydrophone data will have some correlation because of multi-path. Let (r_1, z_1) and (r_2, z_2) be two arbitrary points in the water.

Suppose the water is a stratified medium, in which the sound velocity and density are only functions of the depth. In this case, the noise field can be represented by normal modes. If the medium is finite in depth with appropriate boundary conditions, the normal

modes will be discrete and the propagating modes will be finite in number. We take this case as an example.

In this example, we use a simplified isovelocity homogeneous waveguide bounded above by a pressure release surface and below by a pressure release bottom. The effects of the channel on the signal are limited to absorption and multipath generation. Absorption in the medium can be modeled as a function of frequency. The frequency-dependent attenuation coefficient is given by the following equation

$$\alpha(f) = \frac{0.1f^2}{1+f^2} + \frac{40f^2}{4100+f^2} + 2.75\times 10^{-4} f^2 \tag{5.53}$$

where $\alpha(f)$ is in dB per kiloyard, and f is in kHz.[9]

At arbitrary field points (r_1, z_1) and (r_2, z_2), the spatial correlation is given by[14]

$$C(R, z_1, z_2) = \frac{2\pi q^2 \rho_s^2(z')}{\varepsilon \kappa H^2} \sum_{n=1}^{n_{max}} \sin(\lambda_n z')^2 \sin(\lambda_n z_1)\sin(\lambda_n z_2) J_0(\kappa_n R) \tag{5.54}$$

where H is the water depth

R is the radial distance between the two points $R = |\vec{R}| = |\vec{r_1} - \vec{r_2}|$

q is a constant

$\rho_s(z')$ is the density of the medium at the depth of the noise sources

ε is the propagating attenuation coefficient

κ is the real part of the wavenumber

$\lambda_n = \frac{n\pi}{H}$ is the modal wavelength for the pressure release surface and pressure release bottom case

$n_{max} = \frac{2H}{\lambda} + \frac{1}{2}$ is the number of terms in the modal sum[15]

κ_n is the real part of the modal wave number

We are computing the correlation relationship between the hydrophones. For an equally spacing horizontal array, which is 10m below the surface, R is the hydrophone spacing, z_1 and z_2 are the coordinates in z direction, they are $z_1 = z_2 = 10m$.

Other parameters are,

$$H = 100m$$

$$q = 1$$

$$\rho_s(z') = 1000kg/m^3$$

$$c = 1500m/s$$

Suppose the noise sources are broadband, they are in the frequency range

$$f = 300Hz - 1000Hz$$

then,

$$\lambda = 5m - 1.5m$$

$$n_{max} = 40 - 133$$

$$\alpha(f) = \frac{0.1f^2}{1+f^2} + \frac{40f^2}{4100+f^2} + 2.75\times 10^{-4} f^2 \text{ where } f \text{ is in kHZ}$$

$$\varepsilon = \frac{\lambda\alpha}{1000}$$

$$\kappa = \frac{2\pi f}{c}$$

$$\kappa_n = \frac{2\pi}{\lambda_n}$$

Suppose the number of hydrophones is $N = 3$, the spacing is $h = 1m$ ($R = 1m$). The average cross-spectral density matrix is

$$\underline{C} = \begin{bmatrix} 1.9624 & 0.6636 & 0.1128 \\ 0.6636 & 1.9624 & 0.6636 \\ 0.1128 & 0.6636 & 1.9624 \end{bmatrix} \times 10^6 \tag{5.55}$$

The normalized correlation coefficient matrix is

$$\underline{C_n} = \begin{bmatrix} 1.0000 & 0.3382 & 0.0575 \\ 0.3382 & 1.0000 & 0.3382 \\ 0.0575 & 0.3382 & 1.0000 \end{bmatrix} \tag{5.56}$$

According to the above matrix, the correlated noise time series is generated, shown in figure 5.70.

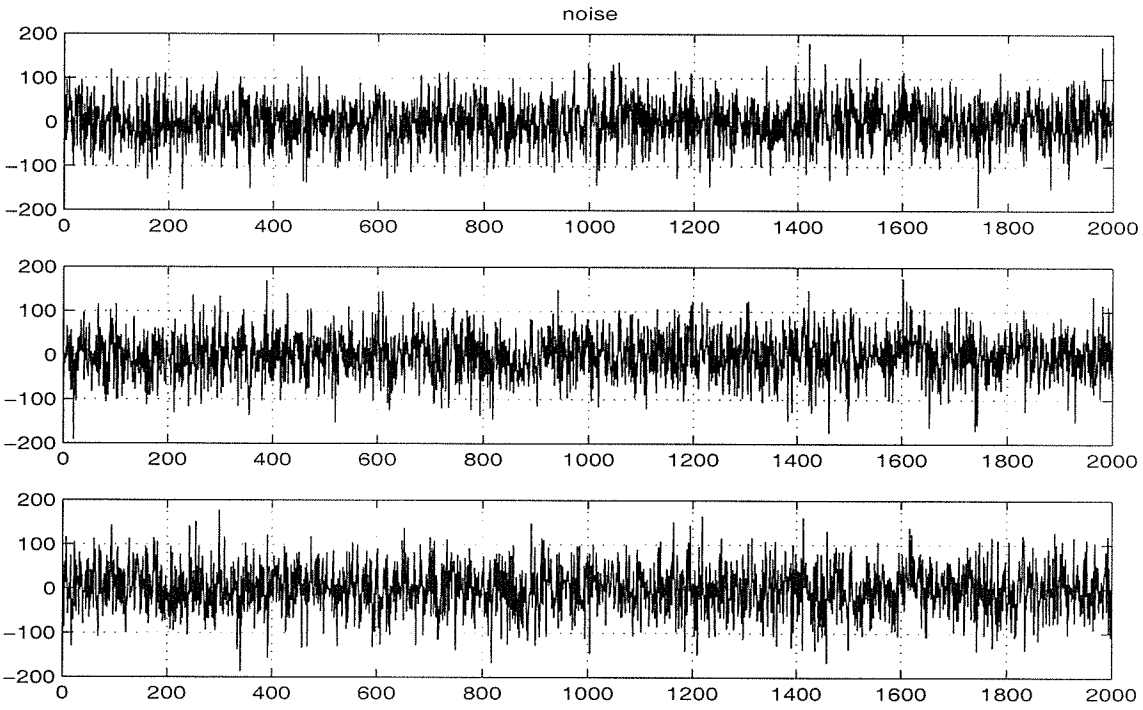

Figure 5.70: Noise in a isovelocity homogeneous waveguide with pressure release surface and pressure release bottom

The source of interest is the same as shown in figure 5.35, but its bearing is $\theta = 30°$. The hydrophone data is shown in figure 5.71.

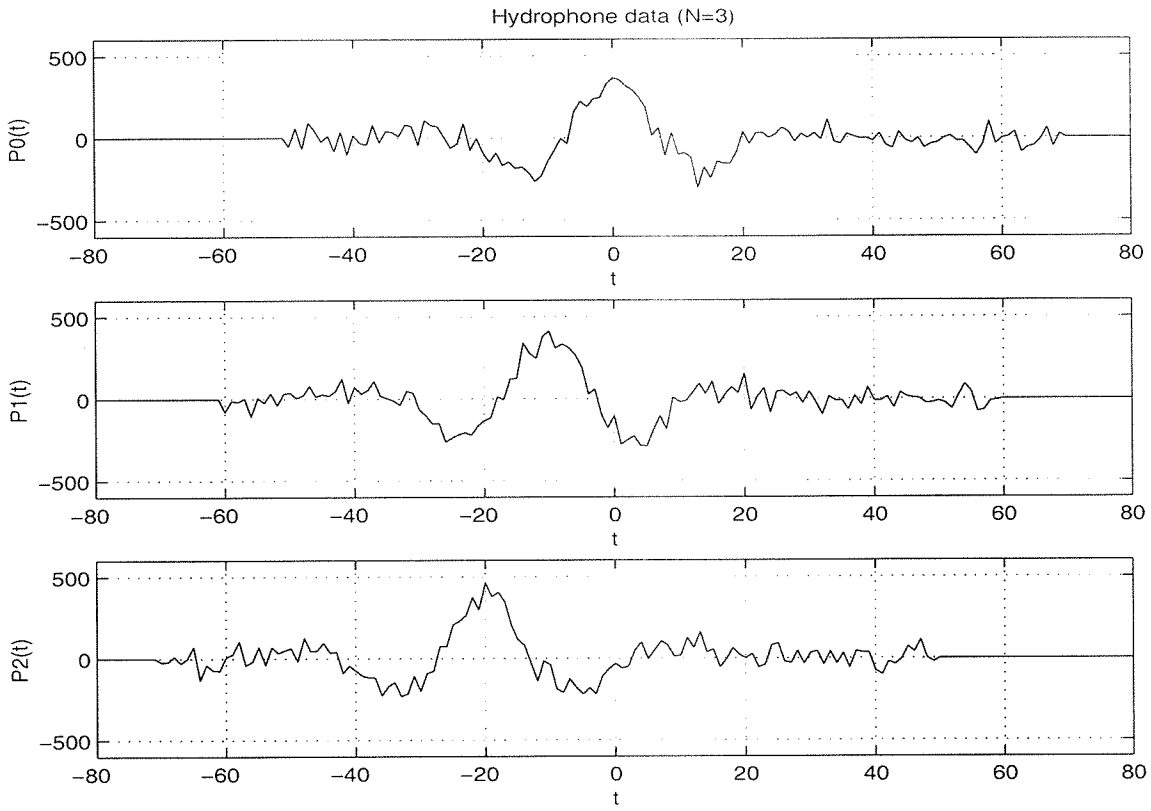

Figure 5.71: Hydrophone data

Maximum likelihood results are shown in figure 5.72 and figure 5.73. The parameters are, grid size $\Delta q = 0.25$, the number of iterations $I = 10000$, initial temperature $T_0 = 1.5 \times 10^6$. The MLE result of the time series is shown in figure 5.72, the standard deviation of the estimated signal is $std(p(t) - q(t)) = 22.4781$, and the MLE result of the bearing is shown in figure 5.73, it's around the true value, $30°$.

Least Squares Estimation results are shown in figure 5.74 and figure 5.75. The parameters are, grid size $\Delta q = 0.05$, the number of iterations $I = 10000$, initial temperature $T_0 = 1.5 \times 10^6$. The LSE result of the time series is shown in figure 5.74, the standard deviation of the estimated signal is $std(p(t) - q(t)) = 34.9986$, and the LSE result of the bearing is shown in figure 5.75, it's a little bit biased from the true value, $30°$.

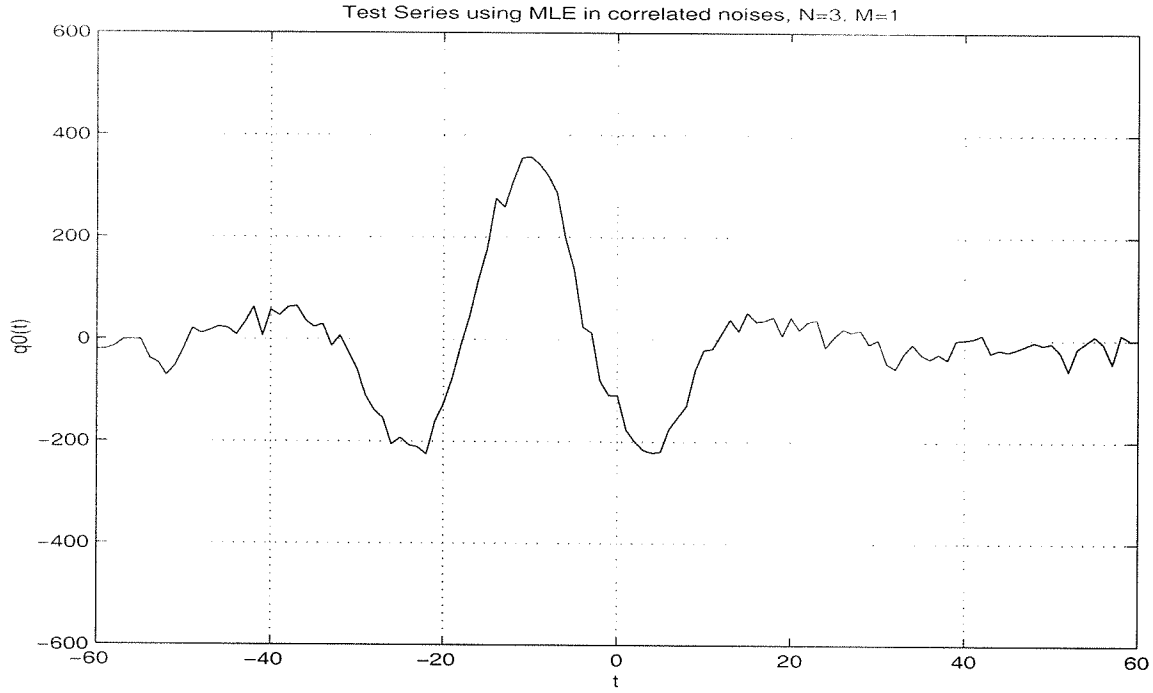

Figure 5.72: MLE result of the time series

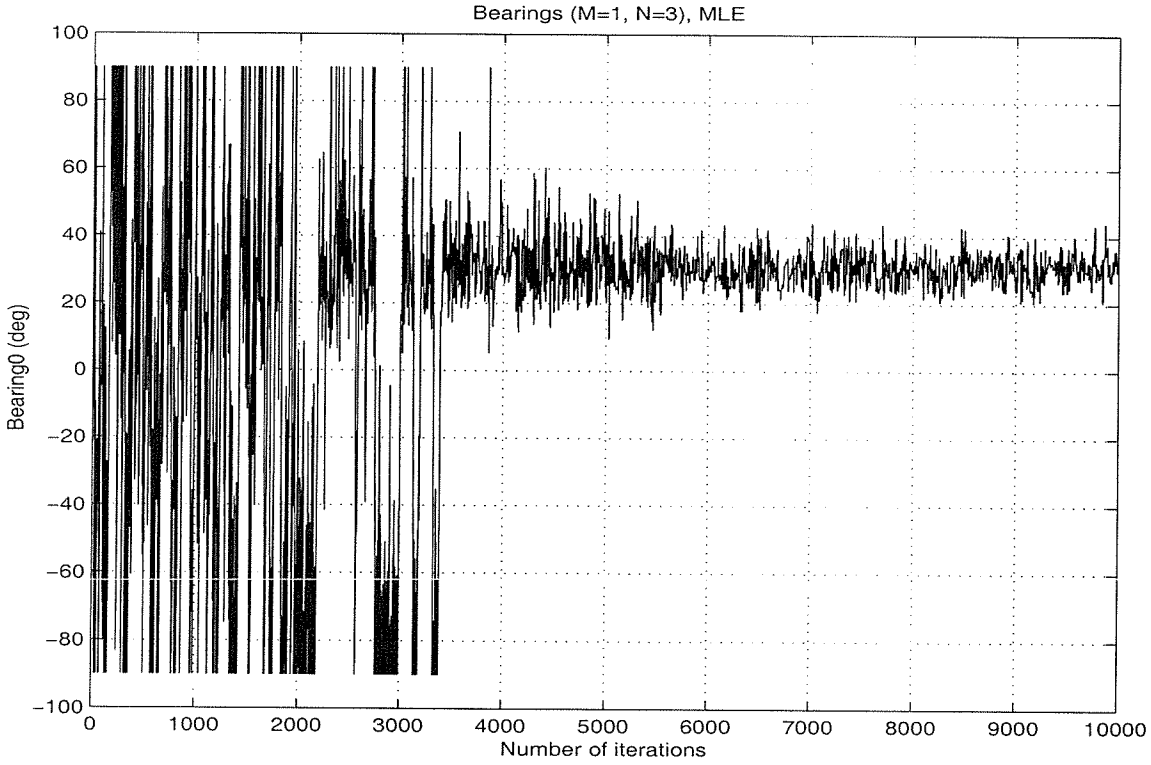

Figure 5.73: MLE result of the bearing

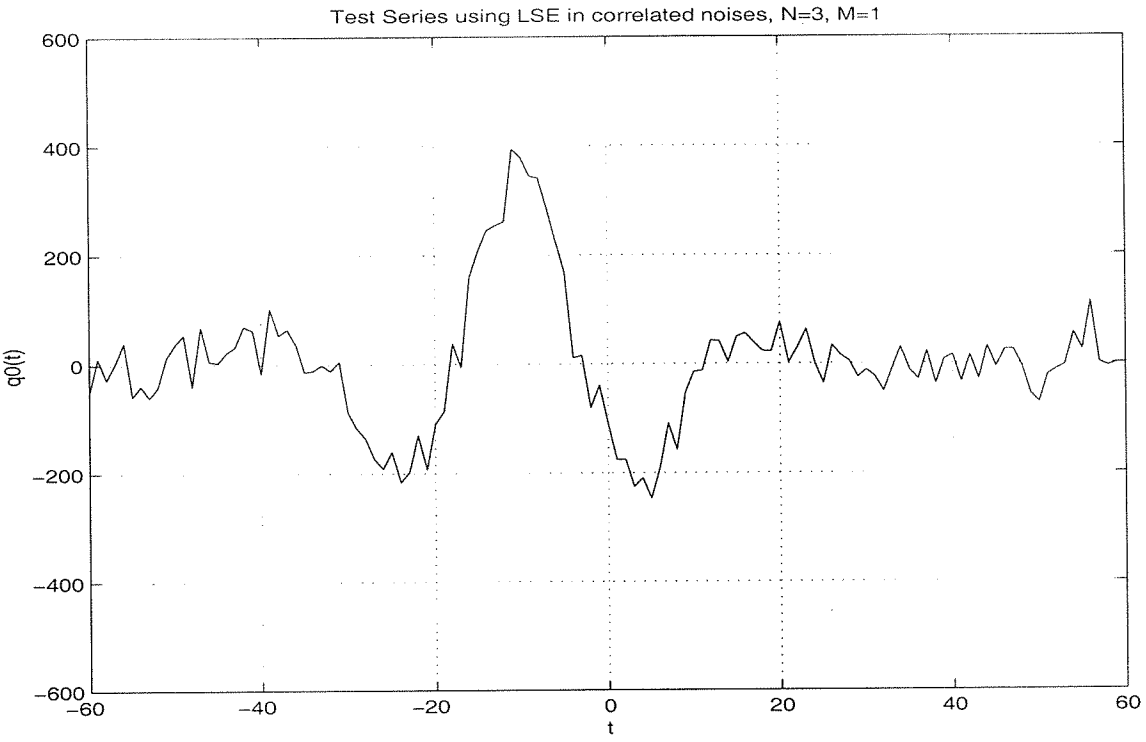

Figure 5.74: LSE result of the time series

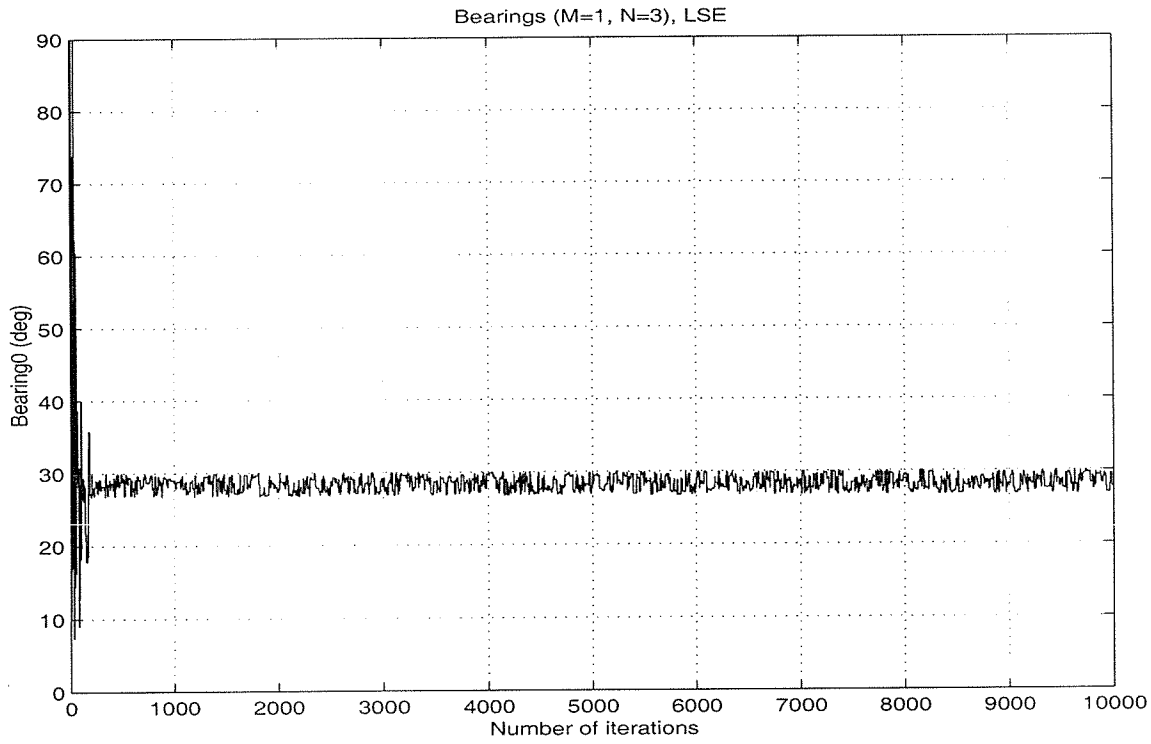

Figure 5.75: LSE result of the bearing

5.3 In spatially uncorrelated noise

In uncorrelated noise, the Maximum Likelihood Estimation and the Least Squares Estimation get the same results. We work with dimensionless variables, the sound velocity c is unity, the hydrophone spacing $h = 20$.

The noise is shown in figure 5.76. The hydrophone data is shown in figure 5.77.

The source is a broadband signal with a bearing of $20°$. The time series is given by the equation:

$$p(t) = \exp\left\{-\left[\frac{t+10}{20}\right]^2\right\}\cos\left[\frac{2\pi(t+10)}{30}\right] \tag{5.57}$$

it is shown in figure 5.35.

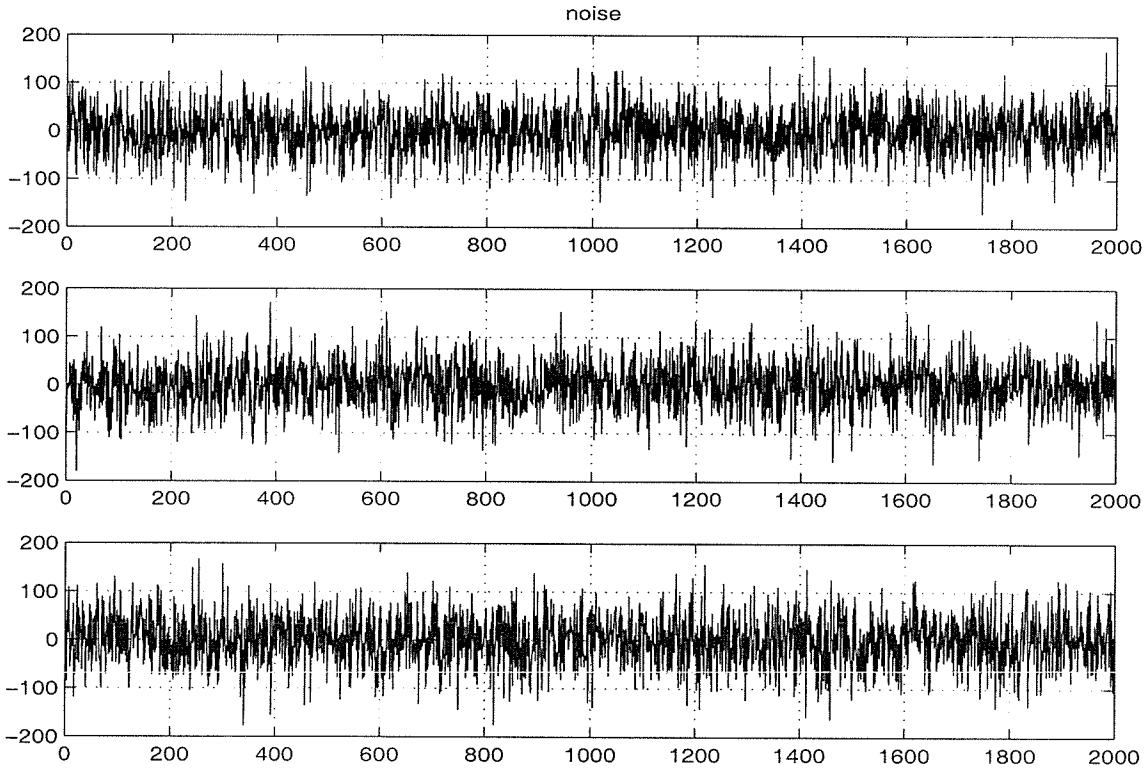

Figure 5.76: The uncorrelated noise

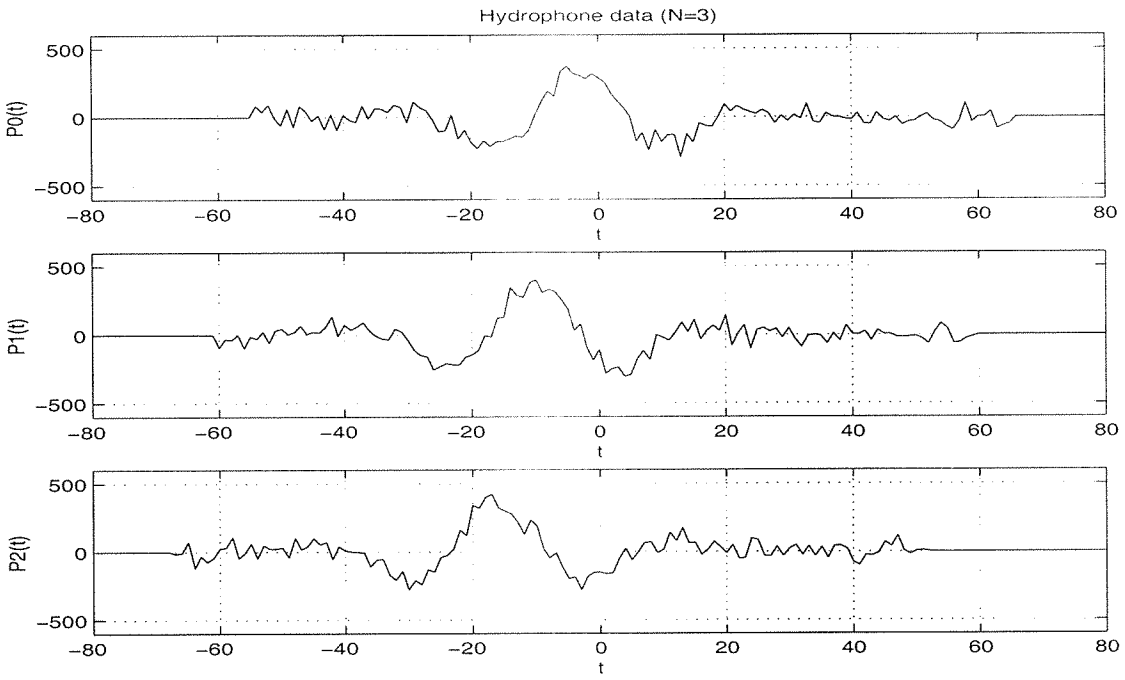

Figure 5.77: Hydrophone data

First, the MLE is used. Take the grid size $\Delta q = 0.25$, the number of iterations $I = 4000$, initial temperature $T_0 = 1.5 \times 10^6$. The MLE result of the time series is shown in figure 5.78, the standard deviation of the estimated signal is $std(p(t) - q(t)) = 37.0401$, and the MLE result of the bearing is shown in figure 5.79, it's around the true value, $20°$.

Then the LSE method is used. Take the same parameters, $\Delta q = 0.25$, $I = 4000$, and $T_0 = 1.5 \times 10^6$. The results are exactly the same as those when using MLE method. The estimated time series is shown in figure 5.80, the standard deviation of the estimated signal is $std(p(t) - q(t)) = 37.0401$. The estimated bearing is shown in figure 5.81.

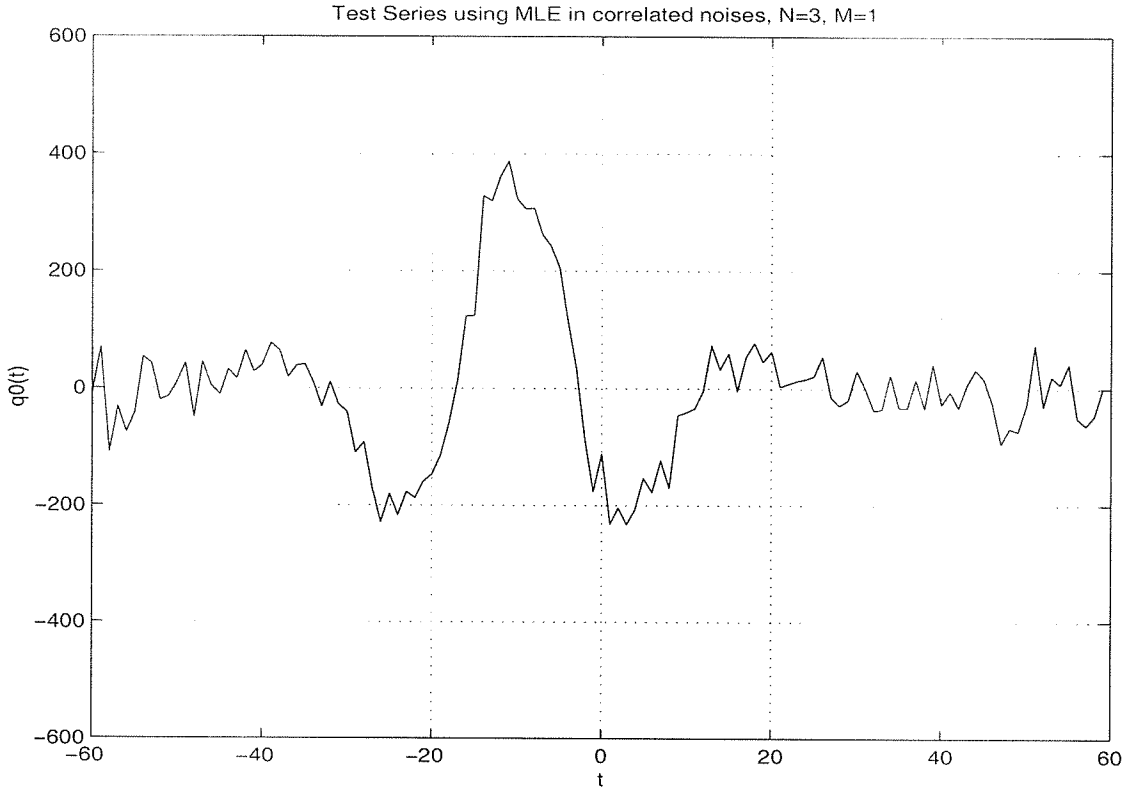

Figure 5.78: MLE result of the time series

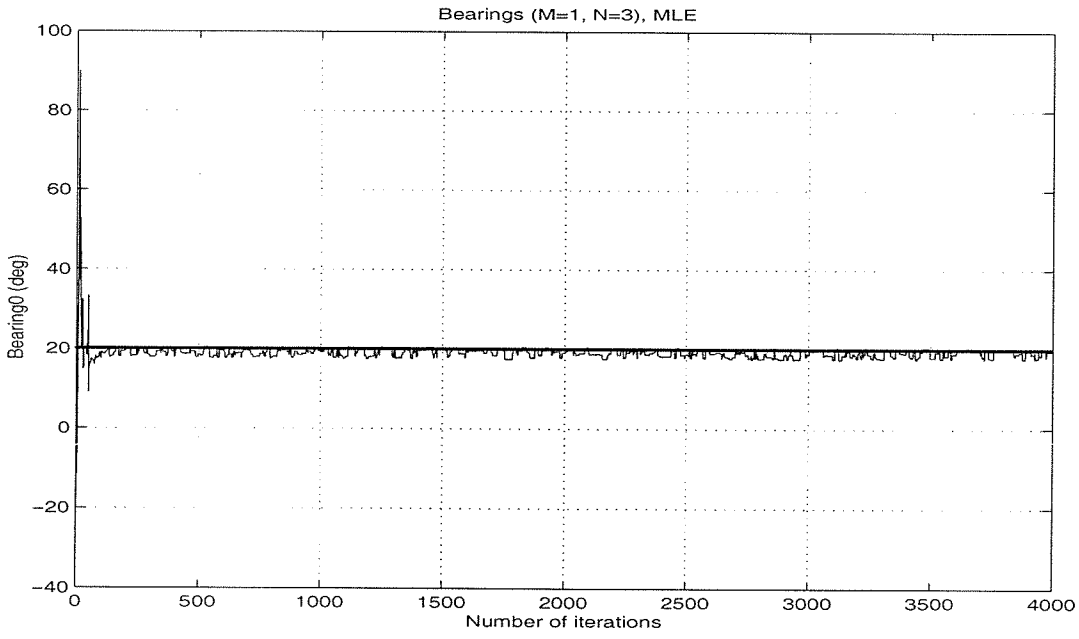

Figure 5.79: MLE result of the bearing

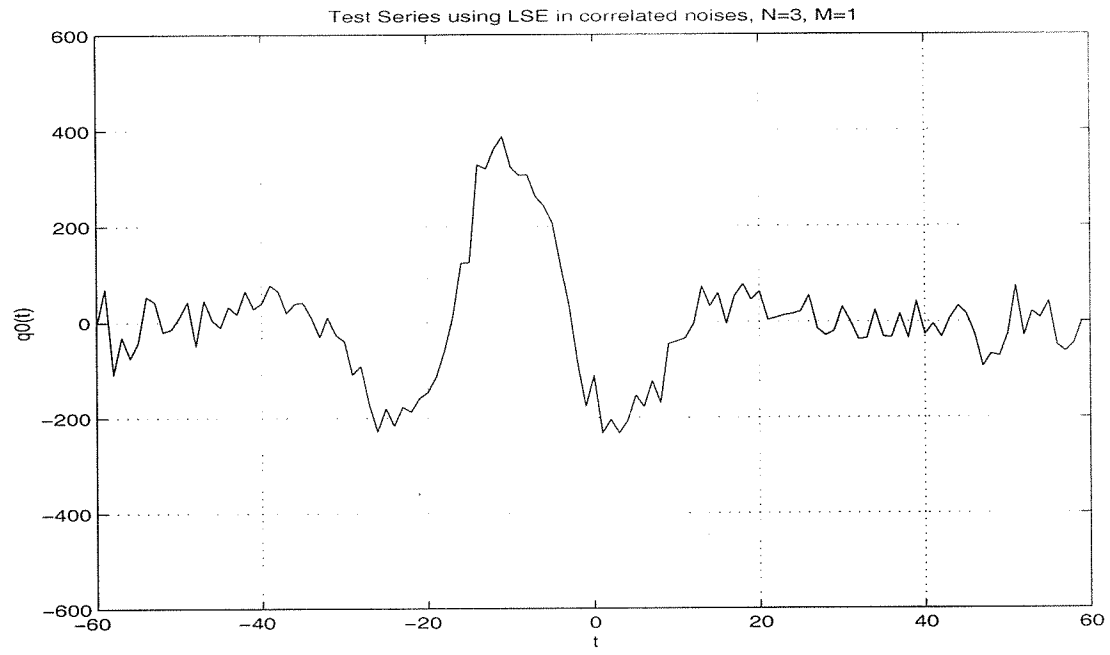

Figure 5.80: LSE result of the time series

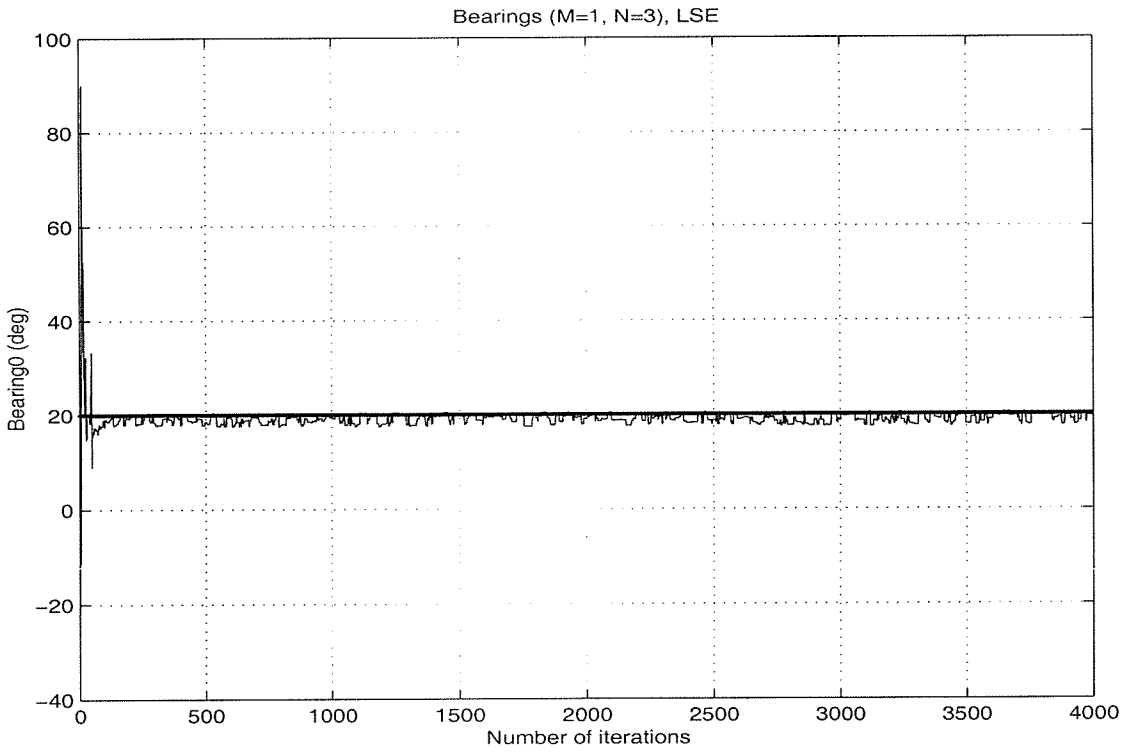

Figure 5.81: LSE result of the bearing

Chapter 6

Conclusions and Discussions

6.1 Conclusions

Maximum likelihood time-domain beamforming achieves good performance in various cases. In the spatially correlated noise background, we get better results using maximum likelihood estimation than using least squares estimation in estimating the time series and bearings of the signals. The simulation results show that, when the spatial covariance matrix is not diagonal, regardless of whether the diagonal elements are inhomogeneous or homogeneous, and the signals are broad or narrow band, maximum likelihood time-domain beamforming performs better than least squares time-domain beamforming. If the covariance matrix is diagonal, the maximum likelihood estimation gets the same results as the least squares estimation does.

Fast simulated annealing algorithm is a useful method in estimation, especially in our maximum likelihood time-domain beamforming, because it is more computationally efficient than exhaustive search.

6.2 Discussions

1. Number of sources unknown

We have proceeded under the assumption that the total number of signals present in the data is known. In practice, that number M is unknown and it also will have to be estimated from the data. Referring back to the signal model, in presence of independent and identically distributed noise, the structural properties associated with the array output covariance matrix $\underline{C}$ can be readily exploited to solve this problem. Statistical tests based on the asymptotic multivariate Gaussian nature of the eigenvalues, have been devised for the real data case to estimate the number of equal eigenvalues with a certain confidence

level. Its use in array processing is reported and the extension of these methods to coherent scenarios is discussed.[16]

2. Temporally correlation

In this thesis, only spatially correlated noise is treated. In practice, the noise is also temporally correlated. In this case, a whitening filter should be used to make the noise uncorrelated in time.

3. Spatial domain

The underwater sound environment is characterized by a multitude of noise-like signals and signal-like noises. In the face of this sometimes bewildering mix of signal and noise, two avenues for signal extraction are available, temporal domain processing and spatial domain processing. The most fundamental tools for temporal domain processing are correlation and spectrum analysis. Temporal domain correlation has a well-known justification based on the matched filter when a priori knowledge of the signal spectrum is available. It should, of course, not be surprising that nearly all of the temporal domain processing concepts have direct counterparts in the spatial domain. As a fundamental relationship, a parallel can be drawn between a sampled time interval of equally spaced, sampled data points and a one-dimensional (line) array of sensors which are equally spaced over some finite spatial aperture.[17]

4. Artificial control parameter and grid size in simulated annealing algorithm

The artificial control parameter and the grid size are based on trial and error. If the temperature is too high, the algorithm might not converge; if the temperature is too low, sometimes we get wrong results. The grid size for time series is small compared to the amplitude of the signals. If it's too small, then the algorithm might not converge. If it's too large, the result we get will not be the best, the variance of the estimation will be larger than the optimal values.

Bibliography

[1] Don H. Johnson. The application of spectral estimation methods to bearing estimation problems. *Proceedings of the IEEE*, 70(9): 1018-1028, September 1982.

[2] W.A. Kuperman, Michael D. Collins, John S. Perkins, and N. R. Davis. Optimal time-domain beamforming with simulated annealing application of a priori information. *The Journal of Acoustic Society of America*, 88(4):1802-1810, October 1990.

[3] Michael D. Collins, Jonathan M. Berkson, W. A. Kuperman, Nicholas C. Makris, and John S. Perkins. Applications of optimal time-domain beamforming. *The Journal of Acoustic Society of America*, 93(4): 1851-1865. April 1993.

[4] Steven M. Kay. Fundamentals of Statistical signal processing: estimation theory. PTR Prentice Hall, Englewood Cliffs, New Jersey. 1993.

[5] Steven M. Kay. Fundamentals of Statistical signal processing: detection theory. PTR Prentice Hall, Englewood Cliffs, New Jersey. 1998.

[6] Alan S. Wilsky, Gregory W. Wornell and Jeffrey H. Shapiro. Stochastic processes, detection and estimation. MIT EECS 6.432 course notes. 1998.

[7] K. C. Sharman. Maximum likelihood parameter estimation by simulated annealing. P*roc. IEEE Conf. Acoust. Speech Signal Process*, ICASSP-5: 2741-2744. 1988.

[8] Richard O. Nielsen. Sonar Signal Processing. Artech House, Inc. 1991.

[9] Robert J. Urick. Principles of underwater sound. McGraw Hill Book Company. 1983.

[10] Don H. Johnson, and Dan E. Dudgeon. Array signal processing: concepts and techniques. PTR Prentice Hall, Englewood Cliffs, New Jersey. 1993.

[11] Edited by Vijay K. Madisetti, and Douglas B. Williams. The digital signal processing handbook. CRC Press, and IEEE Press. 1998.

[12] S. Geman, and D. Geman. Stochastic relaxation, Gibbs distributions, and the Bayesian restoration of images. *Trans. IEEE. Pattern Analysis and Machine Intelligence*, vol. PAMI-6, 6: 721-741, Nov. 1984.

[13] H, Szu and R. Hartley. Fast simulated annealing. *Physics Letters*, 122: 157-162. 1987.

[14] W. A. Kuperman, and F. Ingenito. Spatial correlation of surface generated noise in a stratified ocean. *Journal of Acoustic Society of America*, 67(6):1988-1996. June 1980.

[15] George V. Frisk. Ocean And Seabed Acoustics: A Theory of Wave Propagation. Prentice-Hall, Englewood Cliffs, New Jersey, 1994.

[16] S. Unnikrishna Pillai. Array signal processing. Springer-Verlag, 1989.

[17] Simon Haykin, Editor. James H. Justice, Norman L. Owsley, J. L. Yen, and Avi C. Kak. Array signal processing. Prentice-Hall, Inc., Englewood Cliffs, New Jersey. 1985.